273435

LABORATORY STUDIES OF
ROCKET PLUME RADIATION
AT REDUCED PRESSURE

J. W. Sutton

THE BOEING COMPANY
Aero-Space Division
Seattle 24, Washington
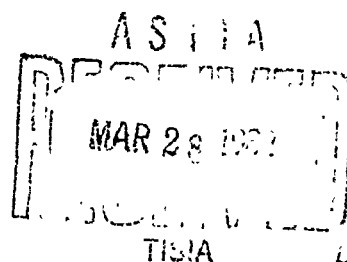
Contract No. AF 19(604)-7439

Project No. 5043

Task No. 79710

FINAL REPORT

December 1961

Prepared
for

GEOPHYSICS RESEARCH DIRECTORATE
AIR FORCE CAMBRIDGE RESEARCH LABORATORIES
OFFICE OF AEROSPACE RESEARCH
UNITED STATES AIR FORCE
BEDFORD, MASSACHUSETTS

LABORATORY STUDIES OF
ROCKET PLUME RADIATION
AT REDUCED PRESSURE

J. W. Sutton

THE BOEING COMPANY
Aero-Space Division
Seattle 24, Washington

Contract No. AF 19(604)-7439

Project No. 5043

Task No. 79710

FINAL REPORT

December 1961

Prepared
for

ABSTRACT

Laboratory studies were conducted of the spatial and spectral distribution of rocket plume radiance at simulated altitudes. Motors of 150 to 200 pounds thrust were operated at sea level and at pressures equivalent to approximately 50,000 and 100,000 feet. The propellant combinations studied were gasoline/oxygen, RP 1/oxygen, JP 4/oxygen, UDMH/N_2O_4 and aluminized solid propellant.

A traversing rocket technique was employed which permitted simultaneous observation of a number of radiometric and spectrometric properties of a common area of the plume. The graphical presentations of these data are interpreted on a qualitative and semi-quantitative basis.

I

CONTENTS

FIGURES

FOREWORD

These studies were conducted at The Boeing Company in the Thermal Radiation
Group of the Applied Physics Section. Dr. J. W. Sutton, Senior Group Engineer,
was principal investigator for the program. Laboratory experimentation and
interpretation of the data was performed by F. W. Cramer, R. R. Sexauer and
J. A. Hammond, Research Engineers, and J. Olson, Associate Engineer, all in
the Thermal Radiation Group. Rocket test operations at Boeing Jet Laboratory
were conducted by R. K. Easter.

1.0 INTRODUCTION

The utilization of the infrared radiation from rocket exhaust for the detection and tracking of missiles creates a requirement for a complete understanding of the spatial and spectral distribution of the plume radiance. Ideally this understanding could come about by proper combination of theoretical knowledge of rocket exhaust expansion processes and of appropriate radiation parameters. The theoretical model thus derived could then be verified by appropriate measurements of actual missiles in flight.

This direct approach has not been satisfactorily accomplished, however, because of the complex nature of the radiation process from the missile in flight and of difficulties of long-range infrared measurements in the atmosphere. The field measurements give no information concerning infrared spatial distribution and only limited information on the true spectral distribution of the source radiation. The basic studies of radiation from heated exhaust gases represent the radiance of idealized sources which do not contain the effects of gradients in gas density and gas velocities which occur in actual missile flight.

The gap between the basic studies and field measurements should be filled by investigation of plume radiance properties for small and large motors operated under controlled conditions. Programs in progress include the use of a radiation research burner to perform high temperature infrared emission and absorption studies (Reference 1), wind tunnel studies of plume radiance of small motors (Reference 2), and measurements of radiance in the Mach cone region of plumes of large liquid-propellant motors (Reference 3).

In the present study motors of 150 to 200 pounds thrust were operated at sea level and at reduced pressures equivalent to approximately 50,000 and 100,000 feet. The rocket motor for each of the studies was mounted on a cart, which was traversed slowly through an altitude simulation tank. Radiometric and spectrometric instruments were attached to ports on the tank aligned to view a common area of the plume through infrared transmissive windows. In this manner simultaneous observations were made of the infrared spectral radiance, the total infrared radiance, visible spectra, ultraviolet radiance, distribution of infrared radiance normal to the plume axis, and the audio-modulation component of infrared radiance. Since small motors were used it was feasible to study a variety of propellant systems, which included gasoline--oxygen, JP 4--oxygen, RP 1--oxygen, unsymmetrical dimethylhydrazine--nitrogen tetroxide and an aluminized solid propellant.

The data obtained have permitted us to develop a semi-quantative representation of rocket plume radiance properties, with respect to both spatial and spectral character. Effects related to ambient pressure and propellant combination were given primary consideration.

The limitations inherent in these data, due to the design of the experiment, must certainly be recognized. In performing the experiments air was allowed to flow through the altitude simulation tank in order to assure afterburning in the plume. T'e air flow was of course not sufficient to provide simulation of the actual mixing conditions occurring in missile plumes in flight under the equivalent altitude conditions. Effects related to the gas dynamics of the motion of the missile and its exhaust through the atmosphere were also absent in these tests.

A further limitation to the applicability of these experimental data arises
from the lack of a reliable scaling model for rocket exhaust radiation
processes. Consideration of the data from the several experimental studies,
together with the best possible data on radiation from missiles in flight,
should provide the basis for such a scaling process. The required under-
standing of plume radiation processes in operational rockets can thus be
achieved.

By extension of these techniques, further studies on laboratory motors can
deal with exotic or as yet undeveloped propellant systems to permit predic-
tion of radiation from exhaust plumes of rockets operating with these systems
under actual conditions.

2.0 EXPERIMENTAL INVESTIGATION OF PLUME RADIATION

The primary activity in this program was the experimental investigation of the spatial and spectral distribution of the radiation from rocket motor plumes. A laboratory motor of nominal 150-pounds thrust burned the following liquid propellant combinations: gasoline/oxygen, JP-4/oxygen, RP-1/oxygen, and UDMH/N_2O_4. A 200-pound thrust aluminized solid-propellant motor was also used.

The experimental firings were conducted in a horizontal altitude chamber at the Boeing Jet Laboratories. Test firings were made at sea level and at pressures equivalent to altitudes of approximately 50,000 and 100,000 feet. For all conditions there was air flow past the nozzle to provide oxygen for plume afterburning.

Through the use of ports and appropriate windows installed near one end of the tank, radiation-measuring instruments were able to view the rocket plume. In order to view the entire plume, the rocket motor was traversed past the instrumentation ports. A schematic of the chamber and instrument installation is shown in Figure 1.

The instrumentation used included a rapid-scan infrared spectrometer, a total infrared radiometer, a scanning lead-sulfide radiometer, an ultraviolet radiometer, a cine-spectrograph, an audio-modulation radiometer and a pulse camera. The instruments were installed and boresighted to view a coincident point on the plume centerline.

More detailed discussion of the experimental procedures is presented in the succeeding paragraphs of this section.

-4-

MAX CART TRAVERSE 18'

INSTRUMENTATION PORTS

SECOND STAGE STEAM EJECTORS

END CAP

TEST CHAMBER

MOTOR

C_L

CART

CART TRACK   A

CABLE FOR TRAVERSING CART

TO FIRST STAGE

STEAM EJECTORS

SCANNING
RAD

U. V. RAD   SPARE PORT

PULSE CAMERA   AUDIO MOD. RAD.

RAPID SCAN MONOCHROM.   TOTAL RAD

CINE SPEC   SPARE PORT
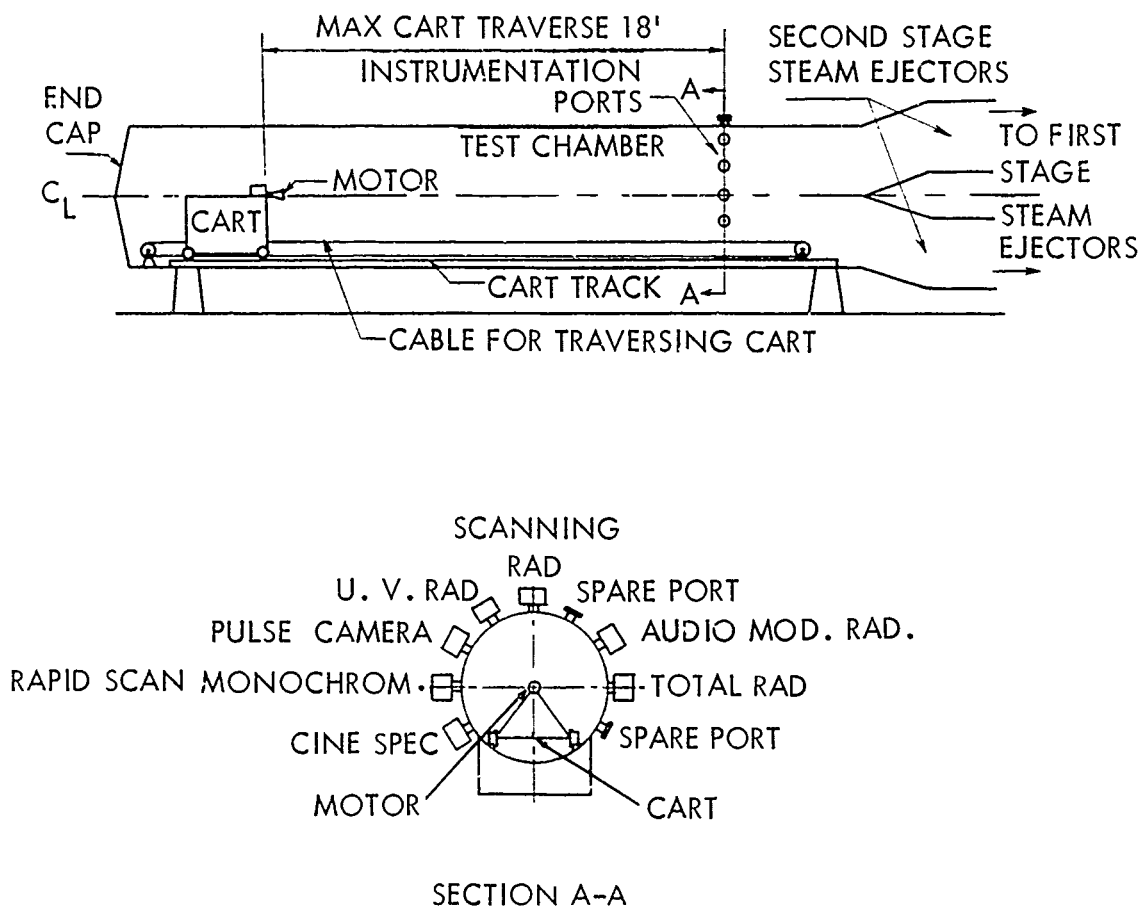
MOTOR   CART

SECTION A-A

Figure 1

INSTALLATION OF RADIOMETRIC EQUIPMENT - SCHEMATIC

2.1   ALTITUDE CHAMBER FACILITY

The altitude facility consisted of a chamber 6 feet in diameter and 36 feet long, connected to a two-stage steam ejector pumping system. The first stage consisted of six 30-inch ejectors and eight 40-inch ejectors and the second stage utilized four 48-inch ejectors. The ejector system has a capability of maintaining steady state pressure equivalent to 100,000 feet with 2.0 pounds per second mass flow. For these tests the system was required to handle only 1.3 pounds per second mass flow, composed of 0.5 pound per second rocket motor exhaust products and 0.8 pound per second bleed air. A general view of this facility is shown in Figure 2.

The test chamber was modified by installation of an annular ring of ports with windows near one end of the chamber. The radiation instrumentation was installed at these ports and boresighted at the plume centerline. The instrumentation boresight and fields of view are shown in Figure 3. A cart, containing the rocket motor, and a track were installed in the tank. A traversing mechanism moved the cart longitudinally down the tank. A maximum separation of 18 feet could be obtained between the motor nozzle and the instrumentation. The cart traverse speed was 2/3 foot/sec for the sea level test condition and 1 1/2 feet/sec for the altitude test condition. The center of the motor nozzle was located on and traversed down the chamber centerline.

2.2   ROCKET MOTOR AND CART

The research motor selected for these studies has a 45 L^* chamber, a 0.45 inch diameter throat and an expansion ratio of 25. The nominal thrust of the motor at 600 psia chamber pressure was 150 pounds. The combustion chamber and throat were water cooled. The injector head was fuel cooled and the

-6-

6 30" 1st STAGE EJECTORS

8-40" 1st STAGE EJECTORS

LOCATION OF PORTS

4 48" 2nd STAGE EJECTORS

Figure 2

BOEING JET LABORATORY FACILITY

DISTANCE VARIES
FROM 0 TO 18'

U. V.
RADIOMETER

MOTOR
NOZZLE

PLUME CENTER LINE

TOTAL
RADIOMETER

SCANNING
RADIOMETER
INSTANTANEOUS
FIELD OF VIEW

RAPID SCAN
MONOCHROMOTOR

CINE
SPECTROGRAPH

SCALE 0 5
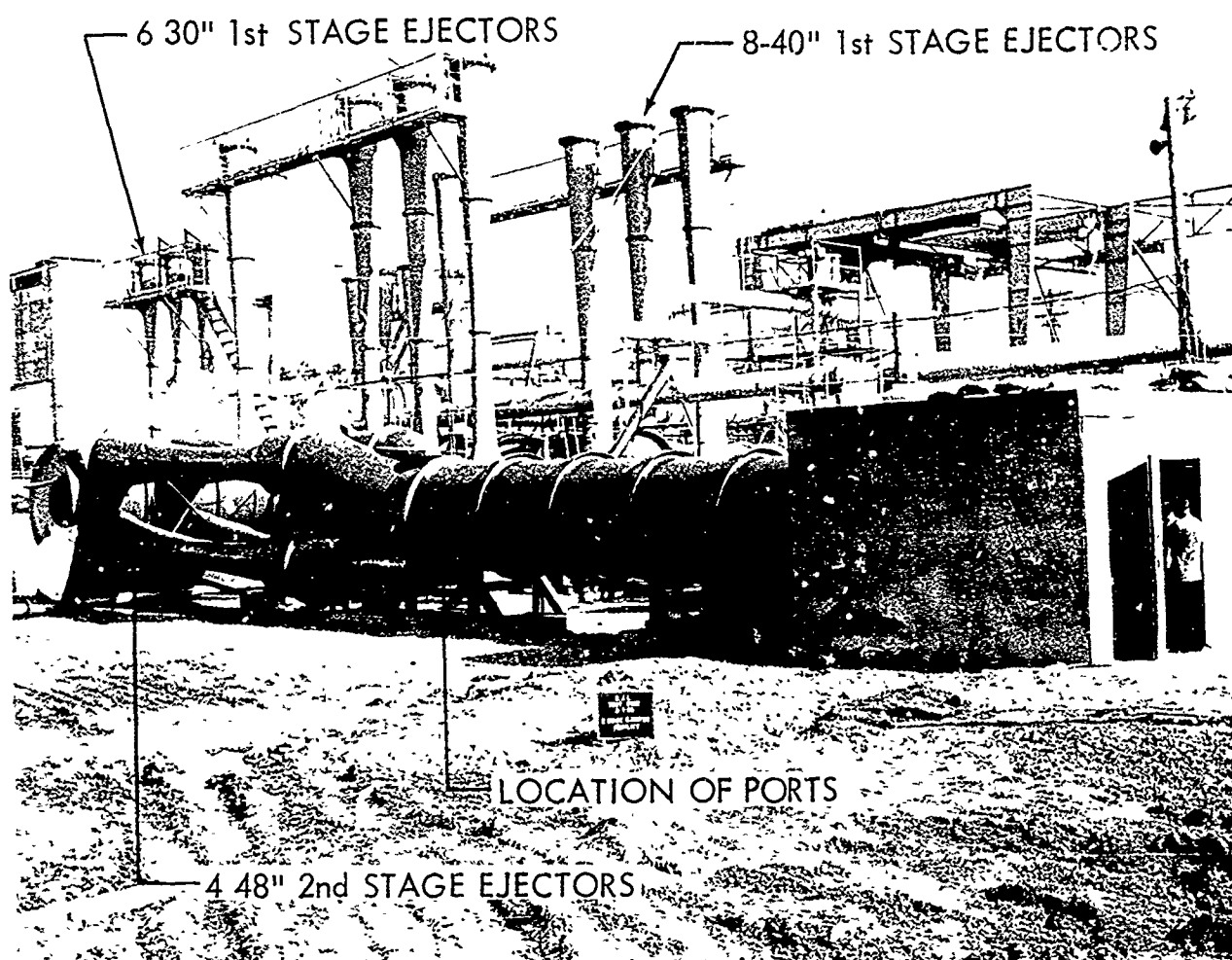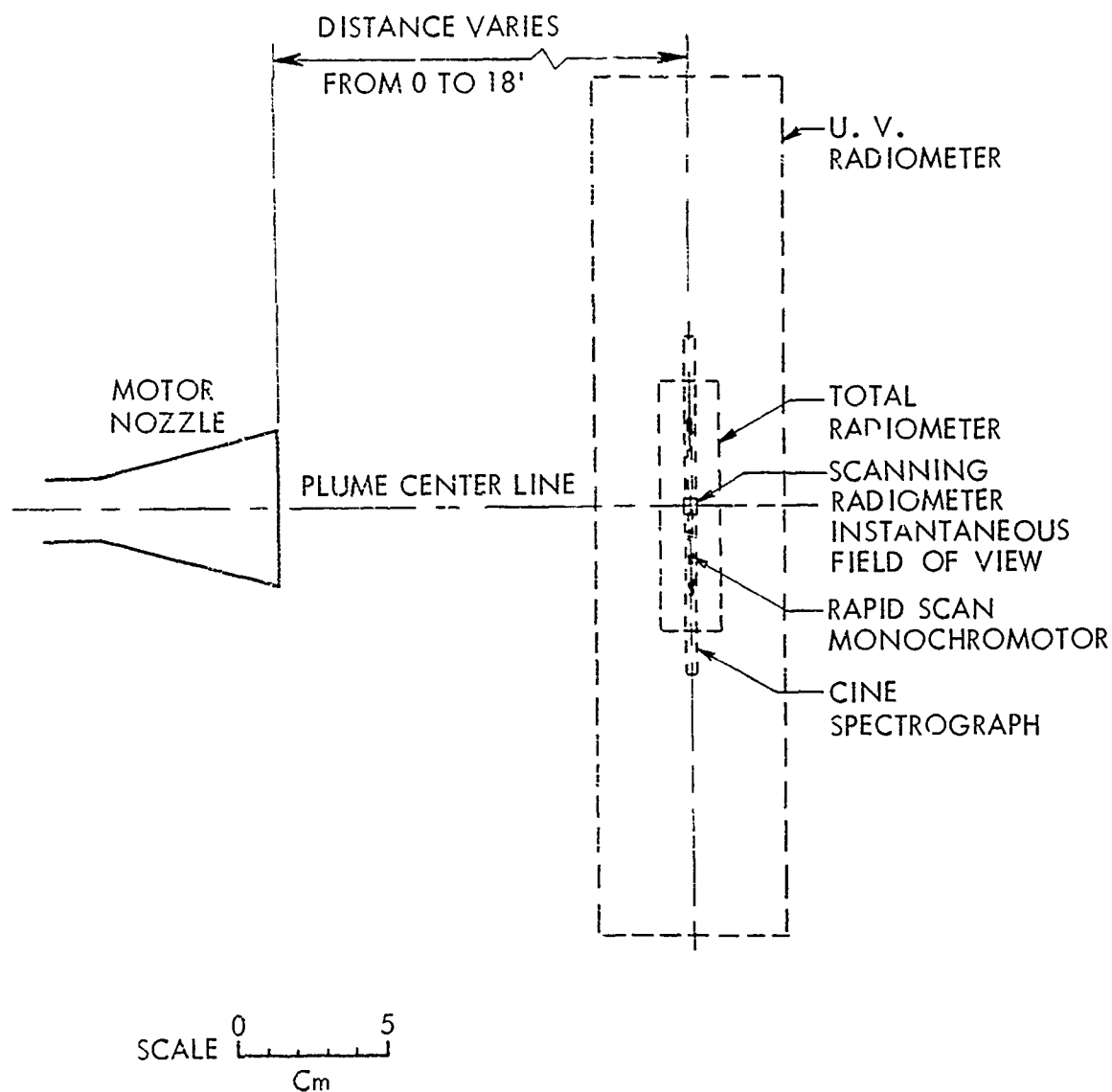Cm

Figure 3

INSTRUMENTATION BORESIGHT AND FIELD OF VIEW

8

nozzle extension was a copper heat sink type. The same motor was used for hydrocarbon and amine propellant systems, except for different injector heads.

The motor was mounted on a cart as shown in Figure 4. This cart contained tanks of fuel, oxidizer and coolant, sufficient to operate the rocket motor for test runs up to 22 seconds. The cart operation was remotely controlled from the control room. Pressures and flow rates of fuel and oxidizer were preset for each run.

In the hydrocarbon-oxygen tests it was intended that the mixture ratio should be at the conventional fuel-rich level, with equivalence ratio (E.R.) equal to 1.6. This value was not attained in all runs, since the fuel and oxidizer flows could not be changed during the run. The regulators that controlled these flows were statically calibrated, but a slight shift in calibration during the dynamic operation resulted in pressure and equivalence ratio change.

The solid-propellant motor used in these tests was manufactured by Thiokol. It contained six pounds of propellant and burned for 6 seconds. The nominal thrust of the motor at 500 psia was 200 pounds. The motor used a graphite nozzle .65-inch diameter at the throat and had an expansion ratio of 6. The propellant formulation was a polyurethane base propellant identified as TPG 3013D, containing 13% aluminum. The motor is shown in Figure 5.

The solid-propellant exhaust products were:

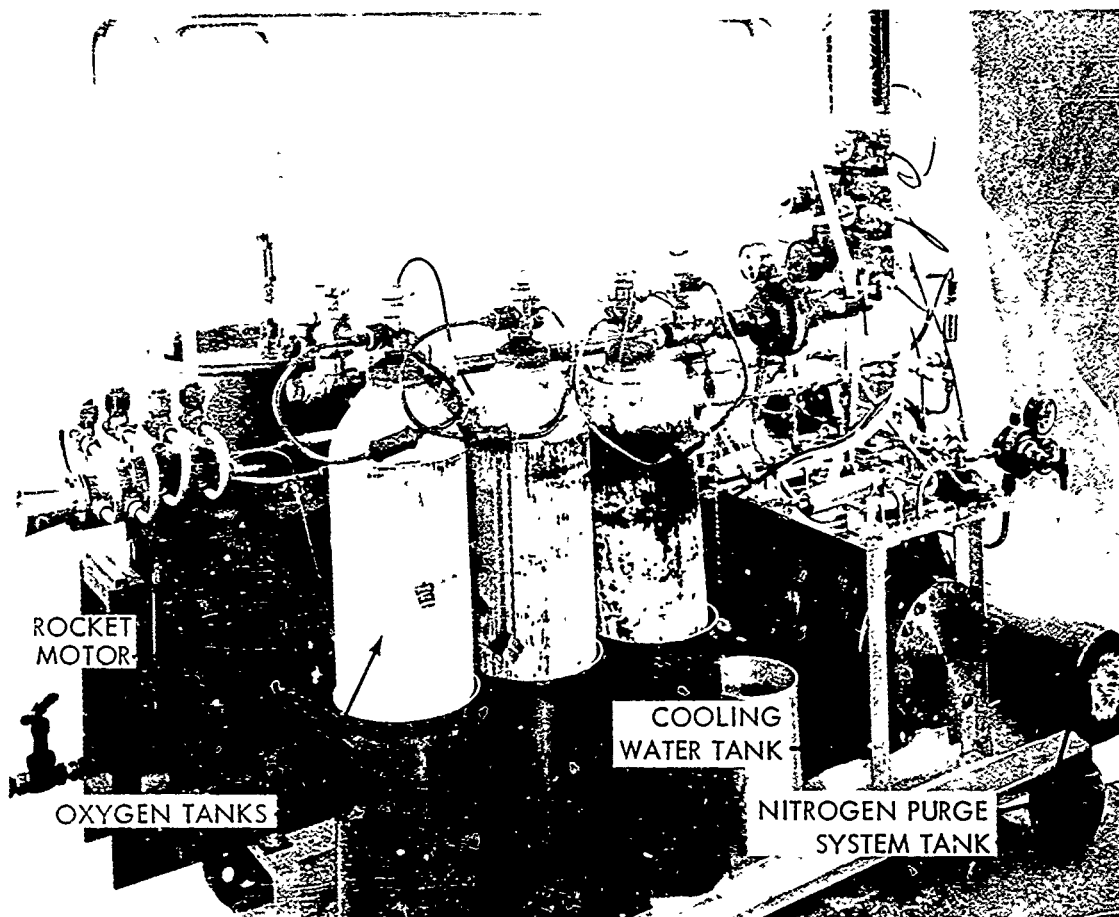| Chemical Species	% Weight
CO	35.1
HCl	20.2
Al_2O_3	24.6
CO_2	3.8
H_2	3.4
H_2O	4.8
N_2	8.1

Figure 4

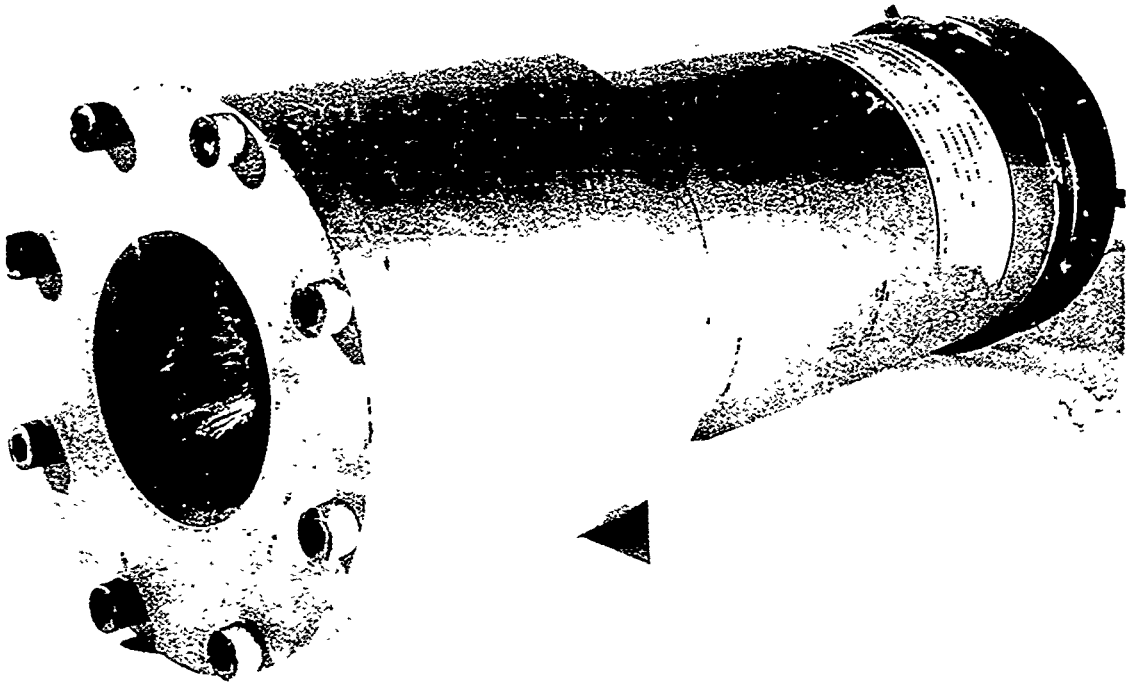CART INSTALLATION OF ROCKET MOTOR

Figure 5

SOLID PROPELLANT MOTOR

For these tests the solid motor was mounted on the cart in place of the liquid motor. The sea level tests were conducted using one motor per test. Because of the short motor burn time and long plume, it was necessary to fire two motors in series to complete one altitude run.

2.3 TEST PROCEDURE

During a typical test run the following sequence of operations was performed:

1. Prepare the motor and cart assembly.

2. Position the motor nozzle exit plane 6 inches downstream from the infrared viewing ports.

3. For altitude tests, start the appropriate steam ejectors and stabilize the test chamber pressure.

4. Turn on instrumentation (infrared and motor).

5. Start motor on condition (equivalence ratio = 1.6, chamber pressure = 600 psia).

6. Cart traverse starts automatically when the chamber pressure reaches preselected level.

7. At end of cart travel, stop motor.

8. Shut down instrumentation and facility.

This operating procedure was modified appropriately for hypergolic fuels and for solid fuels.

The necessary rocket operation parameters were recorded by the Jet Laboratory instrumentation group. Radiation measurements were monitored continuously and recorded in the Mobile Infrared Laboratory. Time-pulse markers and intercommunication between the motor operation and infrared laboratory areas sufficed to establish identifying markers for all events and conditions.

Rocket-operating parameters were recorded continuously, and oxidizer flow, fuel flow, chamber pressure, thrust, characteristic velocity and test chamber pressure were calculated from this information. All measuring devices were calibrated against appropriate standards at regular intervals.

2.4 RADIATION MEASUREMENT INSTRUMENTATION

To obtain the maximum quantity of useful data concerning the spatial and spectral distribution of the plume radiance, several spectrometric and radiometric instruments were aligned to view a common area of the plume.

The spectral data were taken with a Perkin-Elmer Model 108 Rapid Scan Monochromator equipped with CaF_2 prism (Figure 6). The instrument was operated at a rate of 15 scans per second over a wavelength interval of 1.2 to 5.5 microns. The field of view was established by the monochromator entrance slit setting. For a slit width of 0.2 mm the spectrometer field of view at the rocket plume centerline was 5.7 cm high by 0.114 cm wide.

The optical collecting system for the monochromator was a Newtonian type telescope with an 90 mm diameter, 14° off-axis paraboloid and 267 mm focal length. The telescope was focused to image the plume centerline at the entrance slit of the monochromator. A lead telluride detector was used, mounted horizontally in a styrofoam reservoir filled with liquid nitrogen. An off-axis ellipsoid mirror with a six-to-one reduction in image size was used to focus the image of the spectrometer exit slit on the detector.

The wavelength scan indicator of the instrument was modified in the following manner in order to increase its readout accuracy. The sine wave generator on the shaft of the nutating mirror was replaced with a disk containing 20
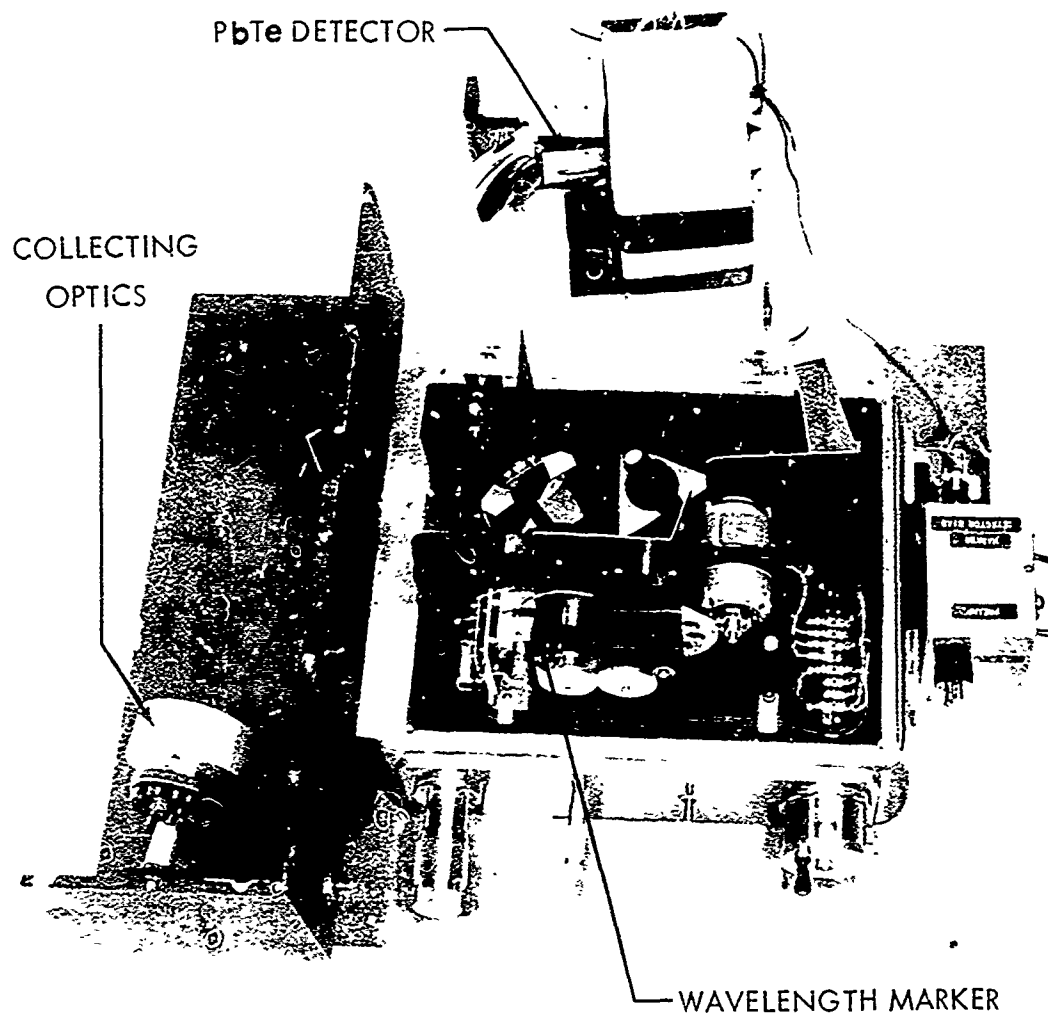
PbTe DETECTOR

COLLECTING
OPTICS

WAVELENGTH MARKER

Figure 6

RAPID-SCAN INFRARED SPECTROMETER

14

slots. This disk interrupted a light beam between a photodiode and a small light bulb, generating a pulse each time the slot appeared between the light and the diode. Consequently, a pulse was generated each 18 degrees of nutating mirror rotation. Since the scan is generated by the rotation of the nutating mirror, each pulse from the diode therefore corresponds to a specific wavelength. The observed resolution was 0.05 microns at 2.7 microns for a slit width of 0.2 mm.

The output of the spectrometer detector was amplified by a pre-amplifier in the instrument and then was transmitted to the trailer laboratory for further amplification and recording. During runs the signal was monitored with an oscilloscope to permit amplifier gain changes as required for recording the wide range of spectral radiances achieved in the experiments.

Total infrared radiation measurements were made with a Barnes Radiometer Model R-8B1 (modified) utilizing a 2.5 x 10 mm Barnes thermistor bolometer detector. The instrument field of view at the plume centerline was 8.25 cm in height by 2.06 cm in width. The instrument spectral response was limited at the long wavelength end to 5.5 microns by using a sapphire window. The short wavelength limit was 0.7 microns or 1.2 microns where a silicon filter was used, as indicated in the appropriate graphs. Using the silicon filter made the spectral response of this instrument equivalent to that of the rapid-scan monochromator. The eight-inch optical system was removed and replaced with an 80 mm diameter, 235 mm effective focal length Cassegrainian system. This change was made because the Barnes 8-inch optics could not be focused at the short plume-to-instrument distance without extensive modifications, and a shorter focal length system was desired to increase the instru-
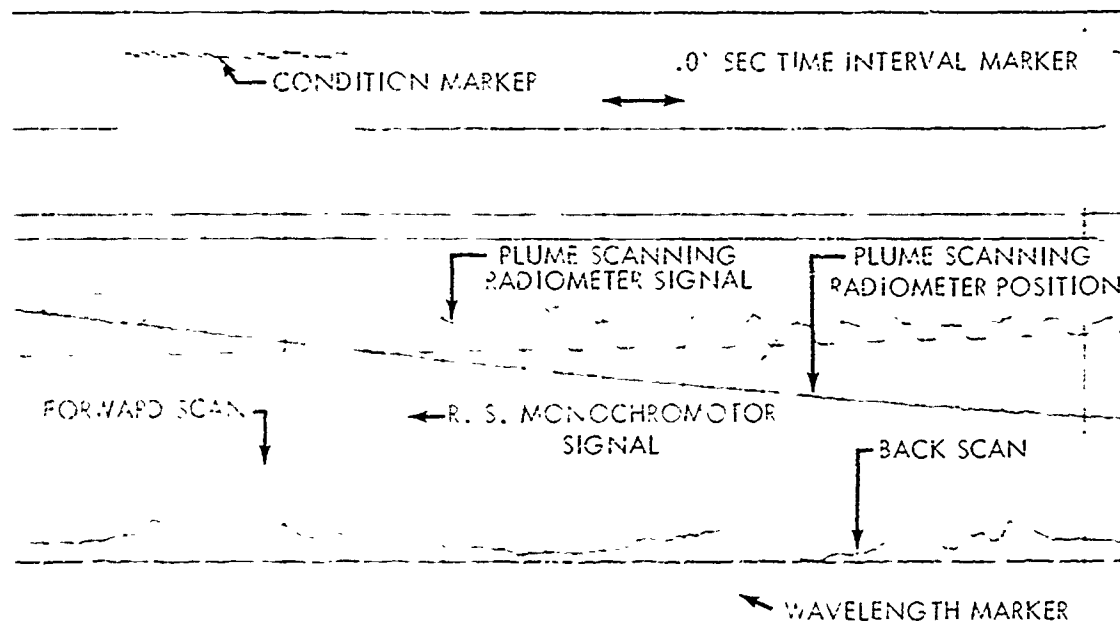
Figure 7

OSCILLOGRAPH DATA TRACE

ment field of view. For this measurement program the entrance aperture was baffled down to some fraction of the available aperture because the intensity of the radiation from the plume would otherwise overdrive the radiometer.

Lateral plume measurements were made with a locally-built radiometer using a 0.5 x 0.5 mm Kodak Ektron detector. A Cassegrainian optical system, with an 80 mm diameter primary and 235 mm focal length, was used as a collector. The input was chopped at 160 cycles per second with the detector output fed into a preamplifier in the unit. The radiometer was mounted on a frame together with an oscillating plane mirror and drive motor (Fig. 8). The instantaneous field of view at the tank centerline was 5 x 5 mm. The oscillation of the mirror swept this field of view laterally across 18 inches on either side of the tank centerline. A linear potentiometer in the mirror drive gave a sinusoidal position signal. With the 1 rps motor used the instrument made 2 scans per second across the plume.

To provide some general information about trends and levels in ultraviolet radiation, a simple radiometer was constructed which utilized a phototube (RCA 935) and a broadband ultraviolet filter (Corning 7-54). The spectral response of this combination peaked at 0.34 micron with half sensitivity points at 0.26 and 0.39 micron (Figure 9). No collecting optics were used in this instrument. The field of view, defined by the geometry of the phototube and a slotted aperture placed near the quartz window, was 6.7 x 28.6 centimeters at the test chamber centerline. The radiation was chopped at 90 cycles to allow AC amplification.

The audio modulation radiation measurements of the plume were made with a locally-built instrument which used a 4.0 x 1.0 mm Kodak Ektron lead sulfide
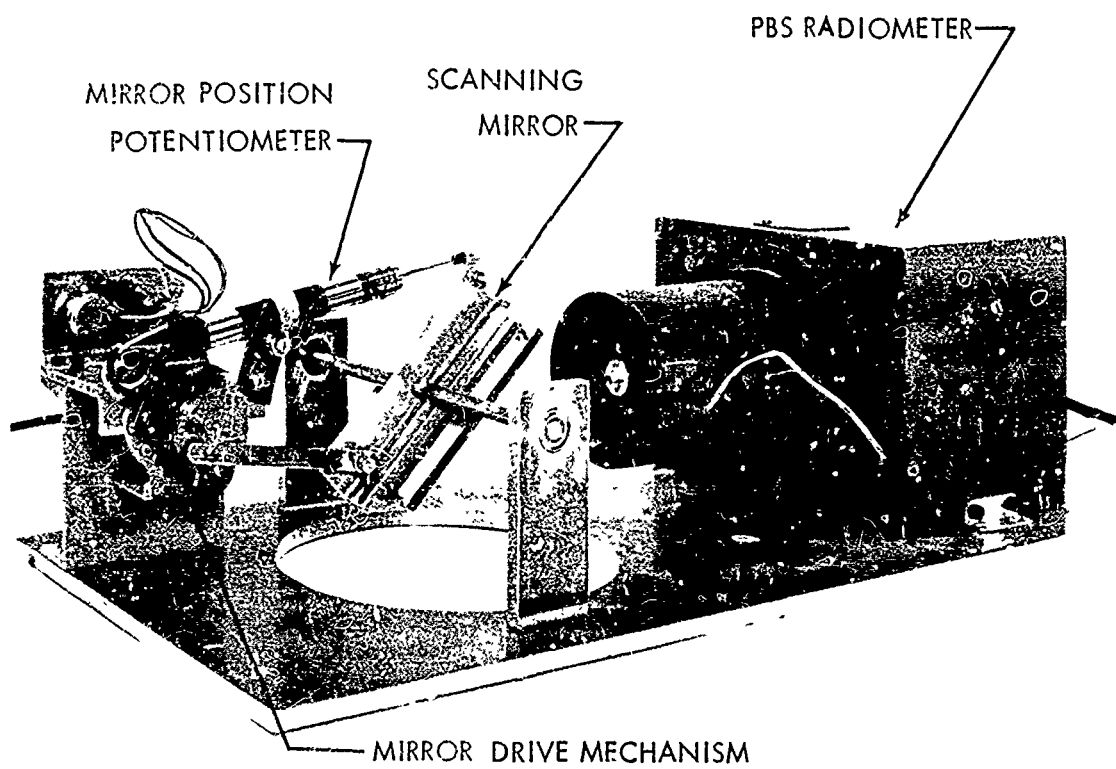
MIRROR POSITION POTENTIOMETER

SCANNING MIRROR

PBS RADIOMETER

MIRROR DRIVE MECHANISM
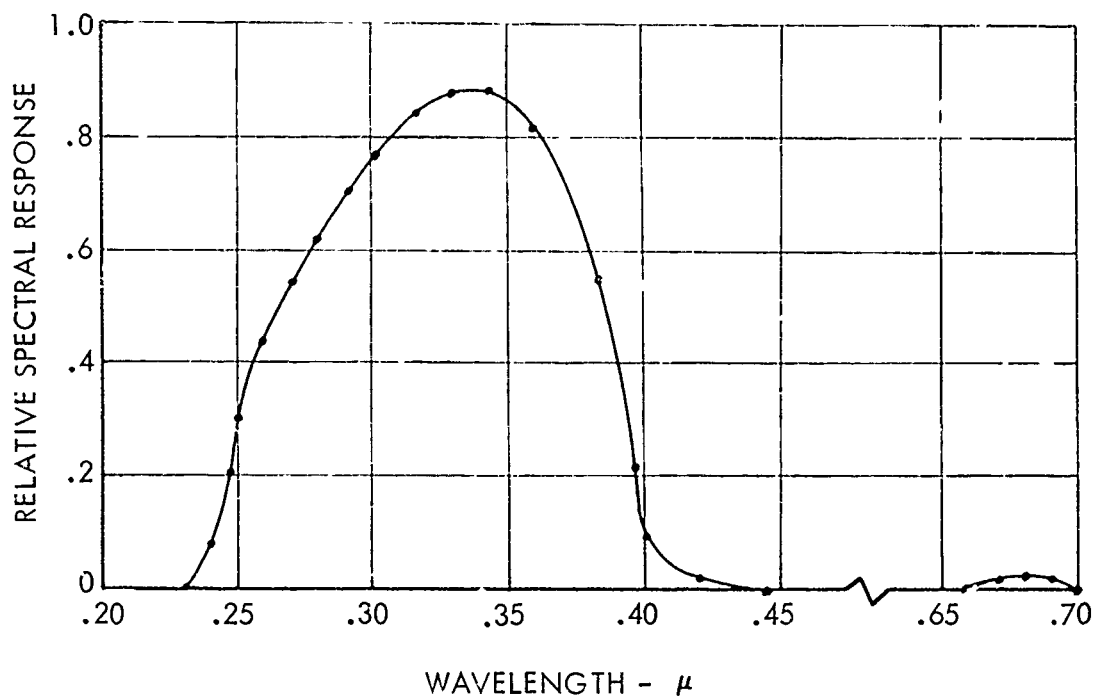
Figure 8

PLUME SCANNING RADIOMETER

18

Figure 9

ULTRAVIOLET RADIOMETER RESPONSE

detector. No optics were used. The field of view, governed by baffles, was a 55 cm diameter circle at the plume centerline. The incoming radiation incident upon the detector was not chopped. The D.C. output from the instrument was amplified and recorded on an F.M. tape recorder.

The altitude chamber vibration at the instrumentation location was measured with an accelerometer and recorded on the second channel of the tape recorder.

Spectral coverage in the visible was provided by a Boeing-constructed cine-spectrograph (Figure 10), capable of frame rates ranging from 12 spectra per second to 64 spectra per second. The instrument utilized a 600 line/millimeter Bausch and Lomb replica transmission grating blazed at 0.55 micron in the first order. Glass achromats were used for the collimating and collecting lenses. A 16 mm Bolex motion picture camera recorded the spectra. The combined system operated at f/4.5. The resolution was limited by film size but was sufficient to separate the mercury yellow doublet. The Plus-X film used in these experiments and the geometry of the instrument limited the spectral response to 0.43 to 0.65 micron. The glass optics and spectral response of the film eliminated the second order ultraviolet.

The cine-spectrograph was placed at one of the lower ports, with its slit focused on the plume centerline. All lenses were normally operated wide open. Exposure was controlled by adjusting the camera frame rate, and thus its shutter speed. Selected spectra were processed with a Jarrell-Ash micro-densitometer to provide two or three plots of relative intensity versus wavelength for each test. It should be noted that the visible spectra can only be compared between conditions during the same test run. Exposure and film processing differences prohibit the comparison of relative intensity between different runs.

16 MM MOVIE
CAMERA

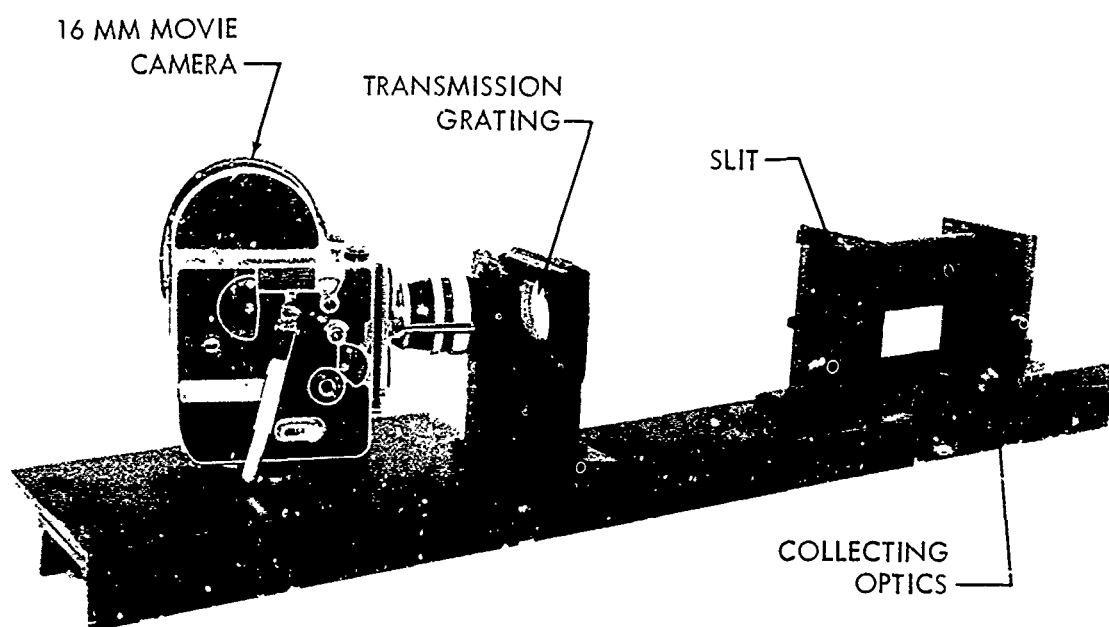TRANSMISSION
GRATING

SLIT

COLLECTING
OPTICS

Figure 10

CINE-SPECTROGRAPH

The signals from the total radiometer and the ultraviolet radiometer were recorded on a 4-channel Sanborn recorder, operated at a paper speed of 25 mm per second. Pulse marker channels recorded a time base, data marks to correlate motor conditions and position, pulse camera markers and total radiometer attenuation. After the earlier tests were completed, cart position was also recorded here. A sample data trace is shown in Figure 11.

Cart position was obtained from a ten-turn Helipot coupled directly to a pulley shaft of the cart drive system. The signal was calibrated for cart position and recorded on the Sanborn recorder.

A Consolidated Engineering oscillograph, operated at 152 cm per second, provided the high frequency capability required to record the rapid scan spectrometer signal and wavelength markers. The scanning radiometer signal and position indication were also placed on this oscillograph. An event marker channel was used to indicate scanning radiometer gain changes. Data correlation was provided by the data marker and the pulse camera marker. Figure 7 shows a sample data trace.

To align the instruments, a 100 watt, clear projection lamp was set-up inside the tank with the lamp filament aligned with the rocket motor centerline directly in the center of the opposing windows.

The monochromator was aligned by moving it until the image of the lamp filament was centered on the entrance slit. At the same time the illumination centering was checked by inserting an aperture in the window and on the paraboloid. The radiometers were equipped with bore-sight tools for alignment purposes. This alignment was checked immediately prior to each run.

PULSE CAMERA INDICATOR

TOTAL RADIOMETER
SIGNAL

ULTRAVIOLET
RADIANCE
SIGNAL

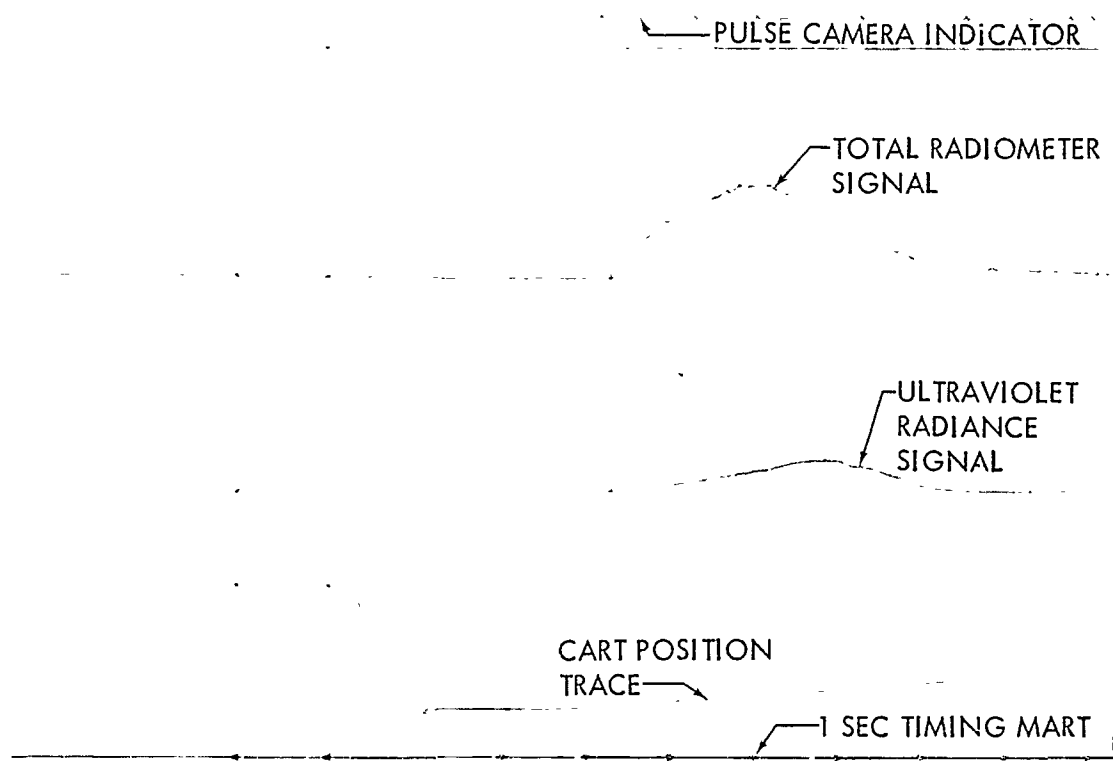CART POSITION
TRACE

1 SEC TIMING MART

Figure 11

RADIOMETER DATA TRACE

With each instrument aligned on the lamp filament, the centers of each instrument field of view coincided as shown in Figure 3.

The plume properties in the visible region were recorded for some of the runs with a 35 mm pulse camera. Boresight alignment pictures were also made to assist in correlation of the photographic observations with the radiometer fields of view.

The optical path between the detector and altitude chamber window in the rapid-scan monochromator was purged with dry nitrogen in order to eliminate the atmospheric absorption in the H_2O and CO_2 bands. Complete elimination of these absorption bands was not possible since the optical path between the chamber window and the plume could not be purged.

2.5 DATA REDUCTION

The raw monochromator data were presented as a series of spectra traced on the oscillograph chart as shown in the sample trace in Figure 7. The scan repetition rate was 15 scans per second; however, half of these were eliminated because only the forward (increasing wavelength) scan was calibrated due to the apparently lower quality, and lower instrument transmission found in the backward scan. Further spectra were eliminated by inspection due to obviously high radiation noise caused by fluctuations inherent in the motor. Spurious structure can be identified by its lack of scan-to-scan correlation in wavelength location, using hand-sketched overlays were necessary. Typical spectra were then chosen at three or more locations down the plume.

Having selected a spectrum for reduction, the chart deflections (D_λ) were picked off for a series of predetermined wavelengths (marker positions)

and at a few other points as required to show structure. The deflection, divided by the galvanometer sensitivity (K) and the overall system gain (G), yielded the detector signal output (V_λ):

$$V_\lambda = \frac{D_\lambda}{KG}$$

The detector signal was multiplied by the spectral radiance calibration factor (C_λ) to obtain the spectral radiance of the source (N_λ) in watts/cm^2-steradian-micron.

$$N_\lambda = C_\lambda V_\lambda$$

The spectrum was then plotted as N_λ versus the wavelength, obtained from the wavelength calibration curve.

The various radiometers measure radiant flux from the plume in their respective spectral bandpass regions, represented by an electrical output signal, V_s. The radiance of the target for each measurement was calculated from the relation:

$$N_T = \frac{V_S}{R\, A_o\, \omega_r}$$

in which R = responsivity of the detector

$\quad\quad A_o$ = entrance aperture

$\quad\quad \omega_r$ = angular field of detector

This latter quantity is given by:

$$\omega_r = \frac{A_D}{f^2}$$

in which A_D = area of detector

$\quad\quad f$ = focal length of optical system

This basic equation was used to reduce all radiometer data (with the exception of the ultraviolet radiometer) using measured values of the respective factors. For the ultraviolet radiometer effective radiance at the peak response of the system was determined, using the effective responsivity of the detector at 0.34 microns.

2.6   CALIBRATION TECHNIQUES

The reference standards for calibration of the various instruments included a Barnes Model 11-131 Blackbody Radiation Reference Source, a high-temperature laboratory furnace with a wedge insert, and a calibrated tungsten ribbon filament lamp. The calibrations were generally made with the instruments at the Jet Laboratory and repeated several times at intervals during the test series.

The rapid scan spectrometer was calibrated using the furnace, into which an oxidized stainless steel 15-degree wedge was inserted. This arrangement gives an emissivity of at least 0.95. The furnace was operated near 1000°C, the precise value being established with a calibrated optical pyrometer.

The furnace itself was mounted on the tank adjacent to the spectrometer with a plane mirror in front of the spectrometer when calibration runs were to be made, as shown in Figure 12. The distance from the furnace opening to the primary mirror of the collecting optics was adjusted to match the distance to the centerline of the rocket plume.

The wavelength calibration curve of the spectrometer was determined through the use of a series of calibrated absorption filters, including polystyrene, Lucite and other plastics. These filters were inserted, one after another,
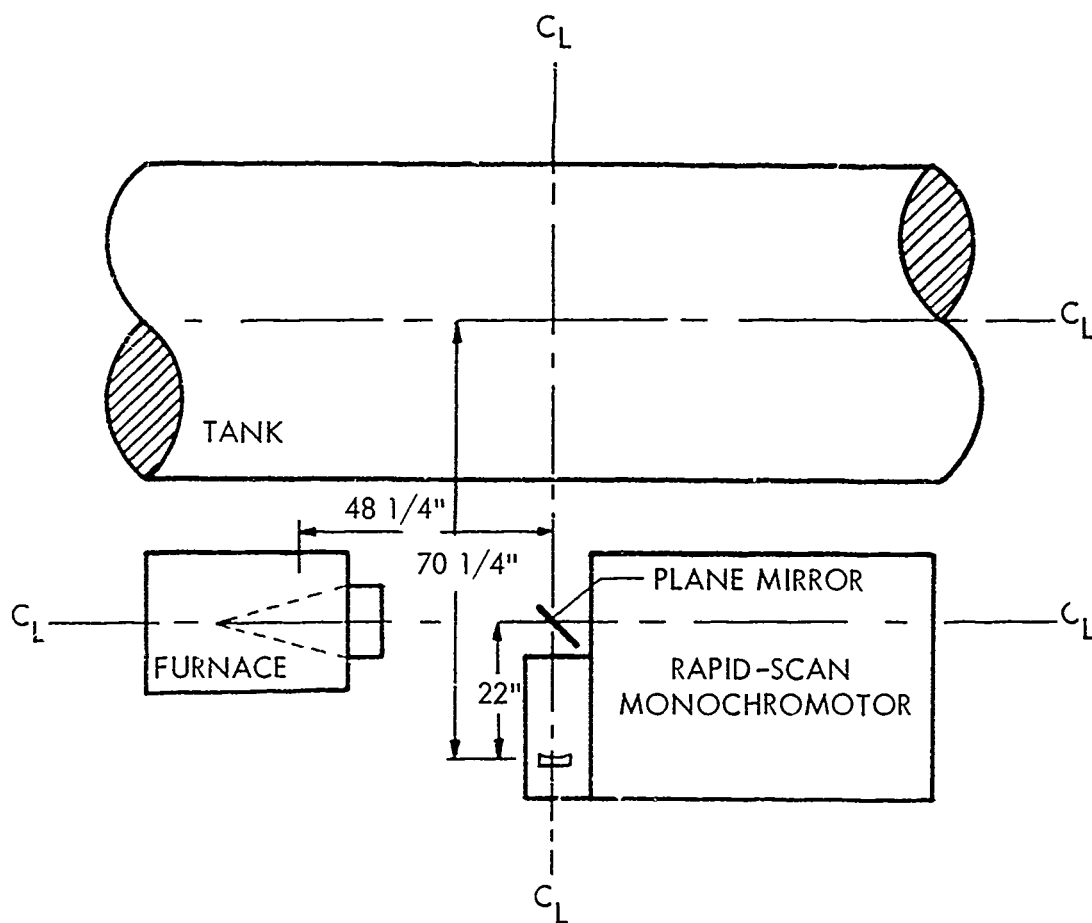
Figure 12

MONOCHROMATOR CALIBRATION ALIGNMENT

at the entrance slit of the spectrometer while it was viewing the blackbody source. Comparison of the known positions of absorption bands with the wavelength markers established a curve like that shown in Figure 13.

For the intensity calibration an observation was made of the blackbody at a measured temperature. The indicated deflection on the oscillograph record was compared point-by-point to the spectral radiant power calculated from the Planck equation. The resulting ratios provided a corresponding series of calibration factors as a function of wavelength, as shown in Figure 13. The data from the experimental runs were then converted directly to spectral radiance, with no need for separate calibration of the nonlinearities within the spectrometer. This calibration was performed after every three or four runs, depending on the time interval between runs.

The infrared radiometers were all calibrated against the Barnes Blackbody Radiation Reference Source. Each instrument was calibrated at a minimum of three temperatures between 700° and 1000°C, and at several aperture sizes. A calibration plot was made of signal voltage versus radiant flux entering the radiometer; the slope of the resulting line was taken as the responsivity.

Since relative values were used for the radiance contours, an absolute energy calibration was not necessary for the scanning radiometer. A strip with electrically heated nichrome wires mounted at 3-inch intervals was used to calibrate the mirror position. This strip was lined up in the test chamber perpendicular to the plume centerline. Scanning the radiometer across this device produced a series of pulses, corresponding to known distances from the centerline, which were recorded on the oscillograph along with the position signal. A template made from this record was used to obtain lateral positions for subsequent test runs.

WAVELENGTH TO MARKER CALIBRATION
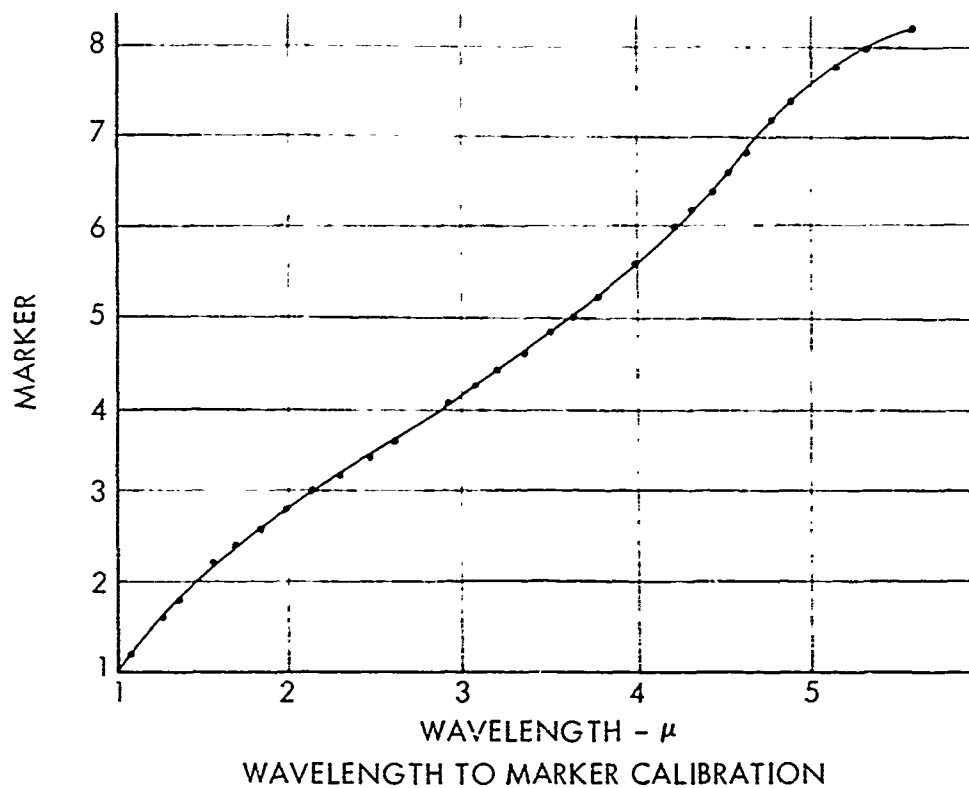

SPECTRAL RADIANCE CALIBRATION
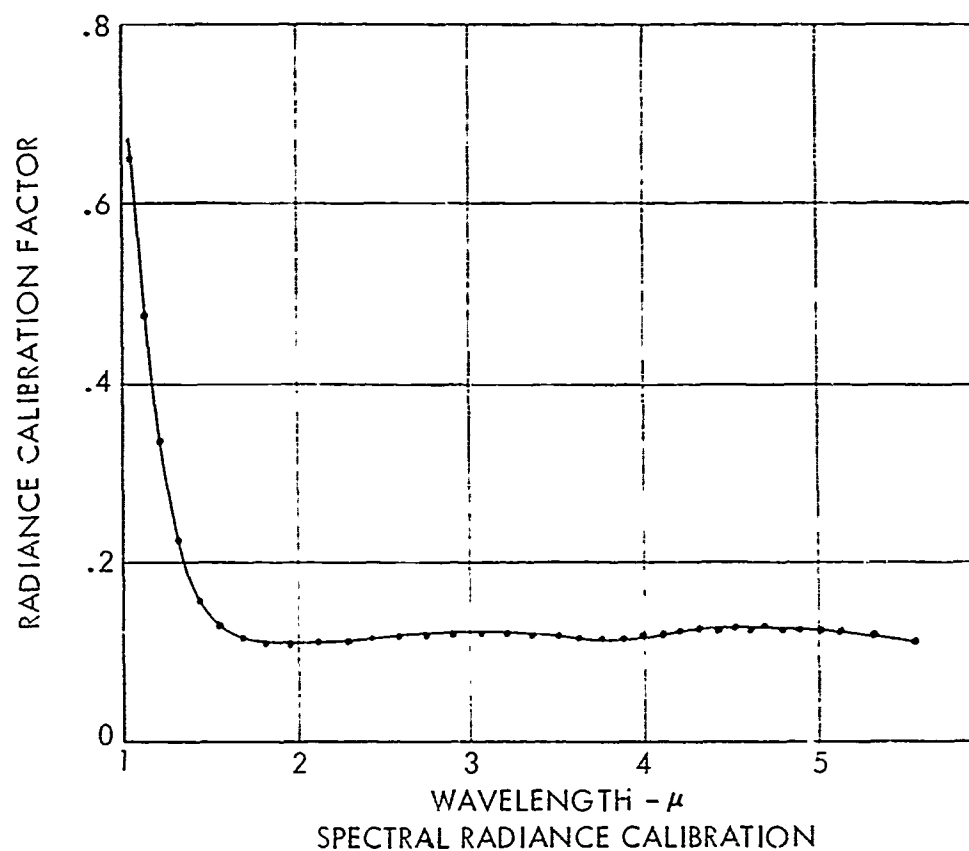
Figure 13

MONOCHROMATOR CALIBRATION

The ultraviolet radiometer was calibrated in terms of effective power at the peak spectral response of the instrument. The standard used was a tungsten ribbon filament lamp calibrated by the National Bureau of Standards (No. L-71).

The cine-spectrograph was calibrated in wavelength against a mercury lamp at several times during the test program. No significant shifts were noted. No intensity calibration was made.

In relating these respective calibrations to the rocket radiation measurements in the altitude tank, experimentally measured transmission factors were used to correct for absorption losses in the sapphire and quartz windows. Atmospheric absorption losses were not estimated, because of their generally small effect in this experimental arrangement and of the difficulty of arriving at valid values.

Only preliminary quick-look data reduction for the audio-modulation of the radiation was performed. This consisted of taking two-second sections of the tape, from selected portions of the test run, and processing them in a half-octave audio analyzer. The frequency response of the analyzer was from 20 to 10,000 cycles and its output was plotted by an x-y plotter. Test chamber vibration data were analyzed similarly.

3.0 PLUME RADIATION CHARACTERISTICS

The experimental measurements of rocket plume radiation for laboratory motors yielded a large quantity of data. The total infrared radiance was presented as a function of position along the plume axis, from the nozzle exit plane for a maximum distance of 18 feet. The ultraviolet radiance was recorded simultaneously.

Fifteen spectral scans per second were recorded for the 1.0 to 5.5 micron region. Visible spectra were recorded using a cinespectrograph, and the visible pattern of the plume was recorded with a pulse camera. An approximate contour map of the plume in the 1.0 to 2.7 micron region was derived from a lateral scanning radiometer. A preliminary survey of audiomodulation in the plume radiance of some of the motors was made with a simple lead sulfide radiometer.

These observations were made for the several propellant combinations, at sea level and at simulated altitudes of approximately 50,000 and 100,000 feet.

On examination of the data it was readily apparent that the mass of detail would be of little practical value to any potential user. Accordingly the investigators have taken the liberty of examining the data for general implications, and attempting a judicious selection of representative runs. The discussions which follow are thus neither a composite nor any sort of average. Each run which has been selected as representative is reported in its entirety, and a narrative accounting of the radiance characteristics is presented. General observations and inferences are presented in the same discussions.

3.1 PLUME RADIATION DATA FOR GASOLINE-OXYGEN

The propellant system investigated in greatest detail was gasoline-oxygen. Preliminary measurements of radiation data were made during the motor and traversing technique development trials. Subsequently a total of twelve runs were made with gasoline-oxygen--six at sea level, three at approximately 50,000 feet and three at approximately 100,000 feet. One run has been selected for each of these altitudes as being representative of the data obtained.

The experimental data for gasoline-oxygen at sea level are shown in the several parts of Figure 14. The brightness distribution along the axis of the plume is shown in the total radiance curve in the 0.6 to 5.5 micron region. The successive shock-compressed regions are clearly defined in this curve, with the maximum level of radiation being attained from the fourth to sixth shock diamonds. A similar position of the maximum in ultraviolet radiance is shown in this curve. Comparison of the plume radiance contour curves with the photograph shows that the visible radiation falls below photographic sensitivity at the position where the infrared radiance is approximately 25 percent of its maximum value. The total radiance curve shows appreciable infrared radiance at a distance twice the photographic length of the plume.

The spectral radiance curves provide some insight into the origin of these various facts, which is substantiated by consideration of the data from the subsequent runs. In the region immediately behind the nozzle. the radiance shows a strong continuum, as a result of scattered radiation from the free carbon particles in the plume. This scattered radiation is probably also

augmented by the continuum radiation of high temperature air (Reference 4), which occurs as a result of the entrainment of air in the exhaust gases. In the region of maximum plume radiance the contribution of the continuum radiation is still significant, but the band contributions of the molecular species--CC, CO_2 and H_2O--are becoming more evident. At greater distances from the nozzle the continuum radiation contribution disappears and the spectrum is one characteristic of the molecular radiators only.

The microdensitometer traces of the visible spectra show few distinctive features. NaD-line appears consistently in our spectra. Bands in the 5,000 angstrom region characteristic of hydrocarbon flames were also found consis ently. The resolution of the cine-spectrograph was found to be lower in the test environment than in the laboratory evaluation, probably due to the high sensitivity of the grating device to mechanical vibrations.

The data for gasoline-oxygen at 52,000 feet, shown in Figure 15, permit the extension of these observations into regions in which the mixing with the air is less significant in its effects. The total radiance curve shows the gradual buildup with the successive shock compressions. The radiance level in this region is approximately 30 percent of the maximum region at sea level. The total radiating area is somewhat greater than at sea level, so that the integrated plume radiant intensity is probably more than 50 percent of the sea level value. The buildup in infrared radiance beyond 10 feet from the nozzle in the measurement at 52,000 foot altitude may be spurious, arising from faulty control of flow in the fuel and oxidizer supply system. The ultraviolet radiance also reaches a maximum value at the same region in the

shock compression pattern. However, it is to be noted that the maximum value attained is only 8 percent of that in the sea level run. Comparison of the infrared radiance contours with the plume photograph again shows that the visible radiation boundary corresponds to between 25 and 50 percent of the maximum infrared radiance value. Thus at least 25 percent of the infrared contribution comes from zones outside the region shown by the visible photograph of the plume.

Infrared spectrometer traces less than 2 feet from the nozzle were generally indistinguishable from the background noise. The region of maximum infrared radiance again shows the continuum contribution, presumably due to both carbon and contribution from the heated air. Beyond the region of maximum radiance, for example at 8.4 feet from the nozzle, the dominant contributions of the molecular species are again evident.

The measurements at 97,000 feet, shown in Figure 16, probably represent the ultimate capability of this facility for motors of 150 pound thrust level. The total radiance curve has apparently leveled off to its maximum value only 2 feet before the available traverse distance is reached. The lateral scanning radiometer indicates 25 percent of maximum radiance values for a width of some 4 feet at this position; some impingement of the plume gases on the tank walls is likely to occur since the duct is only 6 feet in diameter. The maximum ultraviolet radiance has dropped to less than one percent of its sea level value, since it was not detectable with the present instrument at the gain levels being employed in the experiment.

Continuum radiation is not evident in any of the spectrometer traces. The level of spectral intensity in the 2.7 and 4.3 micron regions, however, does

not differ too greatly from the levels observed in the region of maximum radiance at sea level and at intermediate altitude. The plume radiance in this altitude regime is probably strongly dependent on gaseous afterburning reactions, so that the major contributors to the spectral radiation consist of the H_2O, CO_2 and CO.

TOTAL RADIANCE .6 μ TO 5.5 μ

ULTRAVIOLET RADIOMETER .26 μ TO .39 μ

RELATIVE RADIANCE CONTOURS   PbS RESPONSE
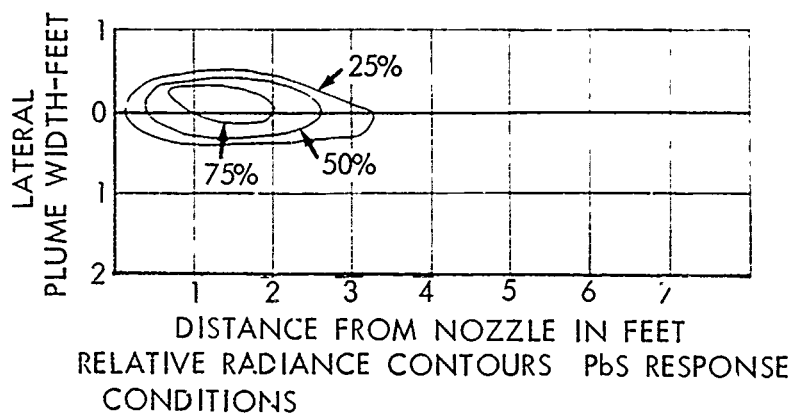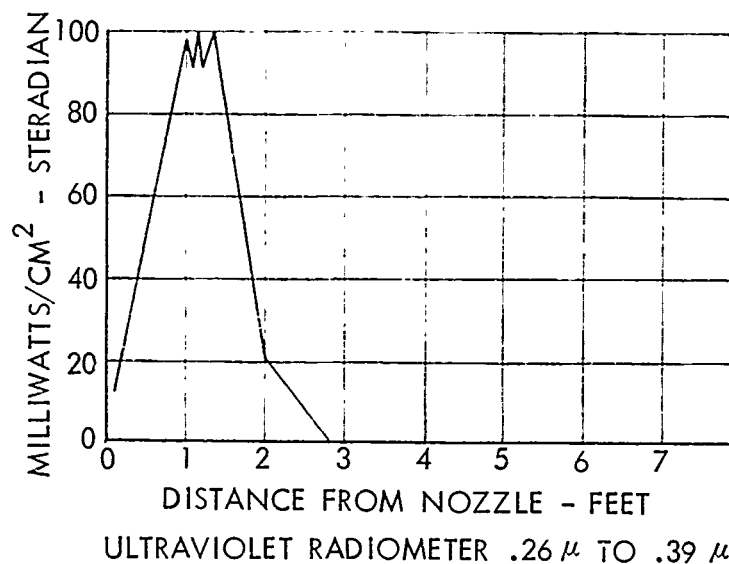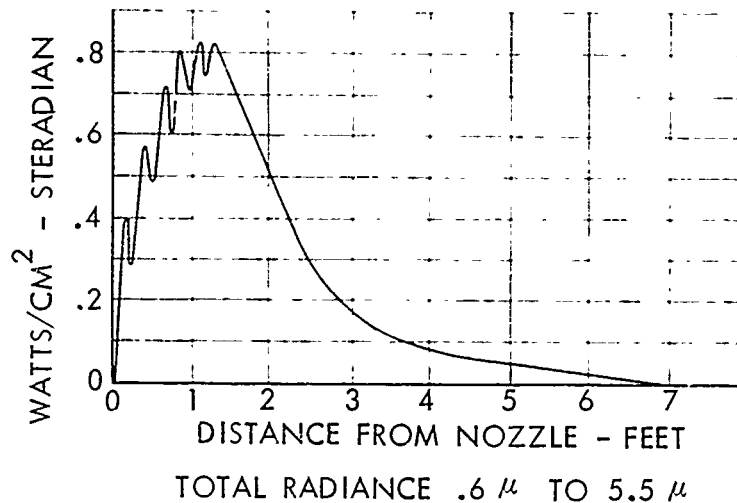
CONDITIONS

PROPELLANT   GASOLINE - OXYGEN
ALTITUDE   SEA LEVEL
E.R.   1.85

Figure 14a

PLUME RADIANCE
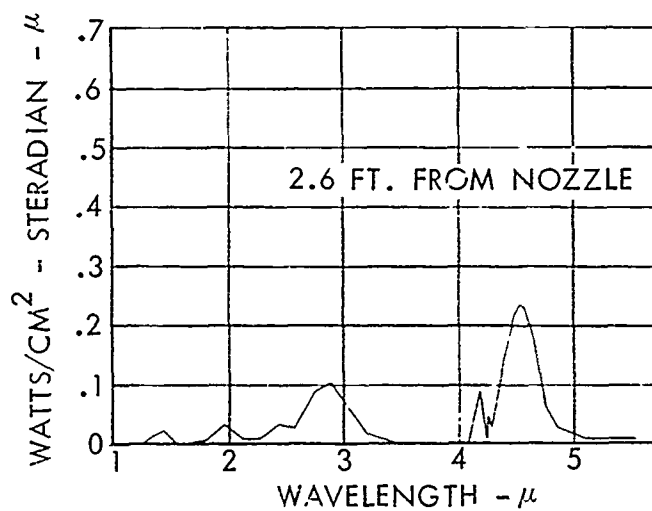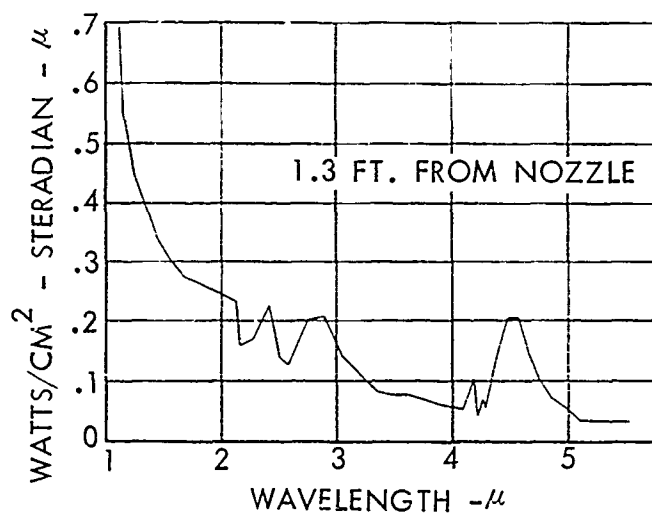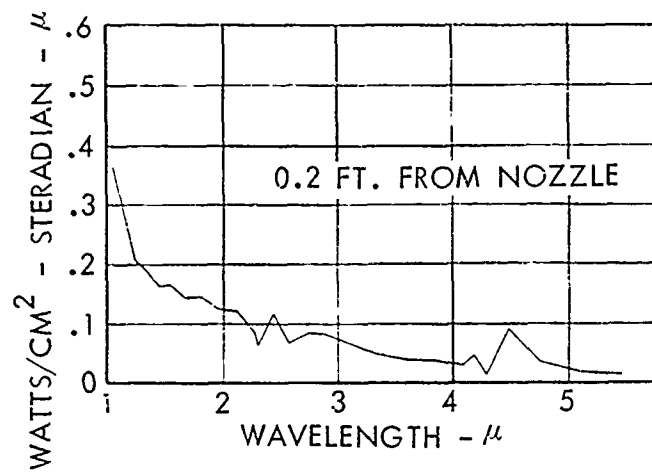
CONDITIONS

PROPELLANT	GASOLINE – OXYGEN
ALTITUDE	SEA LEVEL
E.R.	1.85

Figure 14b

PLUME SPECTRAL RADIANCE

WAVELENGTH - μ
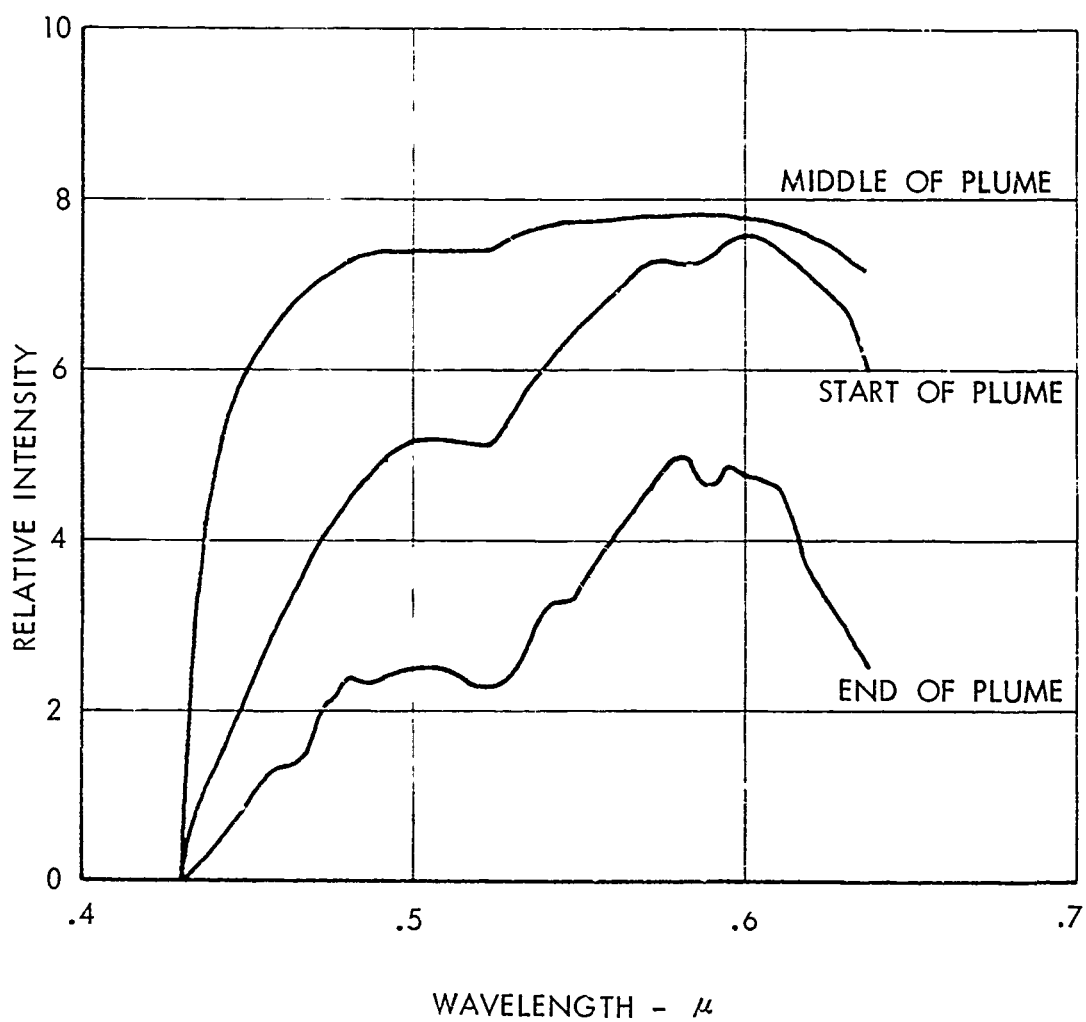
CONDITIONS

PROPELLANT	GASOLINE – OXYGEN
ALTITUDE	SEA LEVEL
E.R.	1.85

Figure 14c

VISIBLE PLUME SPECTRA

FEET
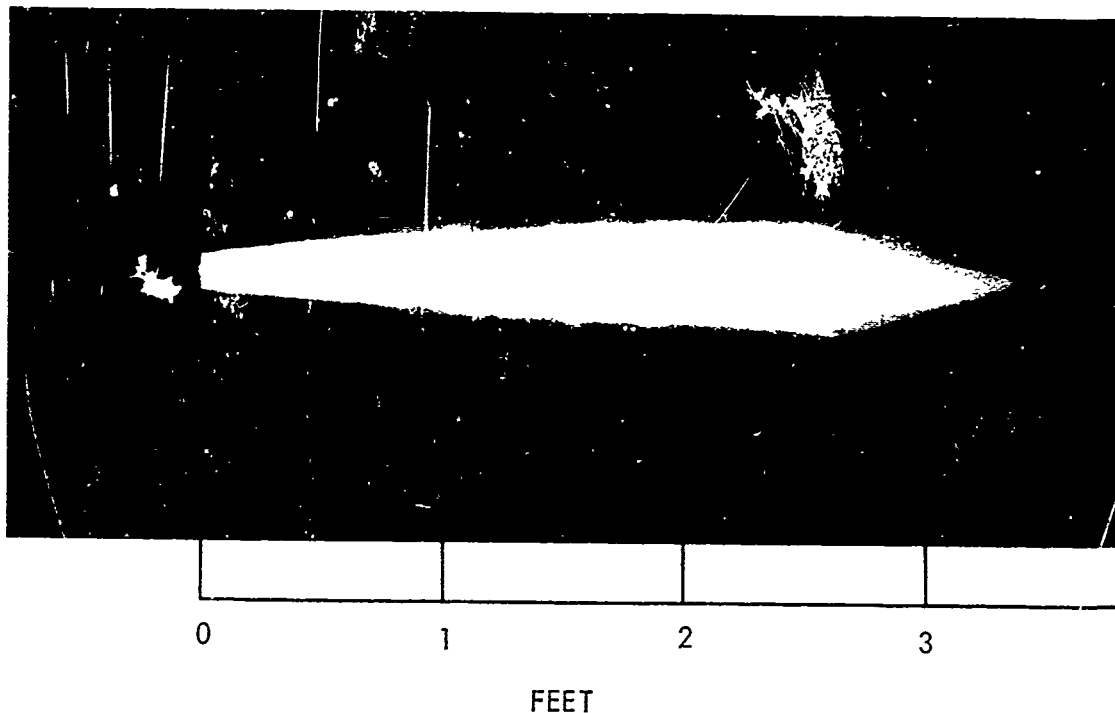
CONDITIONS

PROPELLANT	GASOLINE-OXYGEN
ALTITUDE	SEA LEVEL
E. R.	1.85

Figure 14d

VISIBLE PLUME RADIATION

WATTS/CM^2 - STERADIAN

DISTANCE FROM NOZZLE - FEET

TOTAL RADIANCE .6 μ TO 5.5 μ

1.78 MILLIWATTS/CM^2 - STERADIAN

DISTANCE FROM NOZZLE - FEET

ULTRAVIOLET RADIANCE .26 μ TO .39 μ

LATERAL PLUME WIDTH

25%

75%

50%

DISTANCE FROM NOZZLE - FEET

RELATIVE RADIANCE CONTOURS PbS RESPONSE
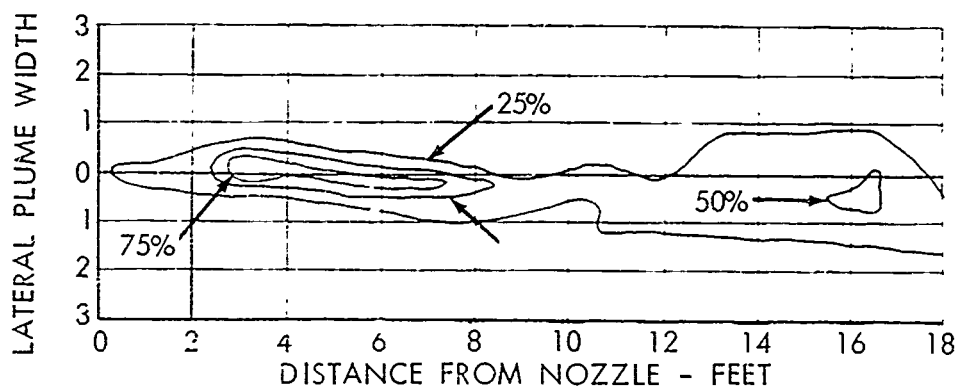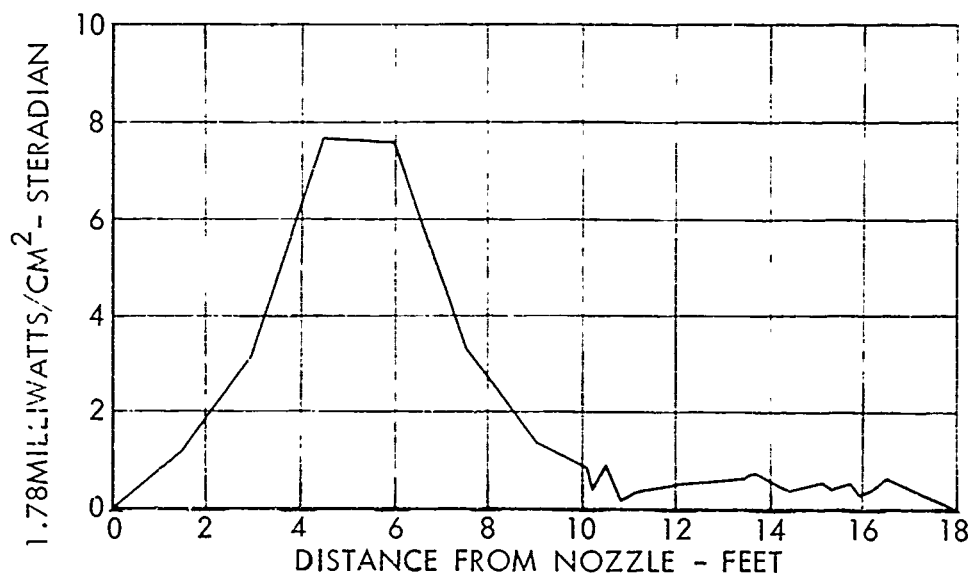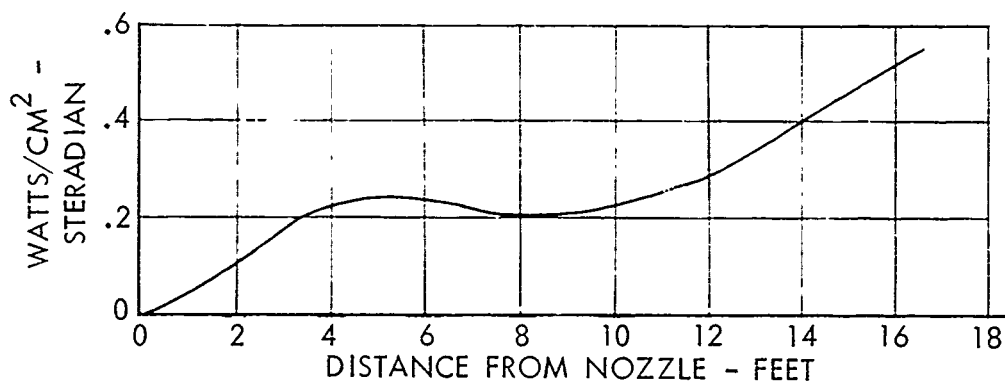
CONDITIONS

PROPELLANT	GASOLINE - OXYGEN
ALTITUDE	52,000 FT.
E.R.	1.85

Figure 15a

PLUME RADIANCE
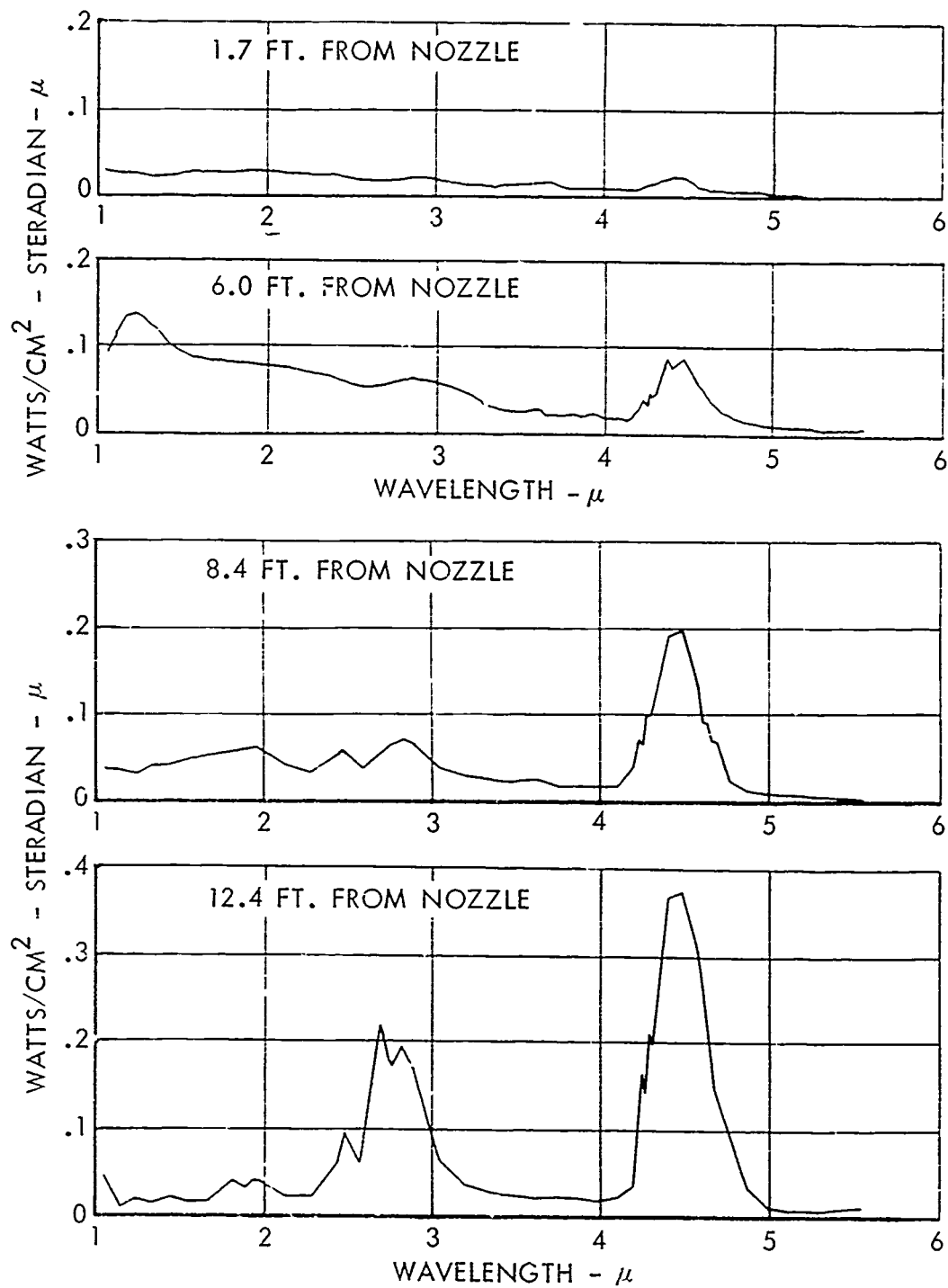
CONDITIONS

PROPELLANT	GASOLINE - OXYGEN
ALTITUDE	52,000 FT.
E.R.	1.78

Figure 15b

PLUME SPECTRAL RADIANCE
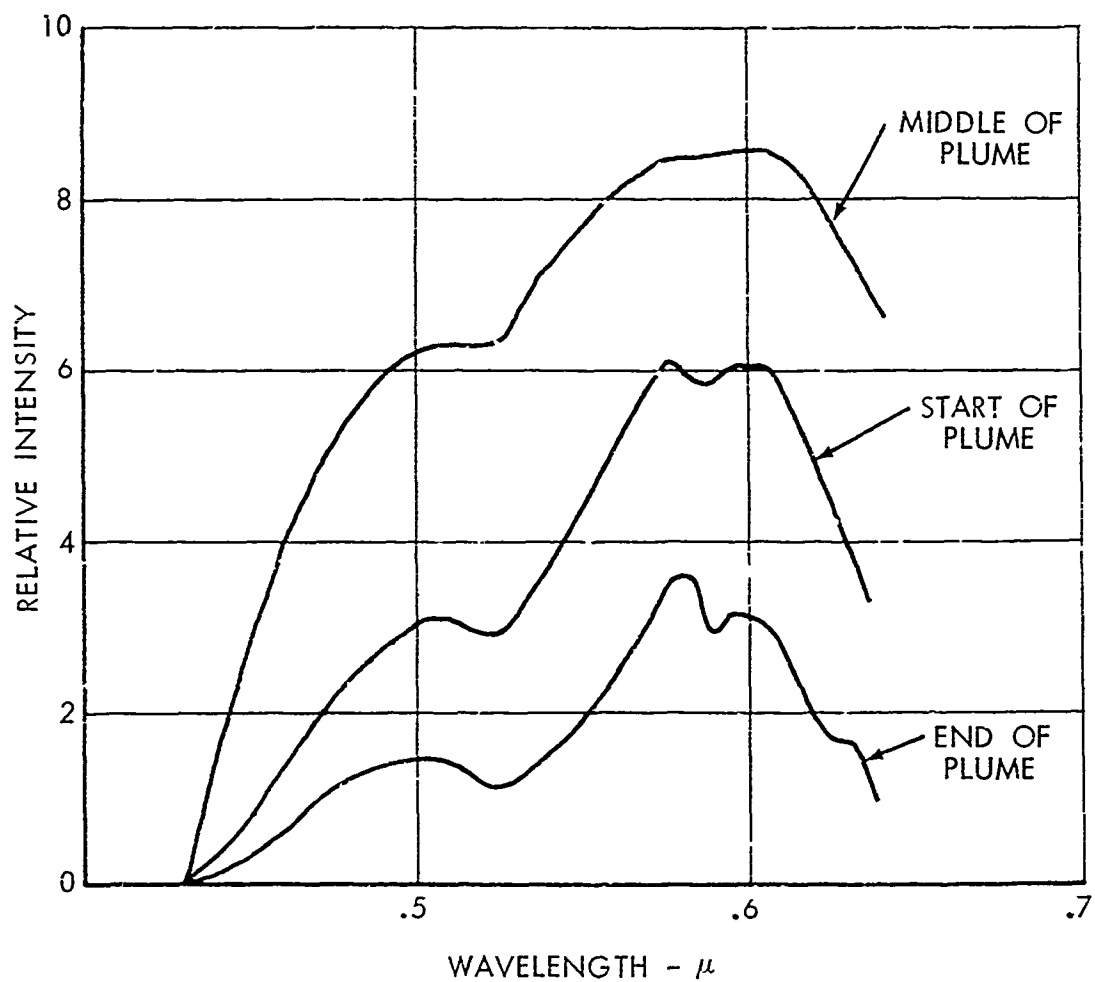
CONDITIONS

PROPELLANT	GASOLINE – OXYGEN
ALTITUDE	52,000 FT.
E.R.	1.78

Figure 15c
VISIBLE PLUME SPECTRA

0 1 2 3 4

NOZZLE   FEET

4 5 6 7 8
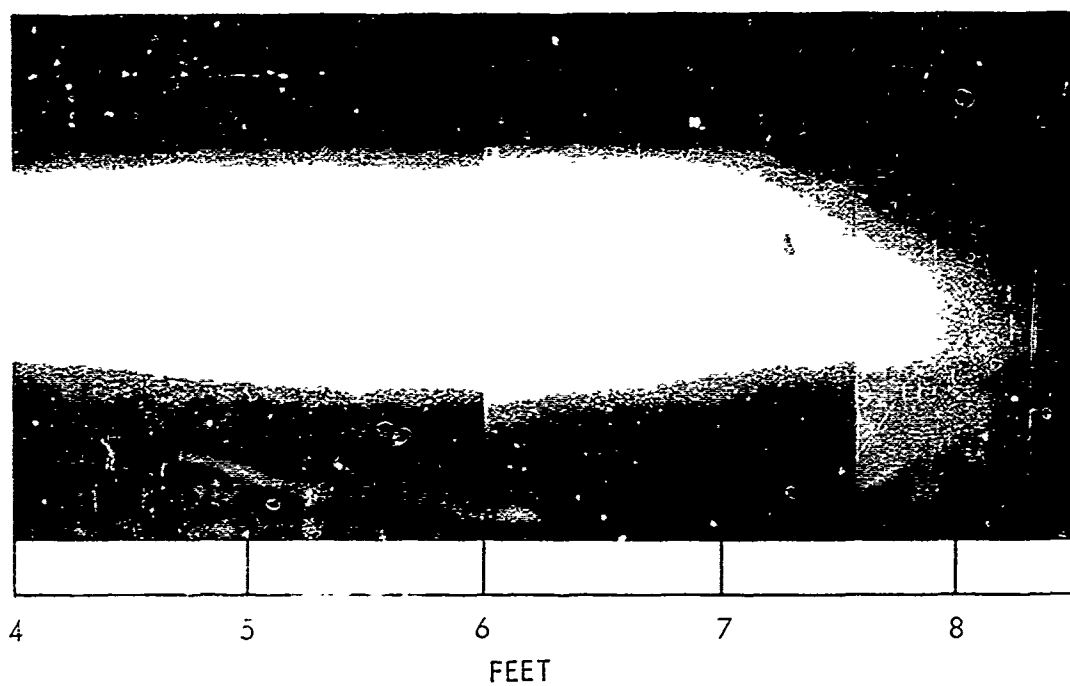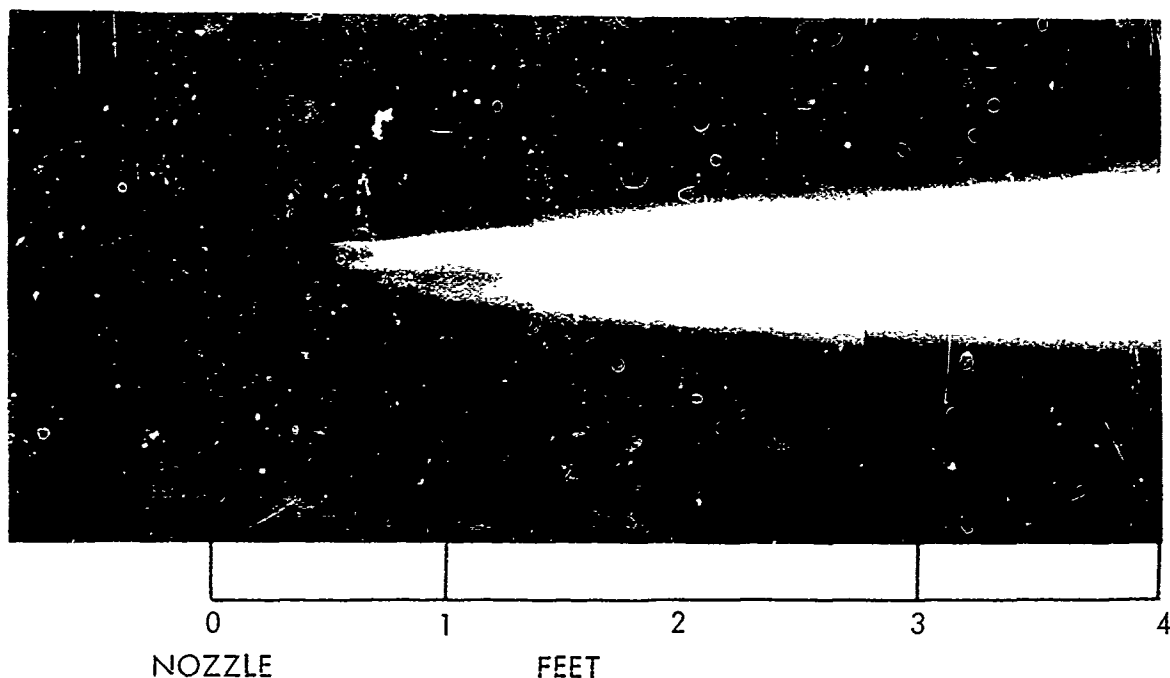
FEET

CONDITIONS

PROPELLANT	GASOLINE–OXYGEN
ALTITUDE	52,000 FEET
E. R.	1.78

Figure 15d
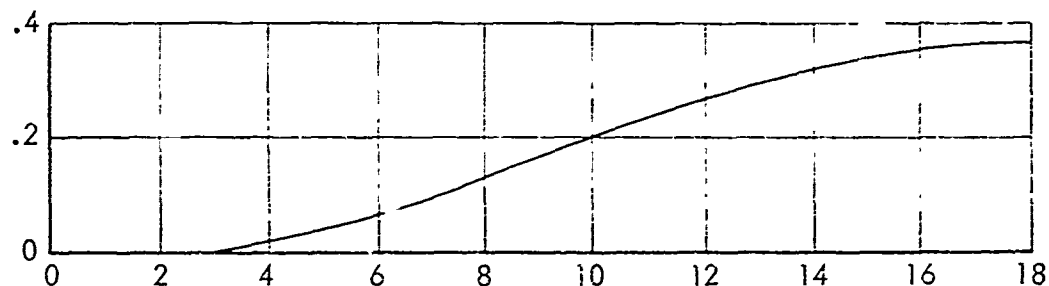
PLUME RADIATION

43

WATTS/CM^2 - STERADIAN

.4

.2

0

0   2   4   6   8   10   12   14   16   18

DISTANCE FROM NOZZLE - FEET

TOTAL RADIANCE .6 μ TO 5.5 μ

LATERAL PLUME WIDTH - FEET

2

0

2

50%   25%

75%

0   2   4   6   8   10   12   14   16   18
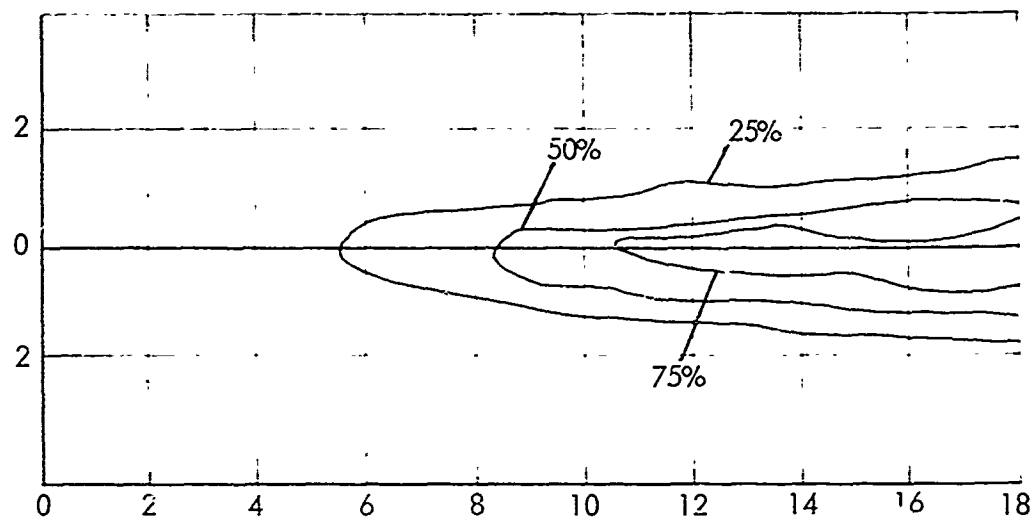
DISTANCE FROM NOZZLE - FEET

RELATIVE RADIANCE CONTOURS PbS RESPONSE

CONDITIONS

PROPELLANT   GASOLINE - OXYGEN
ALTITUDE   97,000 FEET
E.R.   1.59

Figure 16a

PLUME RADIANCE
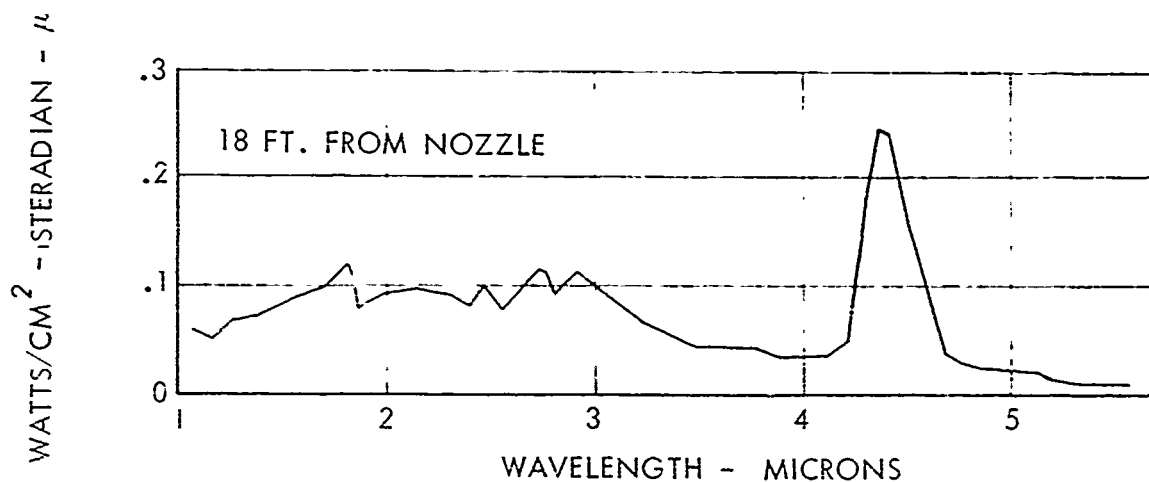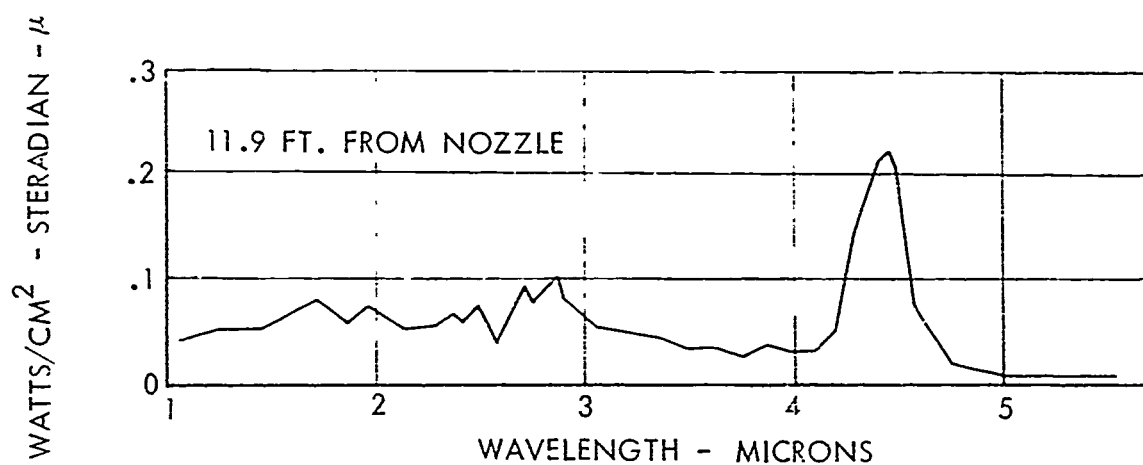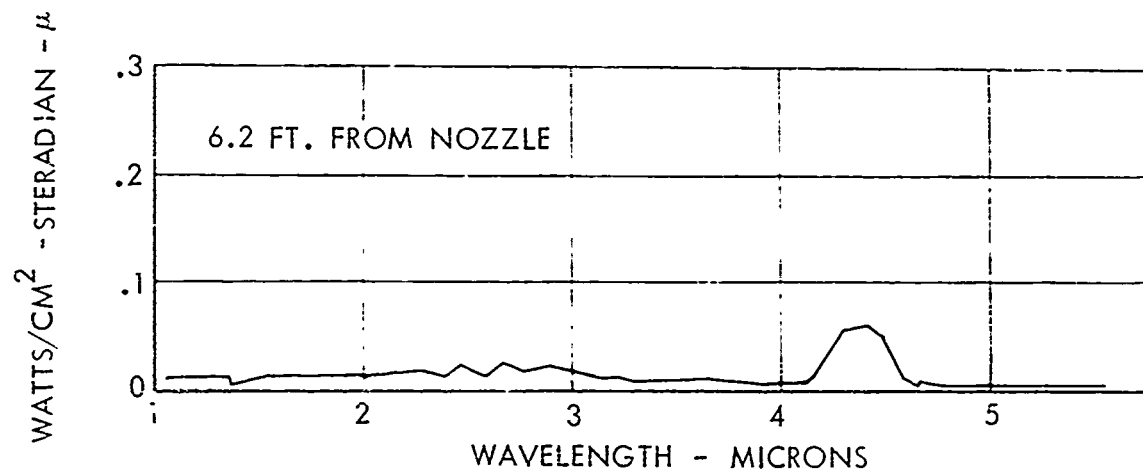
Figure 1ob

PLUME SPECTRAL RADIANCE
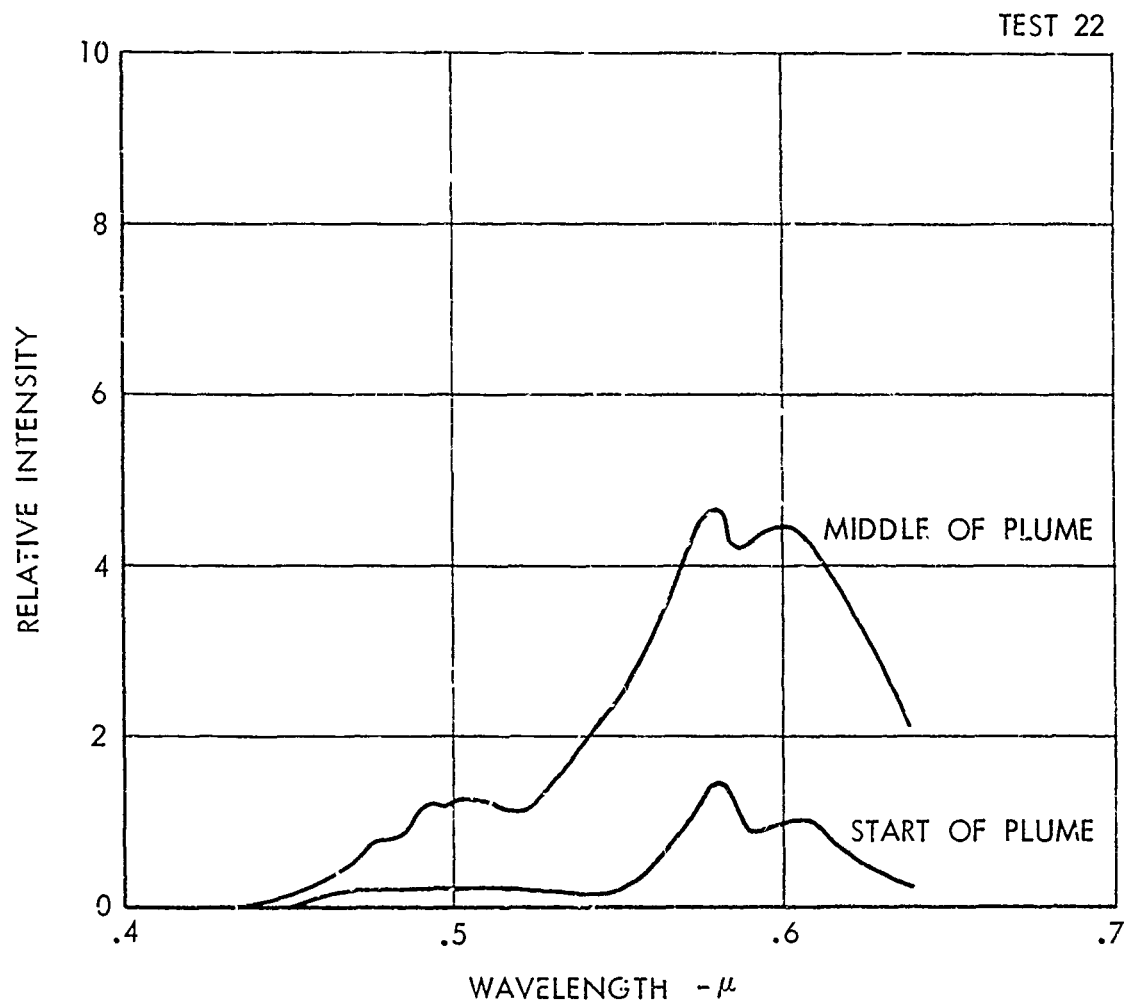
CONDITIONS

PROPELLANT	GASOLINE - OXYGEN
ALTITUDE	97,000 FEET
E.R.	1.59

Figure 16c

VISIBLE PLUME SPECTRA

3.2   PLUME RADIATION DATA FOR RP 1-OXYGEN AND JP 4-OXYGEN

Propellant systems utilizing kerosene-oxygen rather than gasoline-oxygen
were investigated through the use of JP-4 and RP-1 as fuels. The plume
radiation data for selected representative runs are shown in Figures 17
through 21.

The sea level data for RP 1-oxygen shown in Figure 17 are hardly distinguish-
able from the sea level data for gasoline-oxygen. The data for JP 4-oxygen
in Figure 20 are likewise very similar to those for gasoline-oxygen. The
slightly lower maximum value in total radiance and ultraviolet radiance for
the kerosene-oxygen systems is attributed to the fact that the equivalence
ratio is slightly lower. With the leaner mixture less contribution occurs
from afterburning in the plume.

The plume radiation data for the altitude runs with kerosene-oxygen systems
are similarly indistinguishable from those with gasoline-oxygen. The some-
what lower values of total radiance and ultraviolet radiance shown for RP 1-
oxygen at 52,000 feet are not explained, in that the data at 84,000 feet
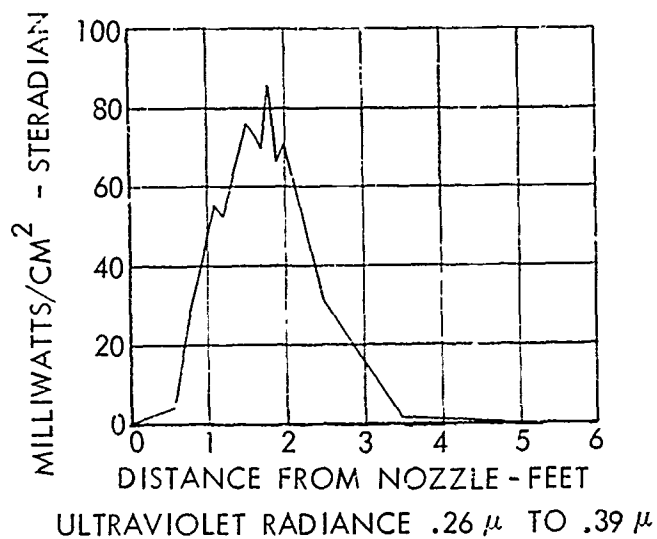again coincide with those for the other hydrocarbon-oxygen systems.

From these data for the several hydrocarbon-oxygen systems it appears that
the degree of saturation in the hydrocarbon liquid fuel does not signifi-
cantly affect the plume radiance properties.

The noteworthy features observed in all of the high altitude runs with
hydrocarbon-oxygen systems were the position of the maximum in both ultra-
violet and total radiance, and the shift in spectral character as the
observations proceed from near the nozzle to positions well removed from

the nozzle. The maximum radiance levels were found to be attained at a distance some °C to 100 nozzle diameters removed from the exit plane of the rocket for altitudes of 80,000 to 97,000 feet. These levels of maximum radiance must be many times greater than the Mach cone radiance, as evidenced by the fact that our instrumentation at no time recorded radiation of appreciable value in the Mach cone region.

The transition in spectral character downstream along the plume axis consists of a shift from spectra in which there is appreciable continuum radiation to spectra in which the molecular radiators dominate. The continuum radiation occurs mainly in the region in which the radiation values are building up, six to ten feet from the nozzle, beyond which the shift to molecular band radiation occurs. For altitudes near 100,000 feet it can be estimated that narrow band radiometers accepting radiation only near 2.7 or 4.3 microns should receive at least five times as much radiation from the zone 18 feet from the nozzle as from points at some 9 feet from the nozzle.

In the highest altitude runs with JP 4-oxygen and RP-1-oxygen appropriate gain changes were made for the ultraviolet radiometer so that radiance values were recorded. The maximum radiance levels in the ultraviolet were found to be 50- to 100-fold lower for the 80,000 to 100,000 foot altitude region than for the sea level measurements. The magnitude of this reduction is considered to indicate that the ultraviolet plume radiance originates nearly entirely in chemiluminescent processes accompanying the afterburning reactions. Long-range measurements of ultraviolet plume radiant intensity should be interpreted only with great caution, since in all likelihood nearly the entire quantity of ultraviolet radiation will originate at positions well removed from the nozzle of the rocket.

TOTAL RADIANCE   1.2 μ TO 5.5 μ

ULTRAVIOLET RADIANCE .26 μ TO .39 μ

RELATIVE RADIANCE CONTOURS   PoS RESPONSE

CONDITIONS

PROPELLANT	RP-1 -- OXYGEN
ALTITUDE	SEA LEVEL
E.R.	1.6
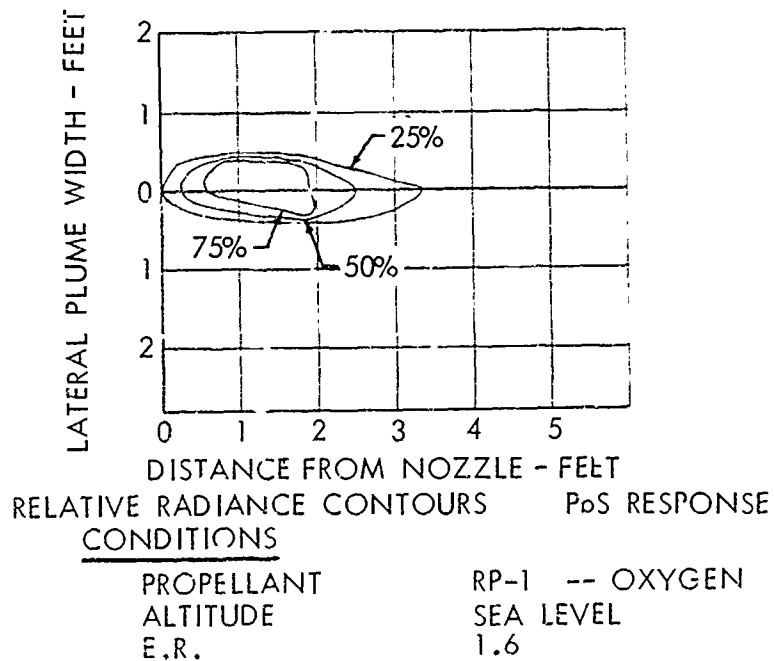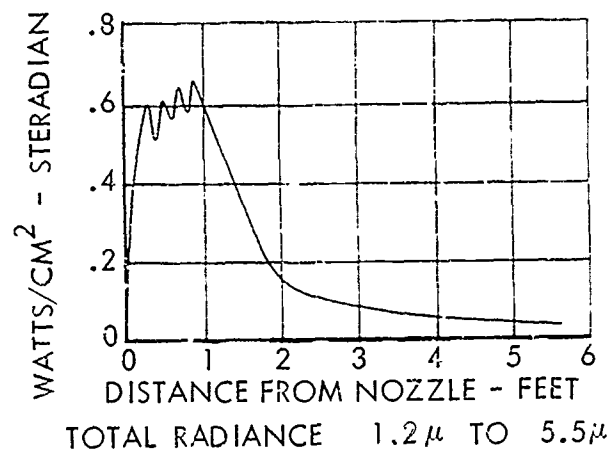
Figure 17a

PLUME RADIANCE

49
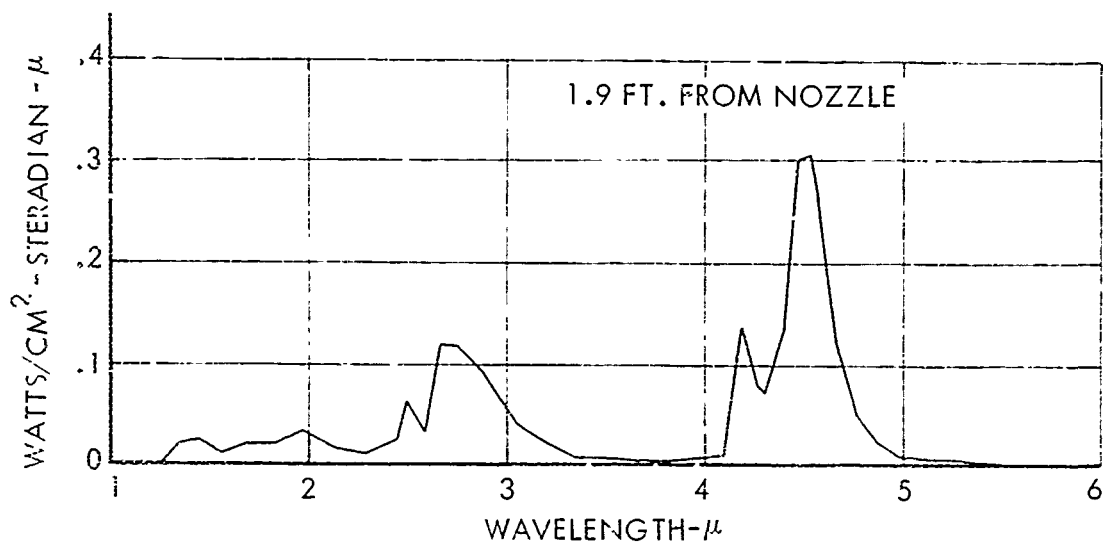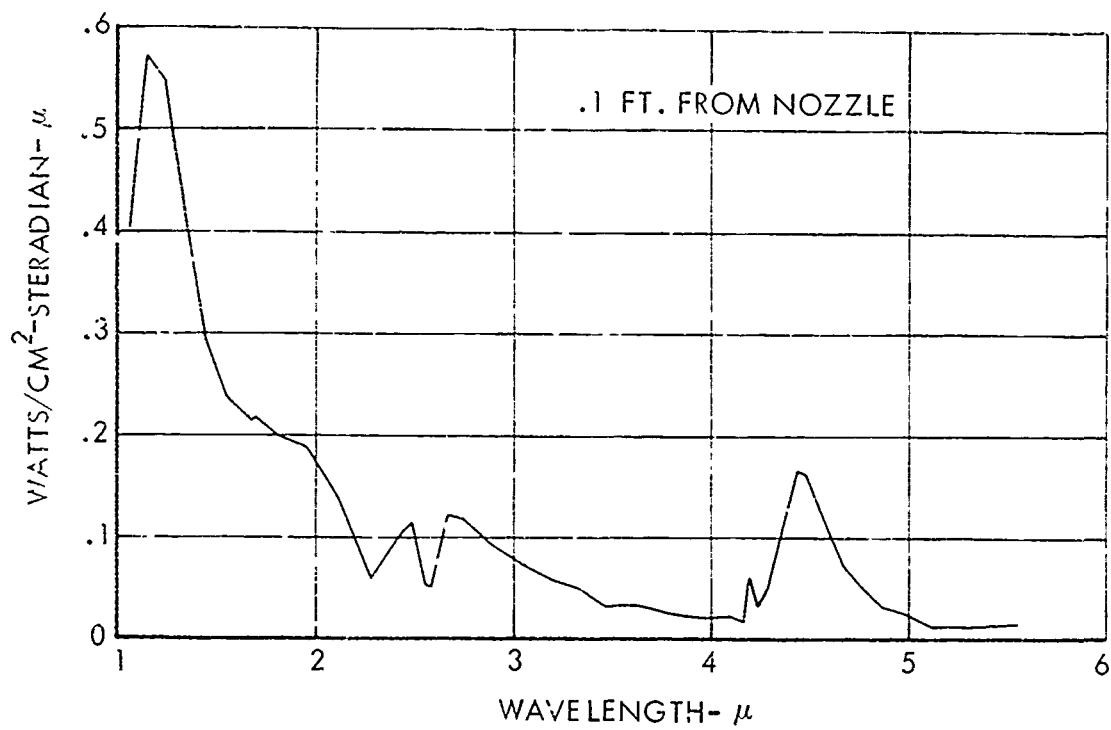
Figure 17b

PLUME SPECTRAL RADIANCE
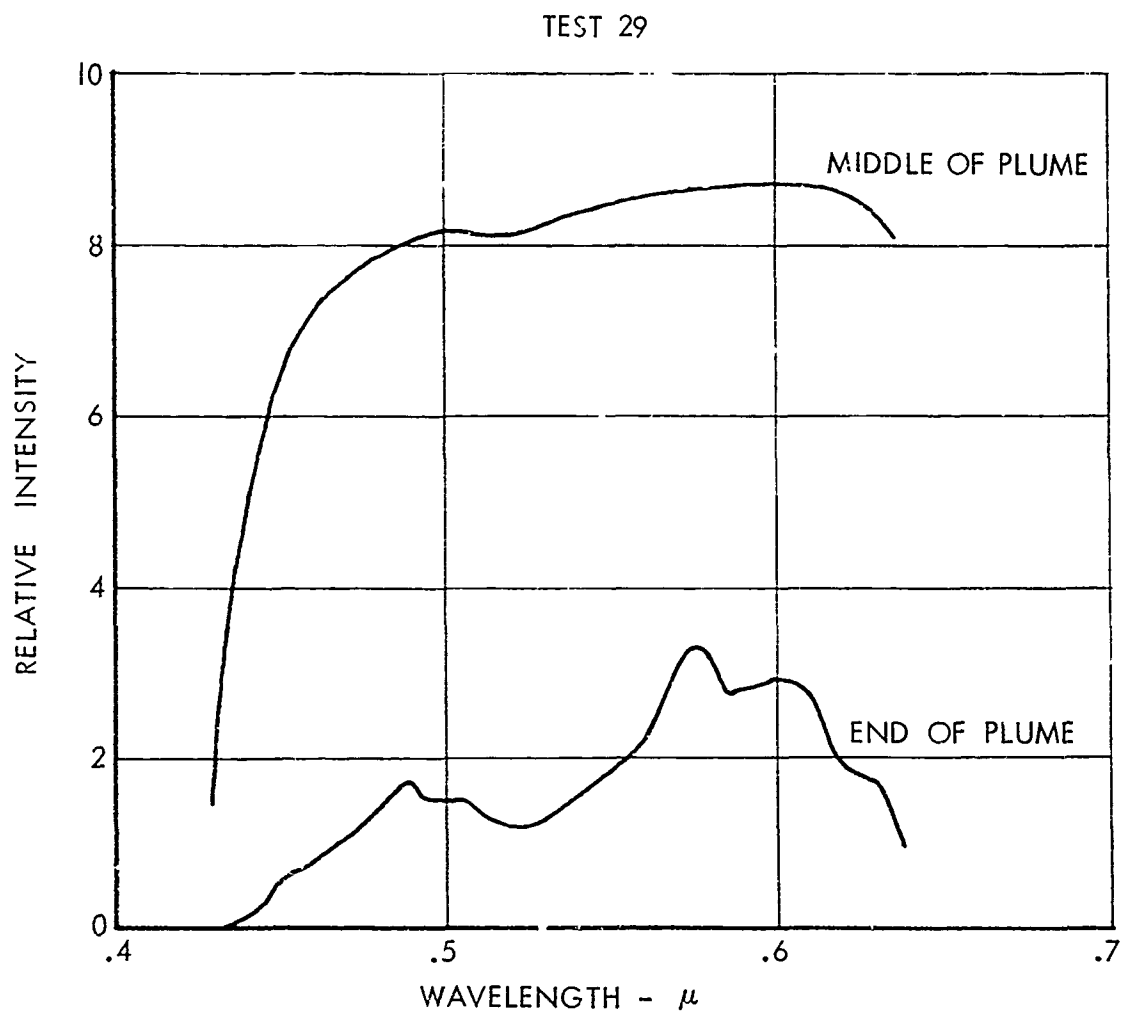
CONDITIONS

PROPELLANT   RP-1 -- OXYGEN
ALTITUDE   SEA LEVEL
E.R.   1.6

TEST 29

VISIBLE PLUME SPECTRA

CONDITIONS

PROPELLANT	RP-1 - OXYGEN
ALTITUDE	SEA LEVEL
E.R.	1.6

Figure 17c

VISIBLE PLUME SPECTRA
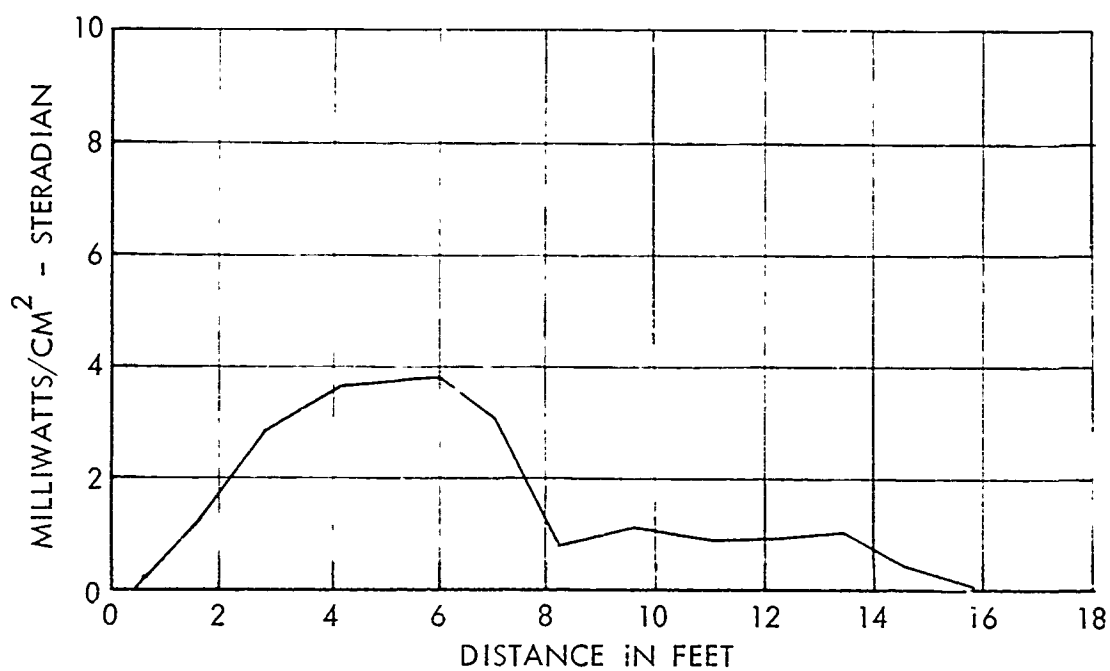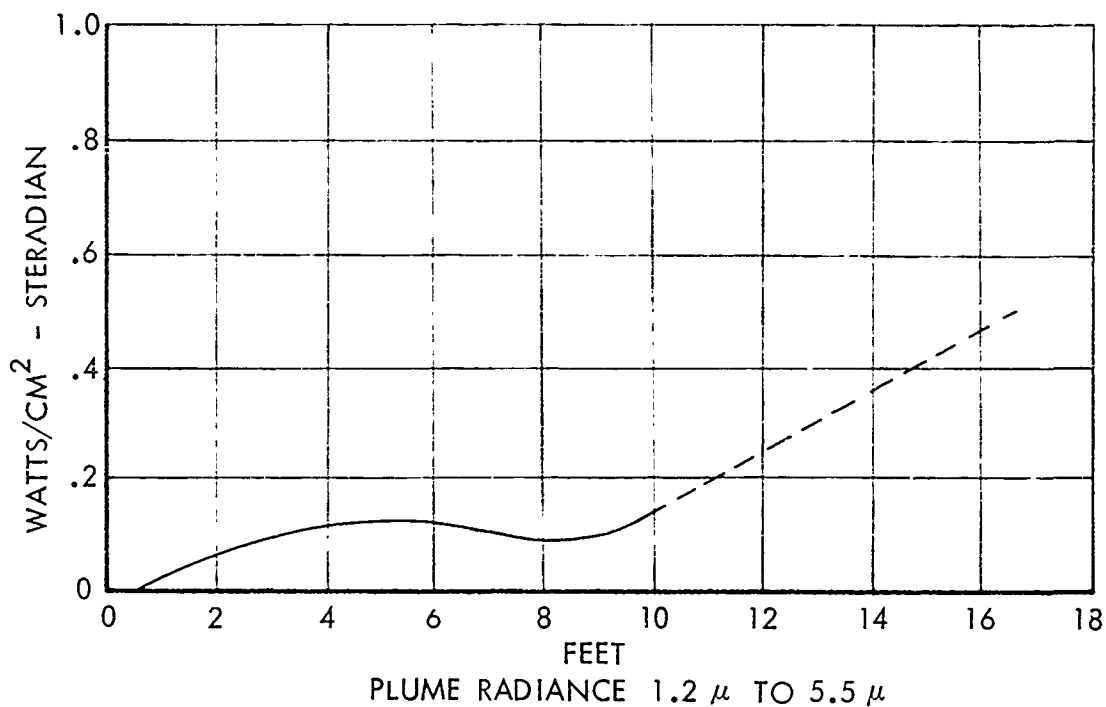
PLUME RADIANCE 1.2 μ TO 5.5 μ

ULTRAVIOLET RADIANCE .26 μ TO .39 μ
CONDITIONS

PROPELLANT	RP-l - OXYGEN
ALTITUDE	53,000 FT.
E.R.	1.70

Figure 18a

PLUME RADIANCE

52
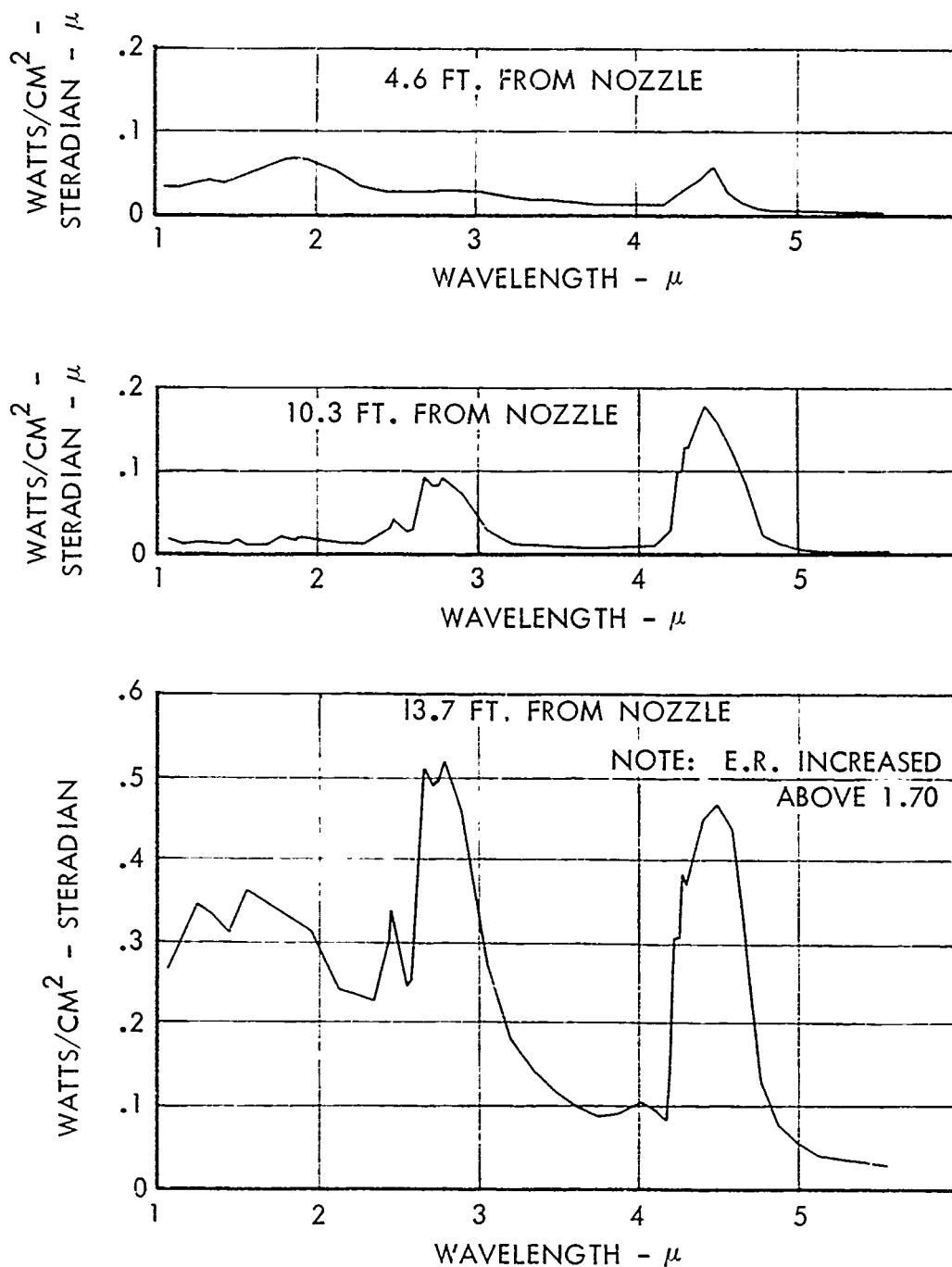
Figure 18b

PLUME SPECTRAL RADIANCE
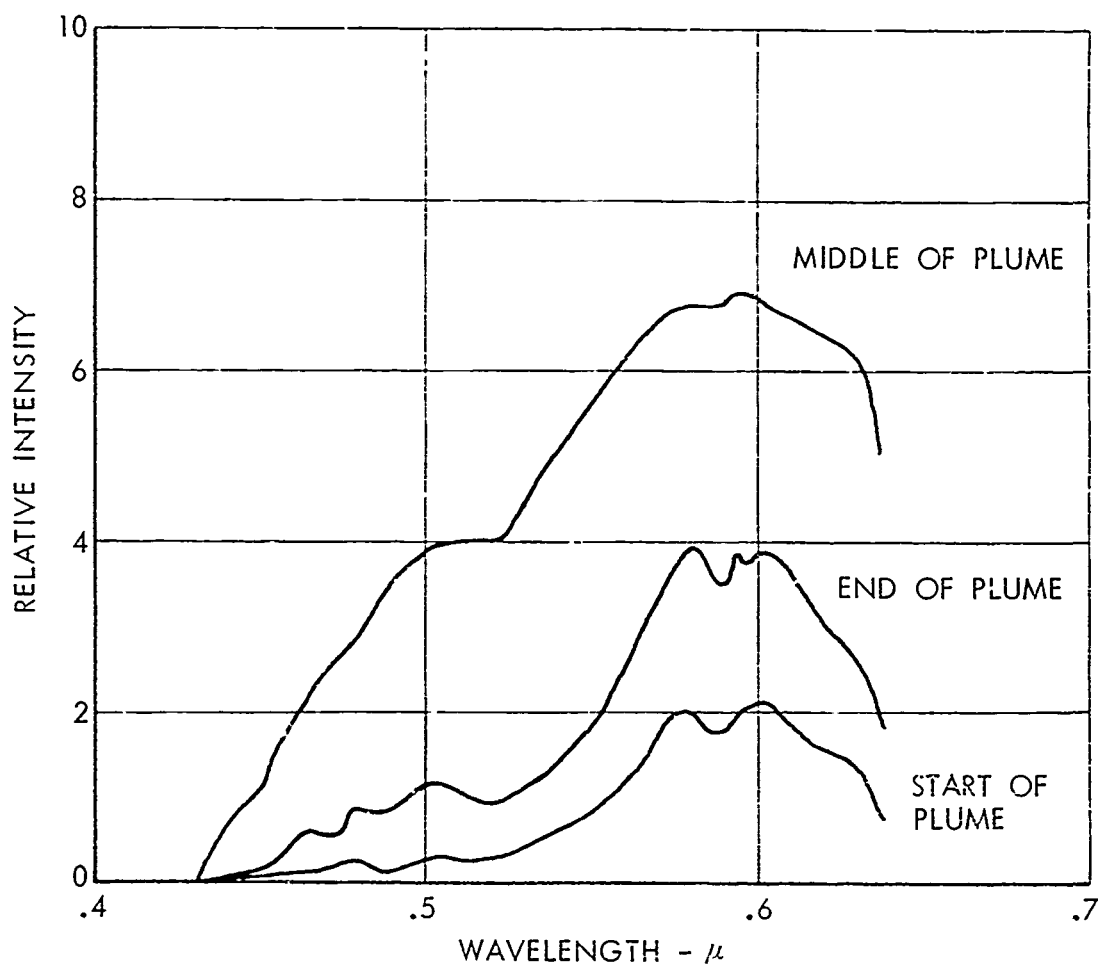
CONDITIONS

PROPELLANT	RP-1 - OXYGEN
ALTITUDE	53,000 FT.
E.R.	1.70

Figure 18c

VISIBLE PLUME SPECTRA

NOZZLE   FEET
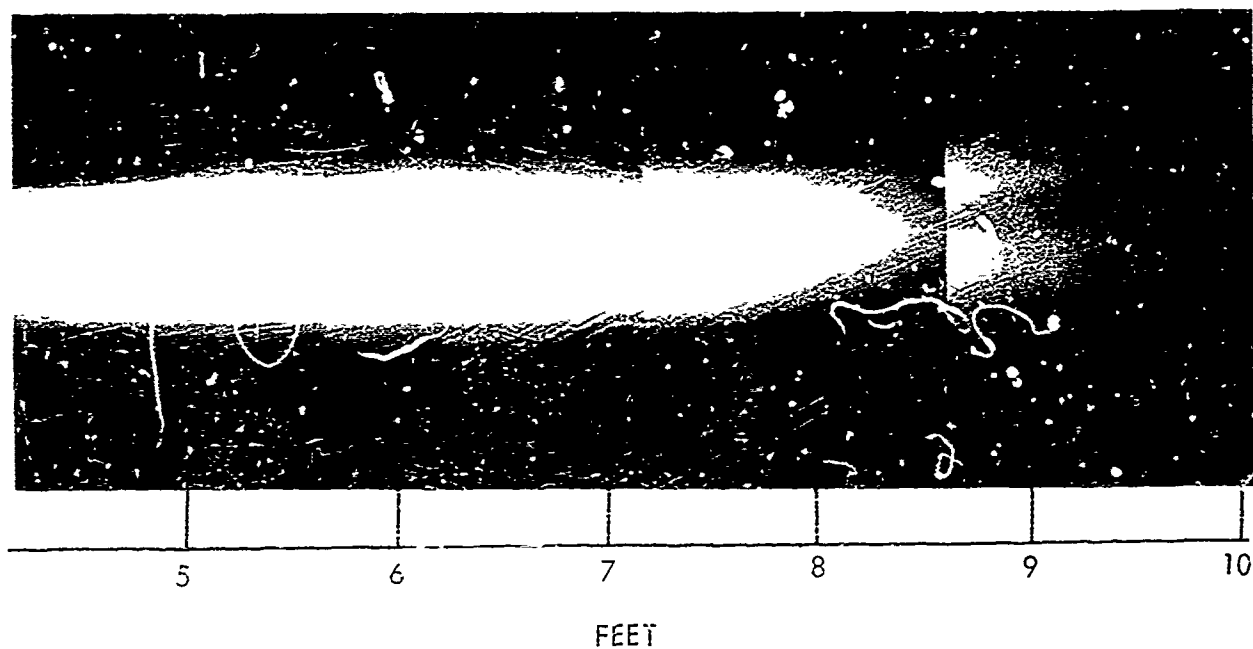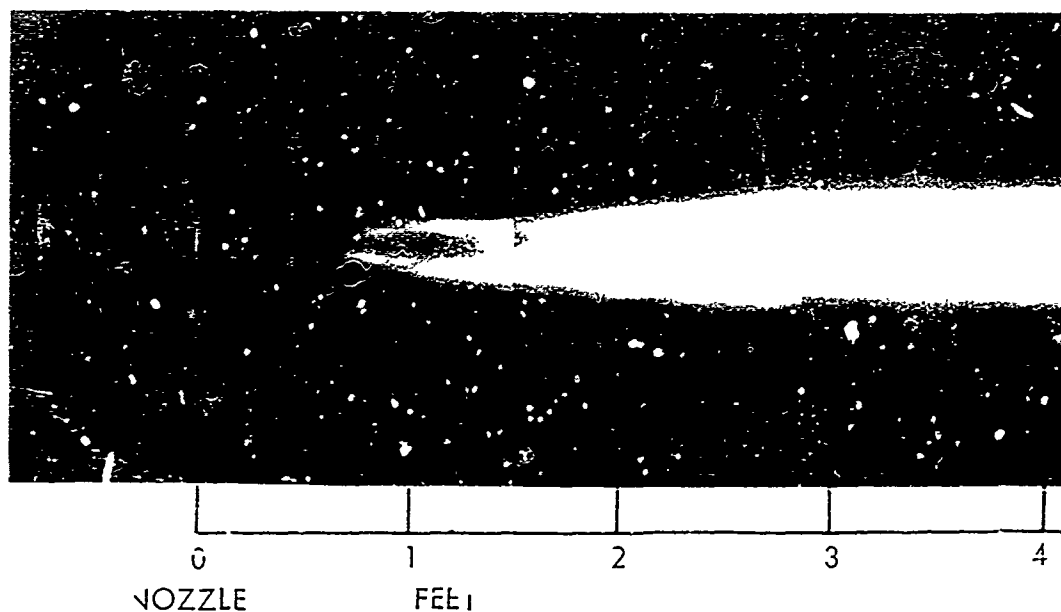
FEET

CONDITIONS

PROPELLANT   RP-1 - OXYGEN
ALTITUDE   53,000 FEET
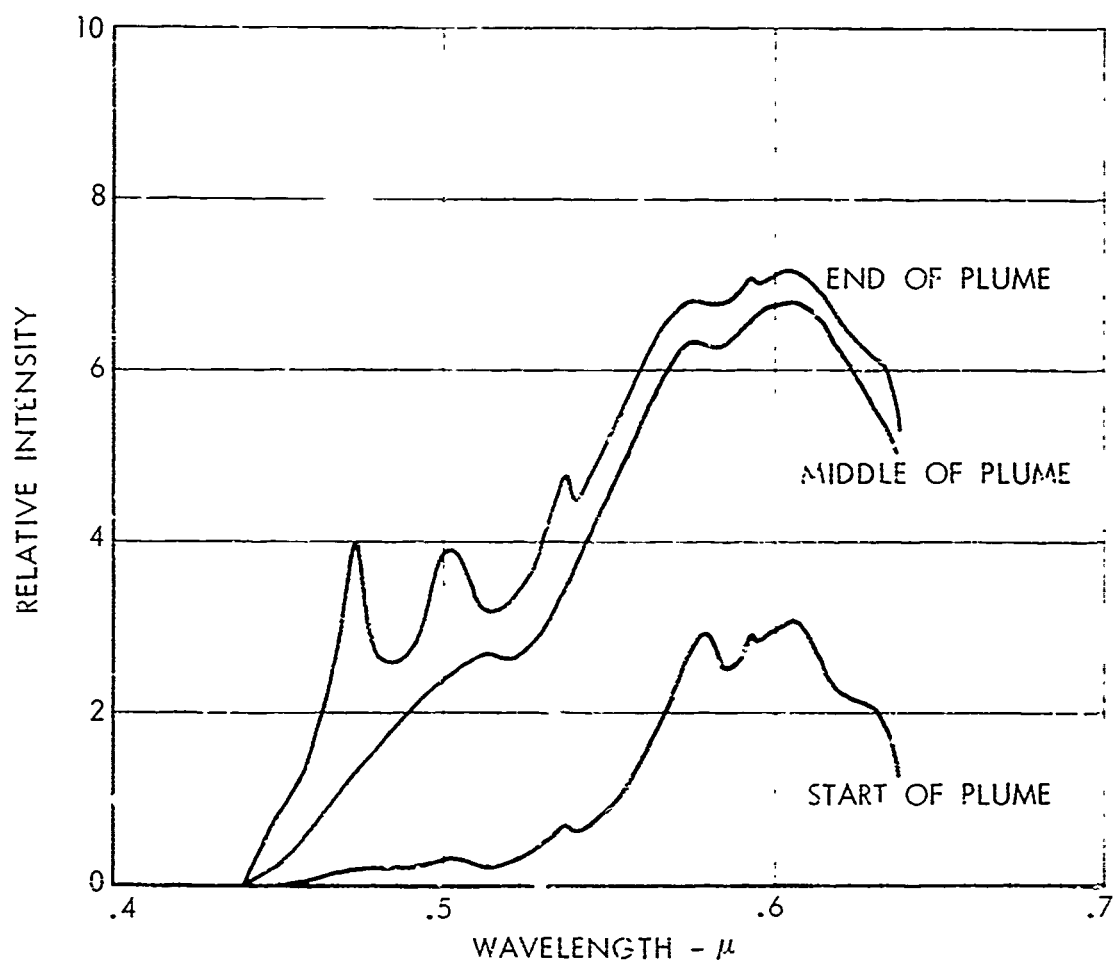E.R.   1.70

Figure 18d

VISIBLE PLUME RADIATION
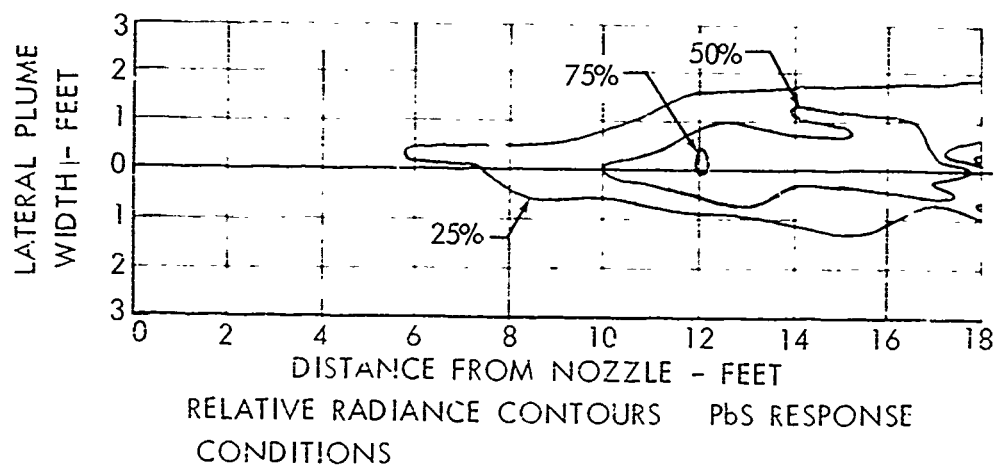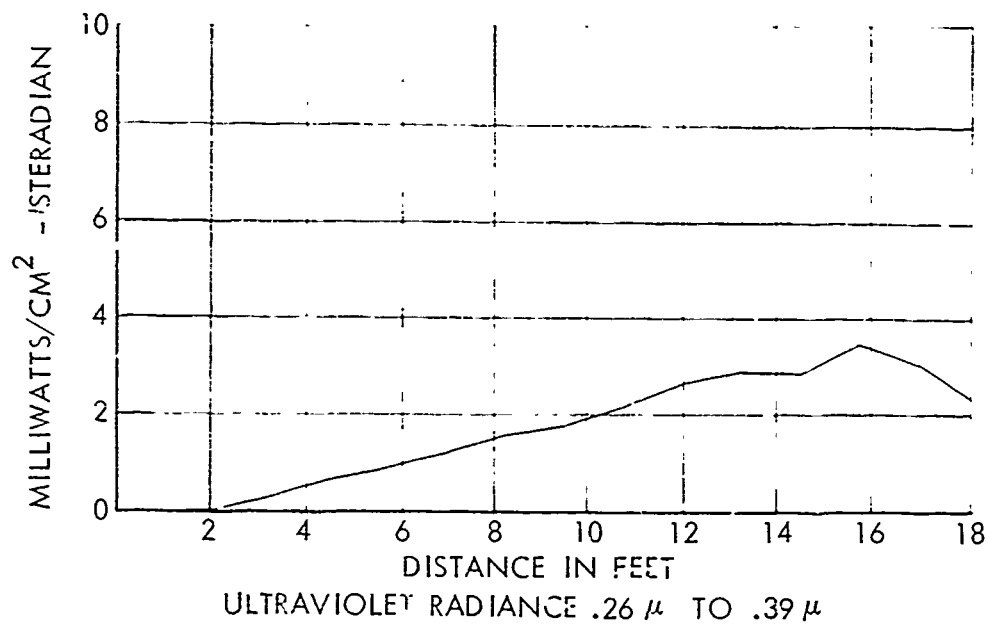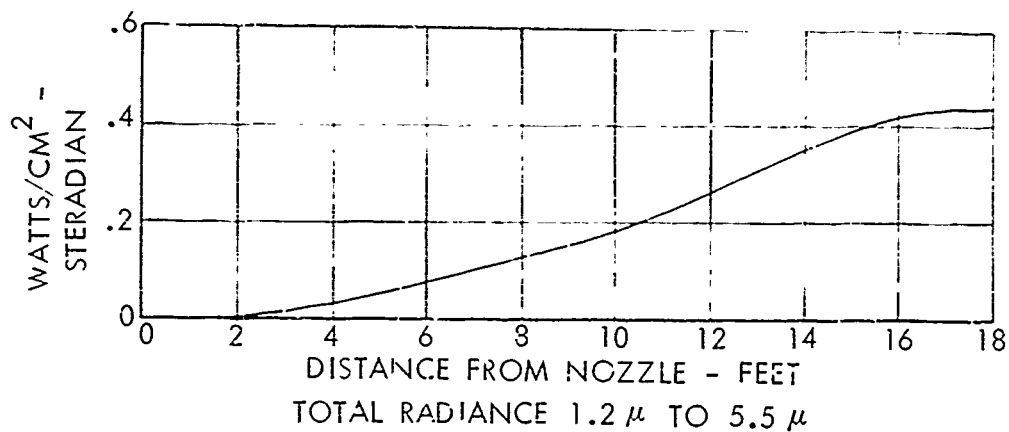
Figure 19a

PLUME RADIANCE
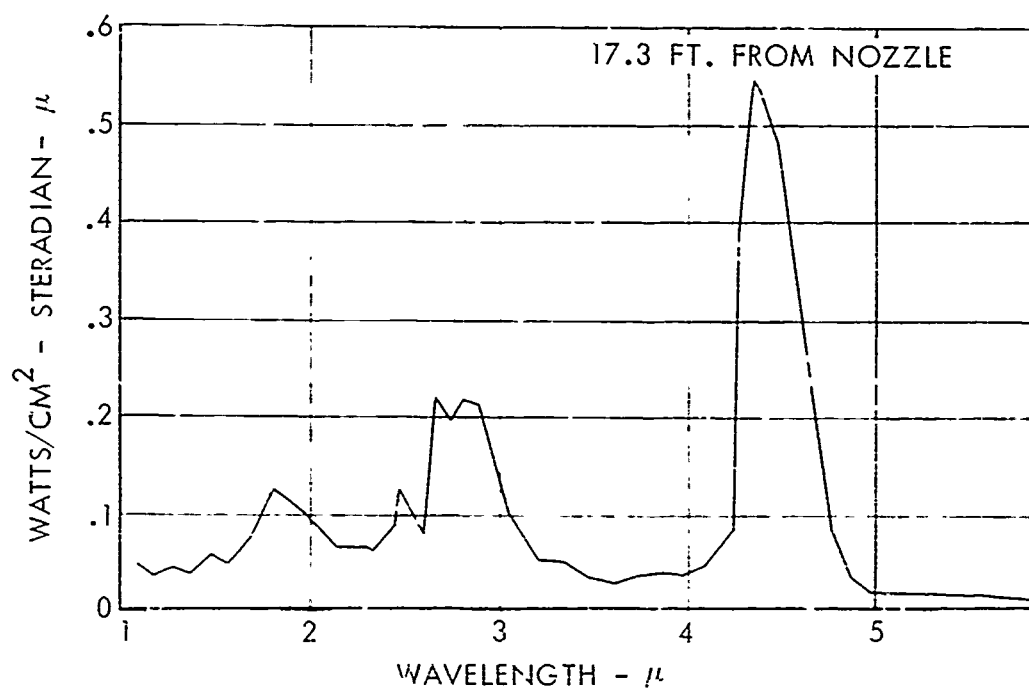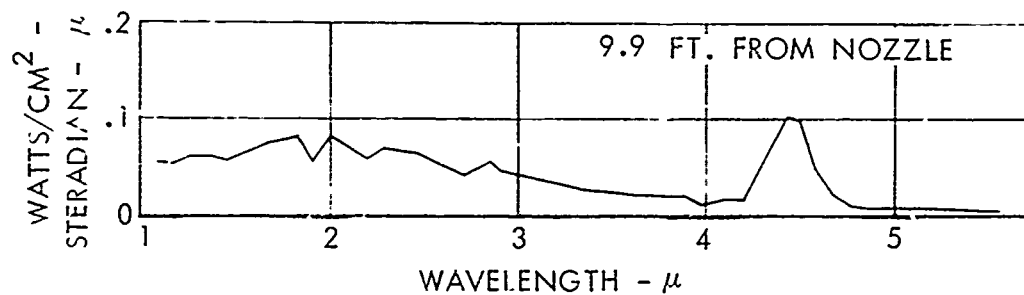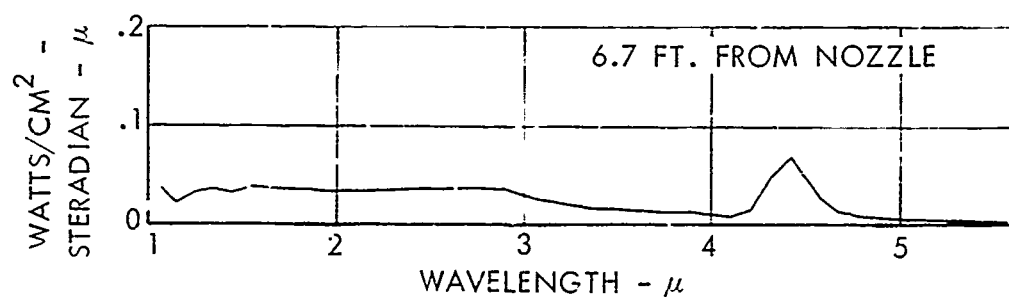
CONDITIONS

PROPELLANT   RP1 - OXYGEN
ALTITUDE   84,000 FT.
E.R.   1.67

Figure 19b

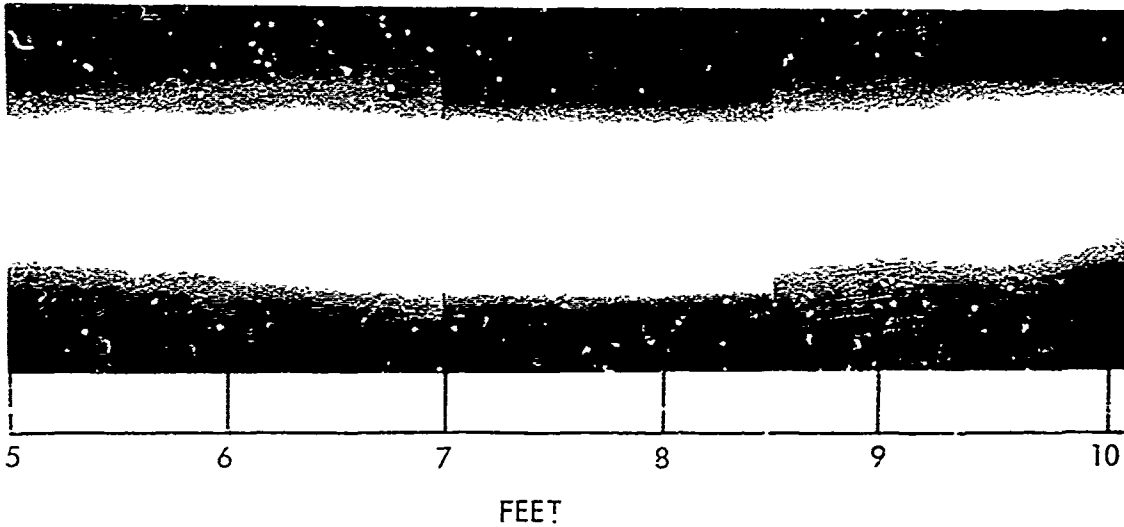PLUME SPECTRAL RADIANCE

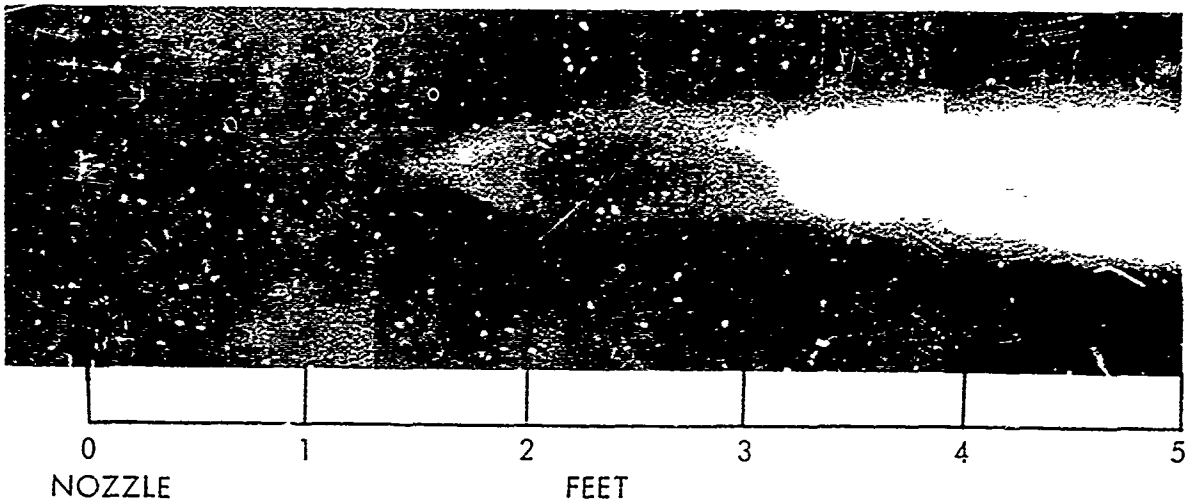CONDITIONS

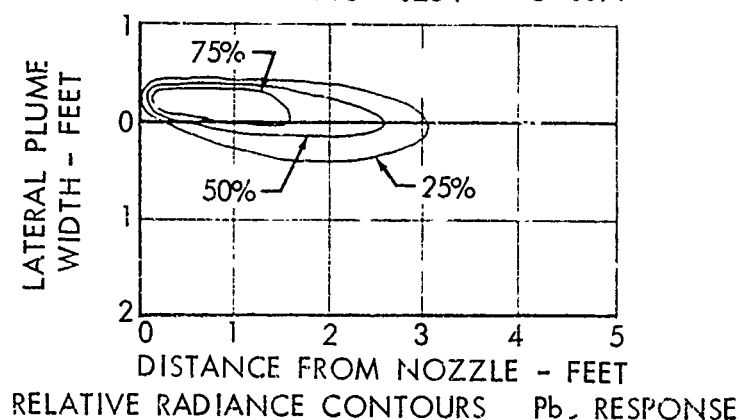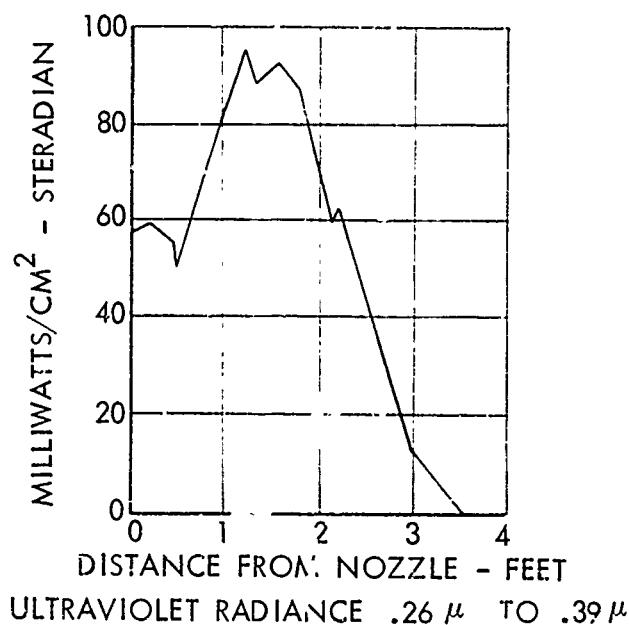| PROPELLANT | RP-1 - OXYGEN |
| ALTITUDE | 84,000 FEET |
| E.R. | 1.67 |

Figure 19c

VISIBLE PLUME SPECTRA

58

0   1   2   3   4   5

NOZZLE   FEET

5   6   7   8   9   10

FEET

CONDITIONS

PROPELLANT	RP-1 - OXYGEN
ALTITUDE	84,000 FEET
E. R.	1.67

Figure 19d

VISIBLE PLUME RADIATION

59

TOTAL RADIANCE .6 μ TO 5.5 μ

ULTRAVIOLET RADIANCE .26 μ TO .39 μ

RELATIVE RADIANCE CONTOURS   Pb₋ RESPONSE
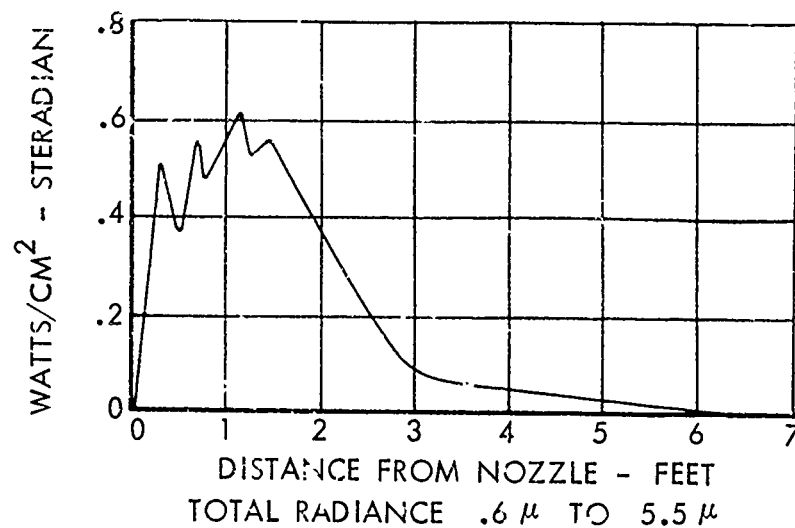
CONDITIONS

PROPELLANT	JP-4 - OXYGEN
ALTITUDE	SEA LEVEL
E R	1.75

Figure 20a

PLUME RADIANCE
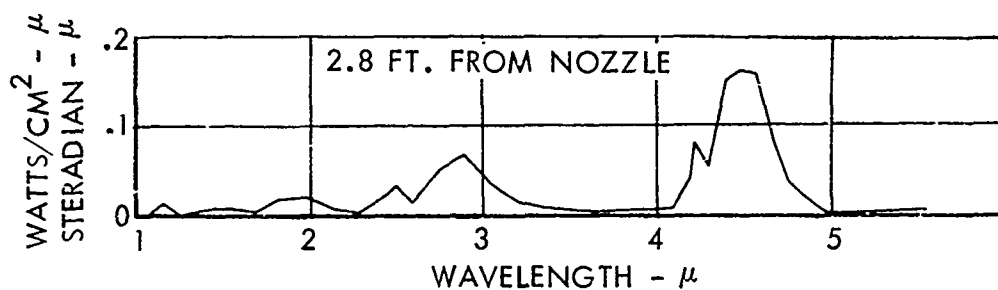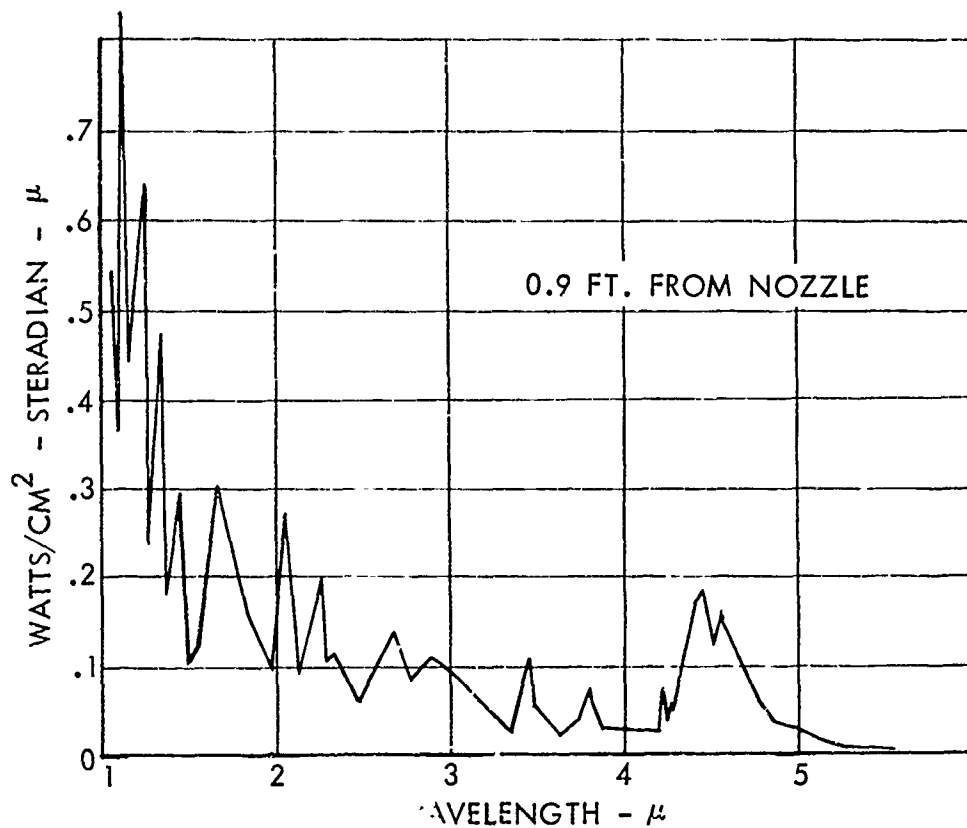
CONDITIONS

PROPELLANT	JP-4 – OXYGEN
ALTITUDE	SEA LEVEL
E.R.	1.75

Figure 20b

PLUME SPECTRAL RADIANCE
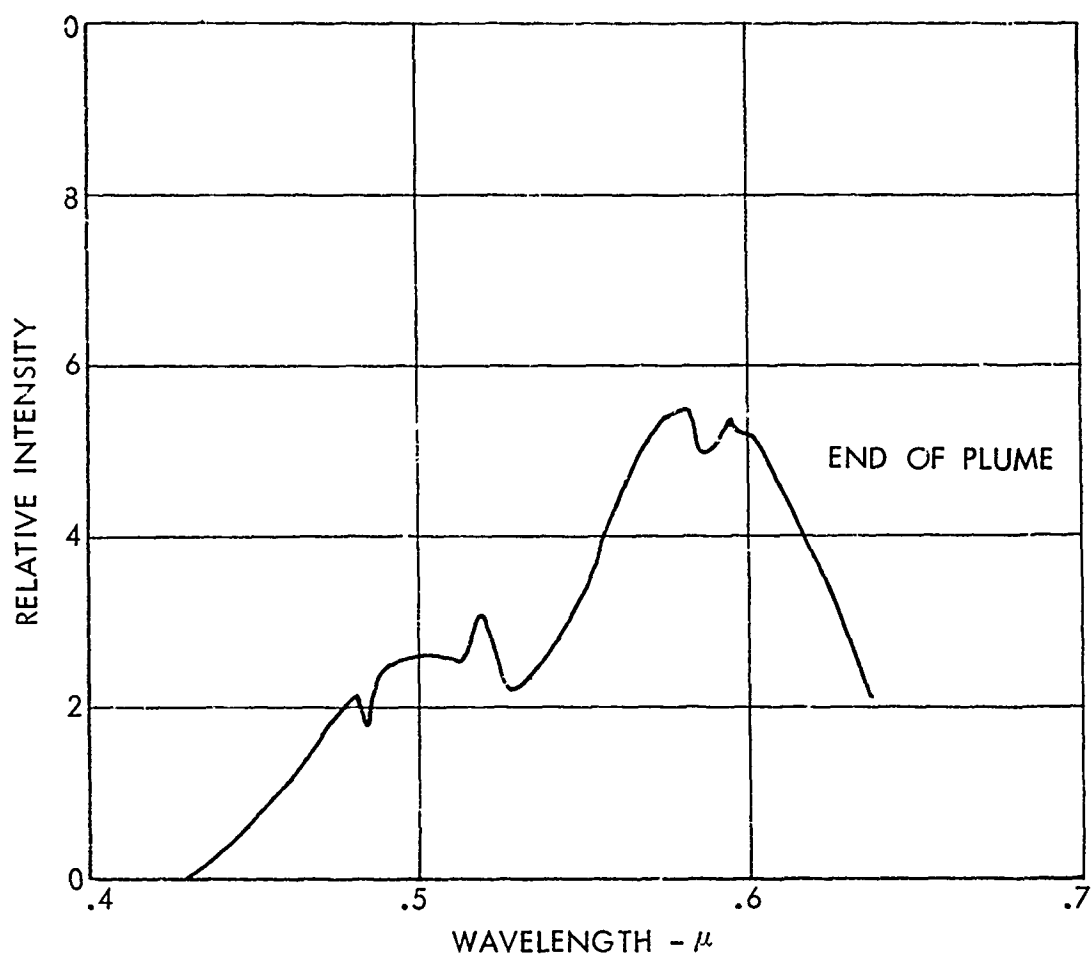
Figure 20c

VISIBLE PLUME SPECTRA

TOTAL RADIANCE 1.2μ TO 5.5μ

ULTRAVIOLET RADIANCE   .26 μ TO   .37 μ

RELATIVE RADIANCE CONTOURS   Pbs RESPONSE
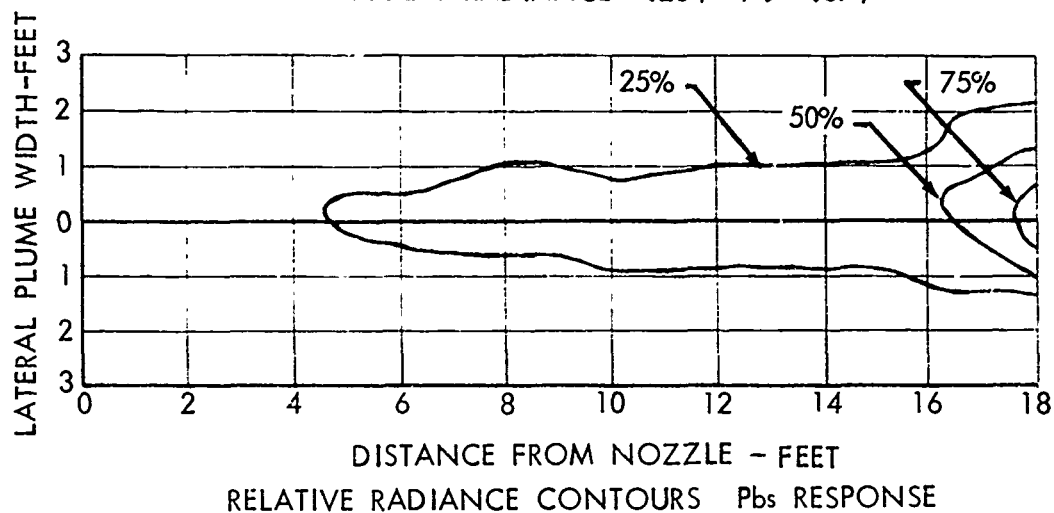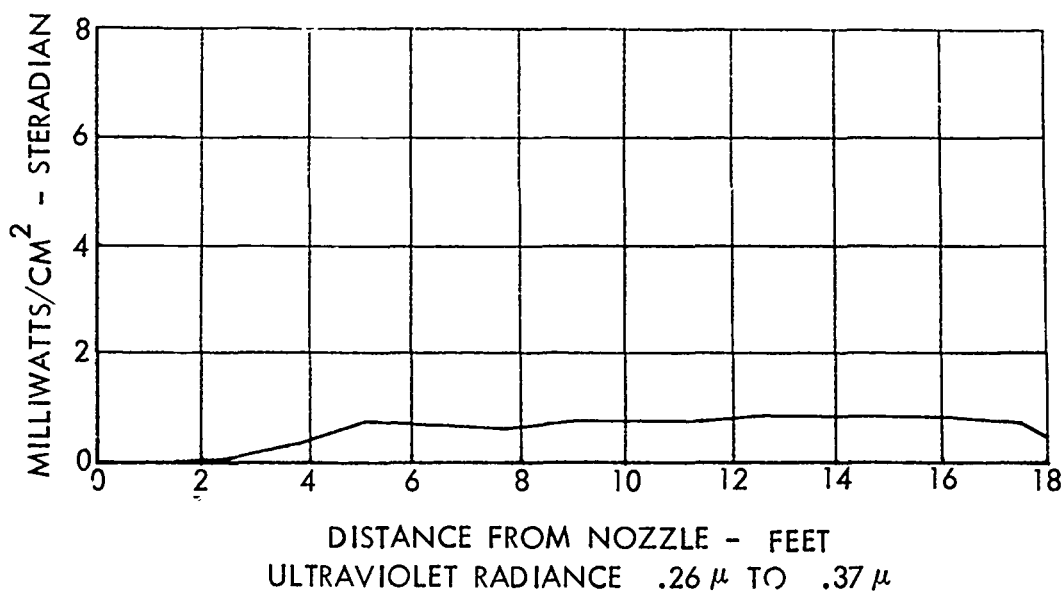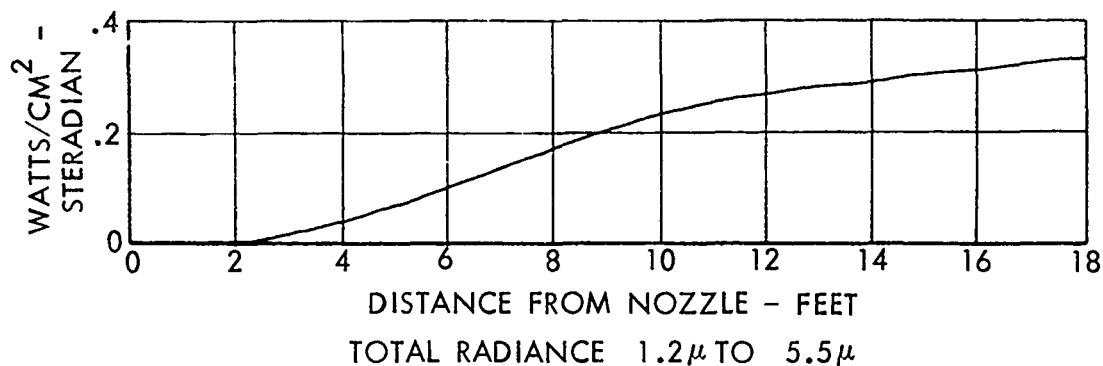
CCNDITIONS

PROPELLANT	JP-4 OXYGEN
ALTITUDE	87,000 FEET
E.R.	1.76

Figure 21a

PLUME RADIANCE
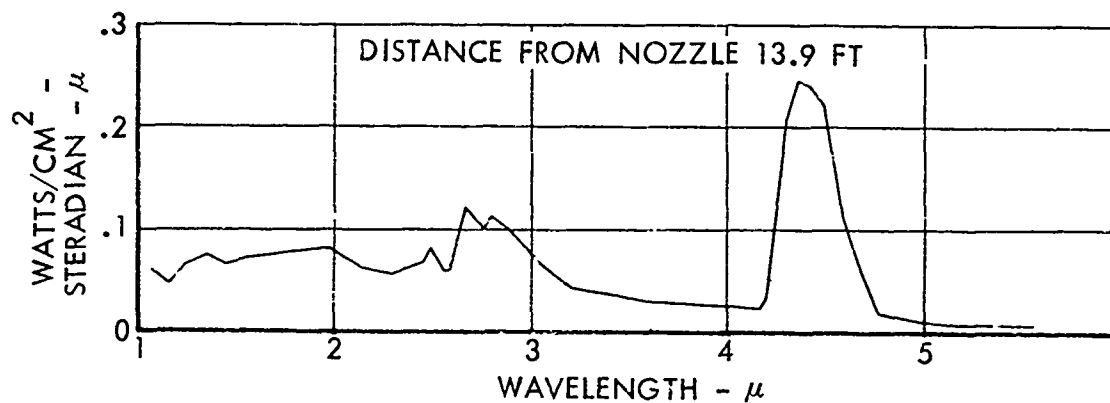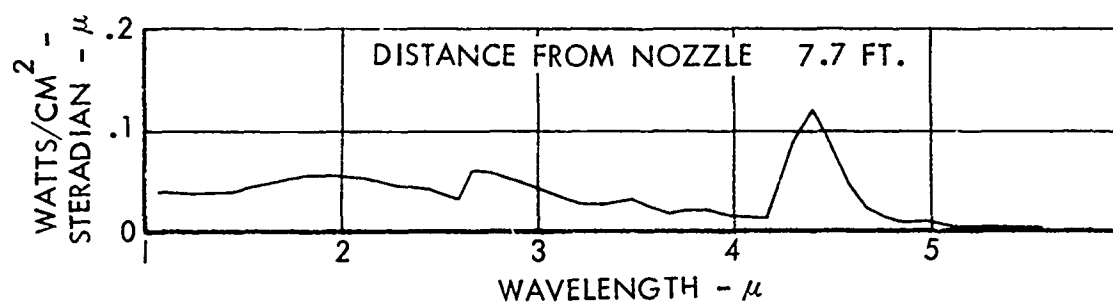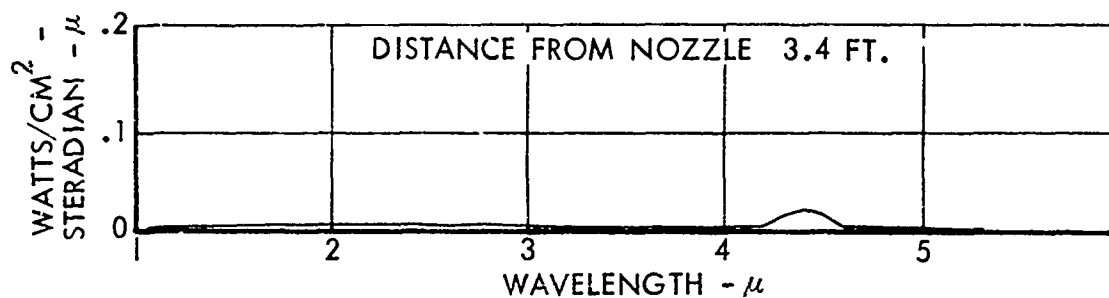
CONDITIONS

PROPELLANT	JP-4 OXYGEN
ALTITUDE	87,000 FEET
E.R.	1.76

Figure 21b

PLUME SPECTRAL RADIANCE
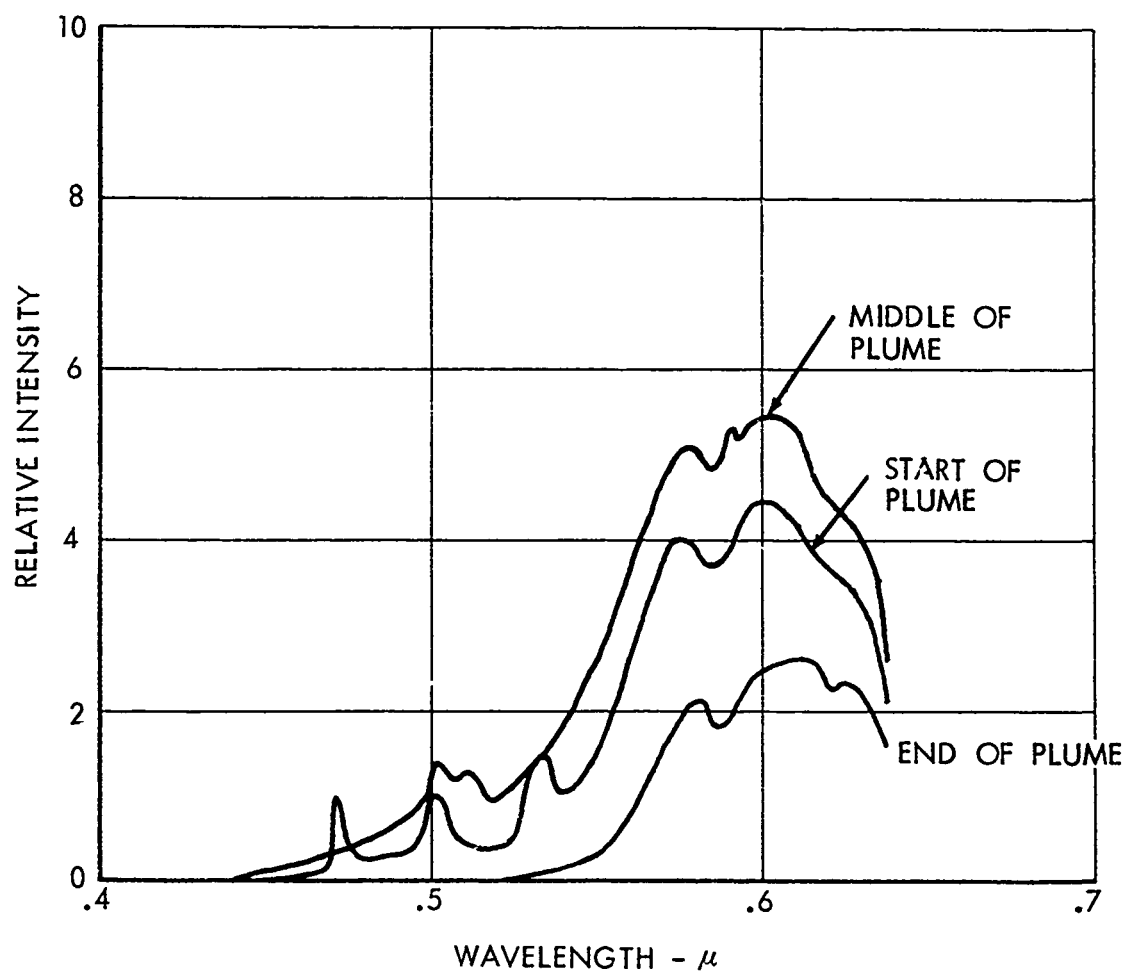
CONDITIONS

PROPELLANT	JP-4 OXYGEN
ALTITUDE	87,000 FEET
E.R.	1.76

Figure 21c

VISIBLE PLUME SPECTRA
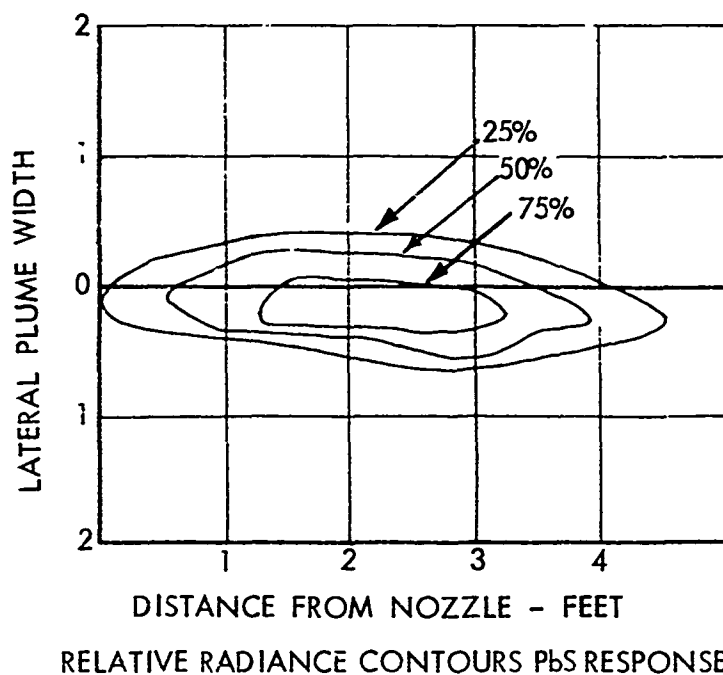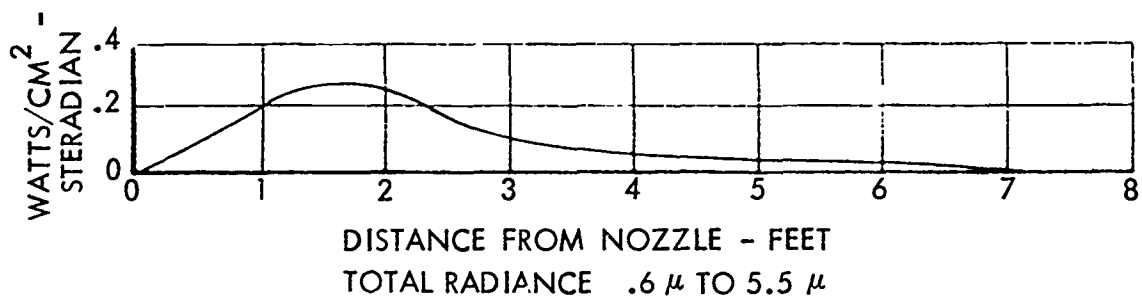
3.3 PLUME RADIATION DATA FOR UDMH-N_2O_4

Five runs were attempted with the propellant system unsymmetrical dimethyl-
hydrazine-nitrogen tetroxide, but useful data were gained from only one of
these runs. In each of the other runs motor failure occurred due to attack
of these constituents on the structure of the rocket under the operating
conditions which were employed. In this one sea level run, shown in Figure
22, the total plume radiance was three- to four-fold lower than for the
hydrocarbon-oxygen systems at sea level.

The infrared spectra for the UDMH-N_2O_4 show no contribution of continuum,
as should be expected from the nature of the exhaust products of this system.
The radiance values in the 2.7 and 4.3 micron regions do not differ greatly
from those obtained with the hydrocarbon-oxygen rocket under comparable
operating conditions. Due to the apparent significance of afterburning in
establishing the strong molecular radiation contributions in the hydrocarbon-
oxygen systems at altitude, it would be dangerous to assume that this same
comparison would be applicable for altitude operation of the UDMH-N_2O_4 system.
Due to the plume composition afterburning can make little if any contribution
to the high altitude radiation source.

WATTS/CM^2 - STERADIAN

.4

.2

0

0   1   2   3   4   5   6   7   8

DISTANCE FROM NOZZLE - FEET

TOTAL RADIANCE   .6 μ TO 5.5 μ

LATERAL PLUME WIDTH

2

1

0

1

2

25%
50%
75%

1   2   3   4

DISTANCE FROM NOZZLE - FEET

RELATIVE RADIANCE CONTOURS PbS RESPONSE

CONDITIONS

PROPELLANT   UDMH - N_2O_4
ALTITUDE   SEA LEVEL
MIXTURE RATIO   2.23

Figure 22a
PLUME RADIANCE

67
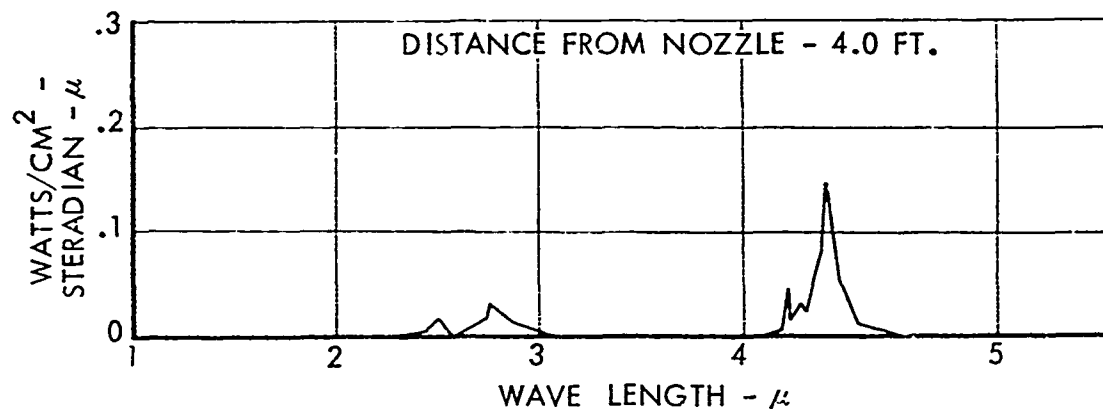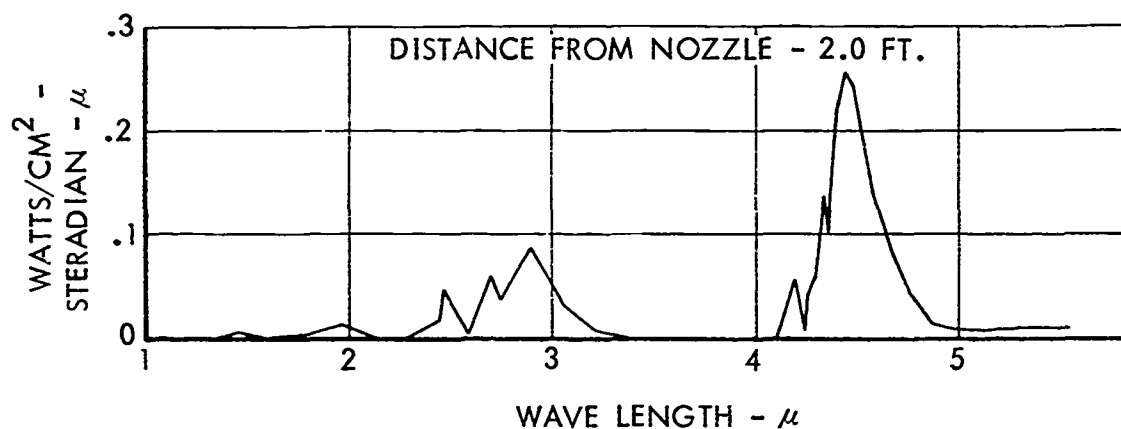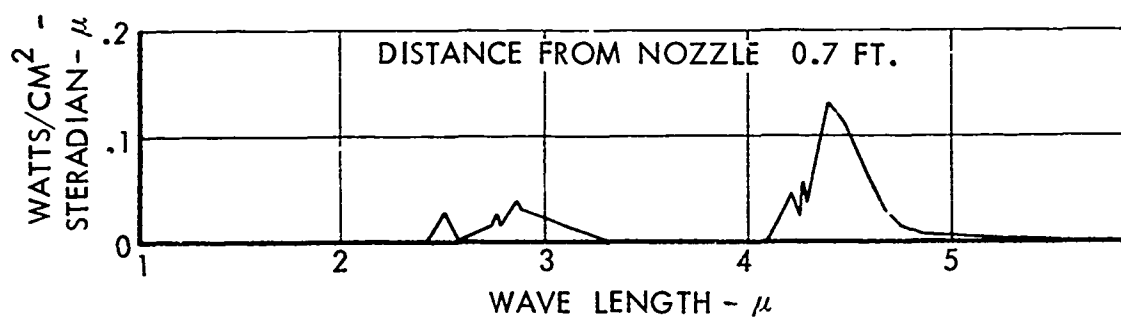
Figure 22b

PLUME SPECTRAL RADIANCE

0   1   2

NOZZLE

FEET
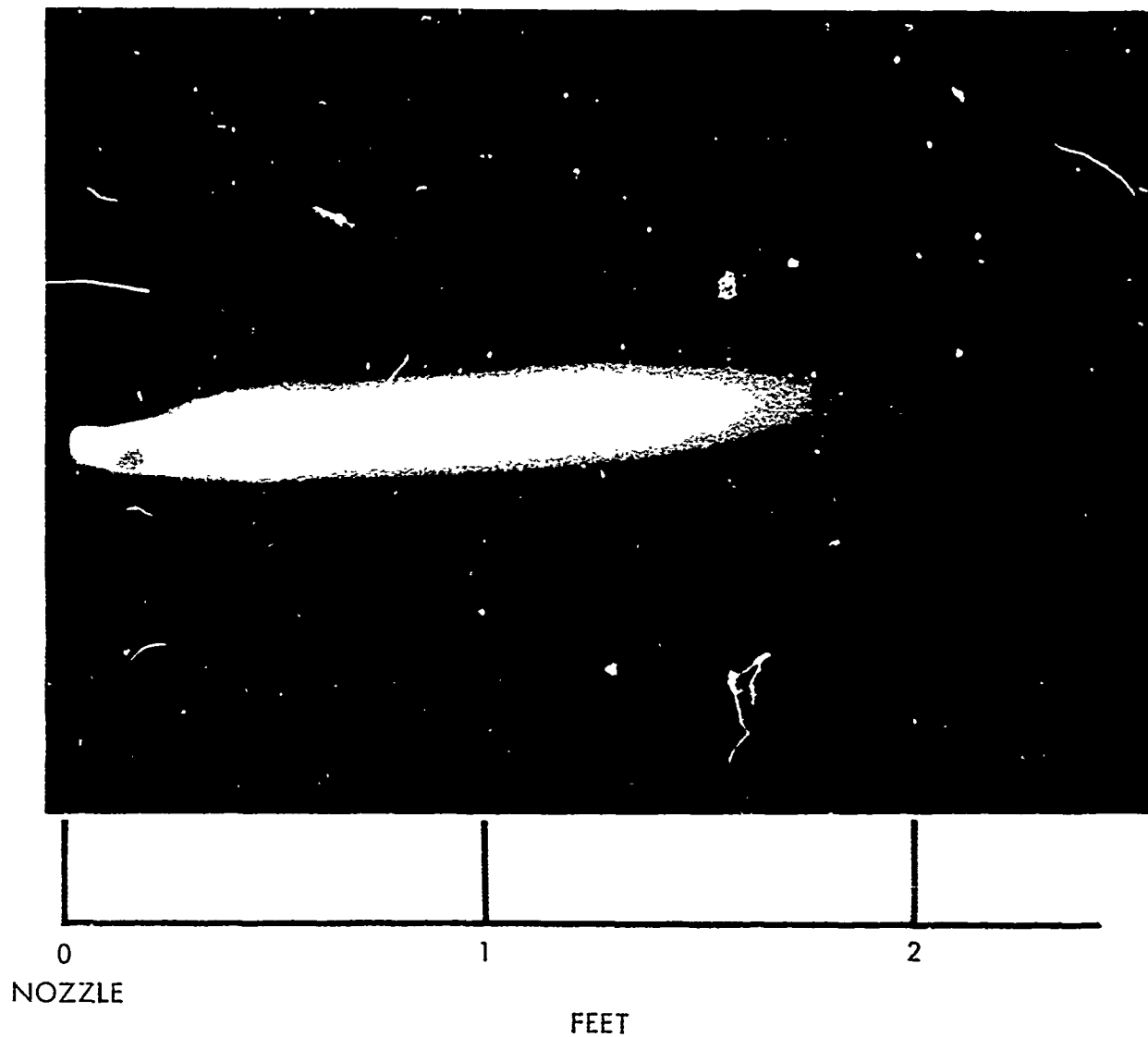
CONDITIONS

PROPELLANT	UDMH – N_2O_4
ALTITUDE	SEA LEVEL
MIXTURE RATIO	2.23

Figure 22c

VISIBLE PLUME RADI ON

69

3.4   PLUME RADIATION DATA FOR ALUMINIZED SOLID PROPELLANT

Observations of plume radiance were made for aluminized solid propellant
rockets at sea level and at 87,000 feet. A modification of the standard
CP test motor was supplied by Thiokol which provided approximately 200
pounds thrust at constant chamber pressure for a period of 7 seconds. The
sea level measurements were made during a traverse of one rocket motor.
In order to survey the plume at altitude it was necessary to traverse two
motors in sequence.

At sea level the total infrared plume radiance was observed to be some three
fold lower than for the liquid propellant motors, although the liquid motors
were operating at a somewhat lower thrust level than the solid propellant
motors. The ultraviolet radiance curve shows two maxima for the solid pro-
pellant exhaust. The first of these maxima, occurring essentially at the
nozzle exit plane, is attributed to the strong scattering power of the
alumina particles in the exhaust for the short wavelength radiation. The
second and somewhat weaker maximum coincides with the maximum in infrared
radiance and may therefore be ascribed to the chemiluminescent processes
accompanying the afterburning reactions, present in the solid exhaust plume
as in those of hydrocarbon-oxygen rockets.

The infrared spectral radiance curves show a smaller contribution of con-
tinuum radiation for the solid propellant rocket than for the several liquid
propellant rockets in the hydrocarbon-oxygen systems. The continuum radia-
tion contribution in the 1 to 3 micron region is largely missing in the solid
propellant exhaust. Two factors may be cited to account for this difference.
The carbon particles in the hydrocarbon exhaust may be of a greater diameter

than the alumina particles in the solid propellant exhaust, and therefore have a greater scattering contribution in the near infrared region. The somewhat lower temperature at the nozzle exhaust plane for the solid propellant rocket may combine with a different gas flow situation in this exhaust to prevent the occurrence of the continuum radiation from high temperature air due to entrainment in the exhaust.

The band radiation in the 2.7 and 4.3 micron regions has essentially the same maximum levels as for the liquid propellant motors which were studied. The visible spectra from the solid fuel motor also shows the strong influence of the scattering power of the alumina particles, in that the early part of the plume shows primarily the continuum radiation extending to very short wavelengths with little evidence of line contribution. The strong contribution of the NaD line is apparent in all of the visible spectra, although sodium is present only as an impurity in this propellant composition.

The solid propellant exhaust at 87,000 feet presents a much more uniform spatial distribution than does the liquid propellant plume. The total infrared radiance attains a reasonably constant value some 3 to 4 feet from the nozzle and maintains this level as far as 1^{2} feet from the nozzle. Measurements did not extend beyond this point since this was the maximum traverse distance in the altitude tank being employed.
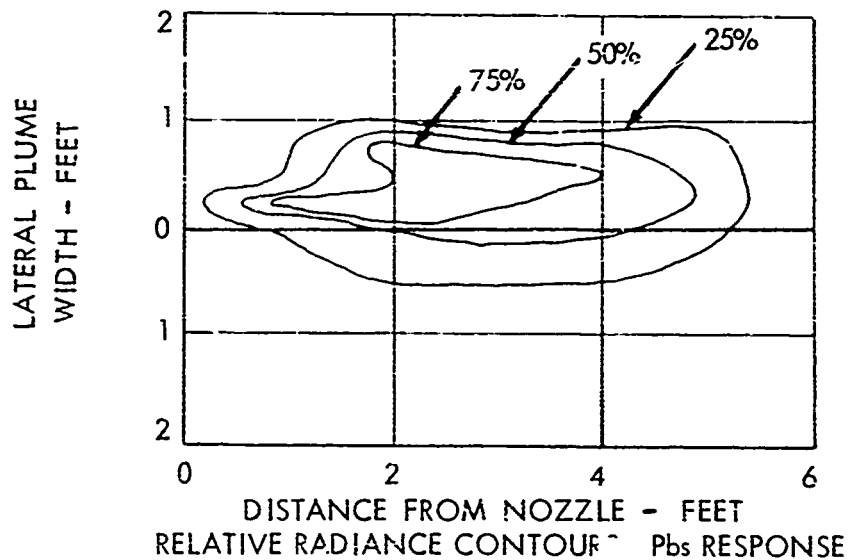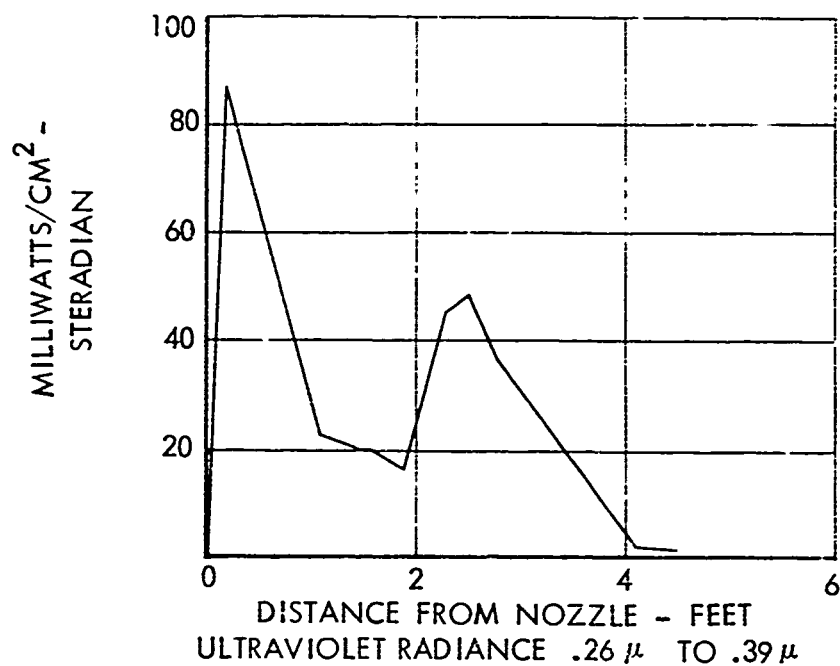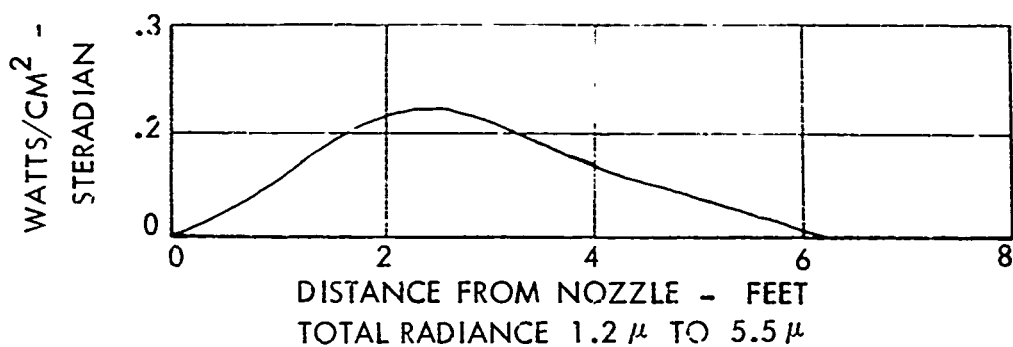
The ultraviolet radiance at altitude is again found to be diminished to some 2 percent of the sea level values. The gradually diminishing value for the solid propellant exhaust as the position is removed from the nozzle

exit plane indicates that the contribution due to scattered radiation domi-
nates with respect to the contribution from chemiluminescent processes in
the exhaust.

The infrared spectral curves again show contribution of continuum radiation
only in the 1 to 2 micron region. As in the sea level measurements the band
contributions in the 2.7 and 4.3 micron regions are found to be not greatly
different from those in the hydrocarbon-oxygen rocket exhaust. If any differ-
ence exists it is that the level of radiation in these bands is slightly lower
for the solid propellant exhaust than for the hydrocarbon-oxygen exhaust,
although the thrust level was some 25 percent greater for the solid propellant
rockets.

The visible plume spectra show the line contributions of the various metal
species present in the solid propellant exhaust. It should be noted that
this spectrum, which might be considered to have signature characteristics,
does occur in the region near the nozzle. The strong contributions to visible
spectrum in the liquid propellant exhaust were found to occur consistently
in the afterburning region, well removed from the nozzle plane.

The photograph of the high altitude solid rocket plume presents an interesting,
if unexplained, view. The directed flow of the alumina particles is some-
what altered by the gas shock pattern impressed on it. The first compression
effect is observed only 1.0 foot from the nozzles, as compared with a spacing
of 1.5 feet in the liquid motor plumes under comparable conditions. The
total effect of particle cooling and reheating due to gas compression and
afterburning is to yield a gradually diminishing visible radiation pattern.

WATTS/CM^2 - STERADIAN

.3
.2
0
0   2   4   6   8

DISTANCE FROM NOZZLE - FEET
TOTAL RADIANCE 1.2 μ TO 5.5 μ

MILLIWATTS/CM^2 - STERADIAN

100
80
60
40
20
0   2   4   6

DISTANCE FROM NOZZLE - FEET
ULTRAVIOLET RADIANCE .26 μ TO .39 μ

LATERAL PLUME WIDTH - FEET

2
1
0
1
2

75%   50%   25%

0   2   4   6

DISTANCE FROM NOZZLE - FEET
RELATIVE RADIANCE CONTOUR Pbs RESPONSE

CONDITIONS

| PROPELLANT | SOLID FUEL MOTOR |
| ALTITUDE | SEA LEVEL |

Figure 23a

PLUME RADIANCE

73
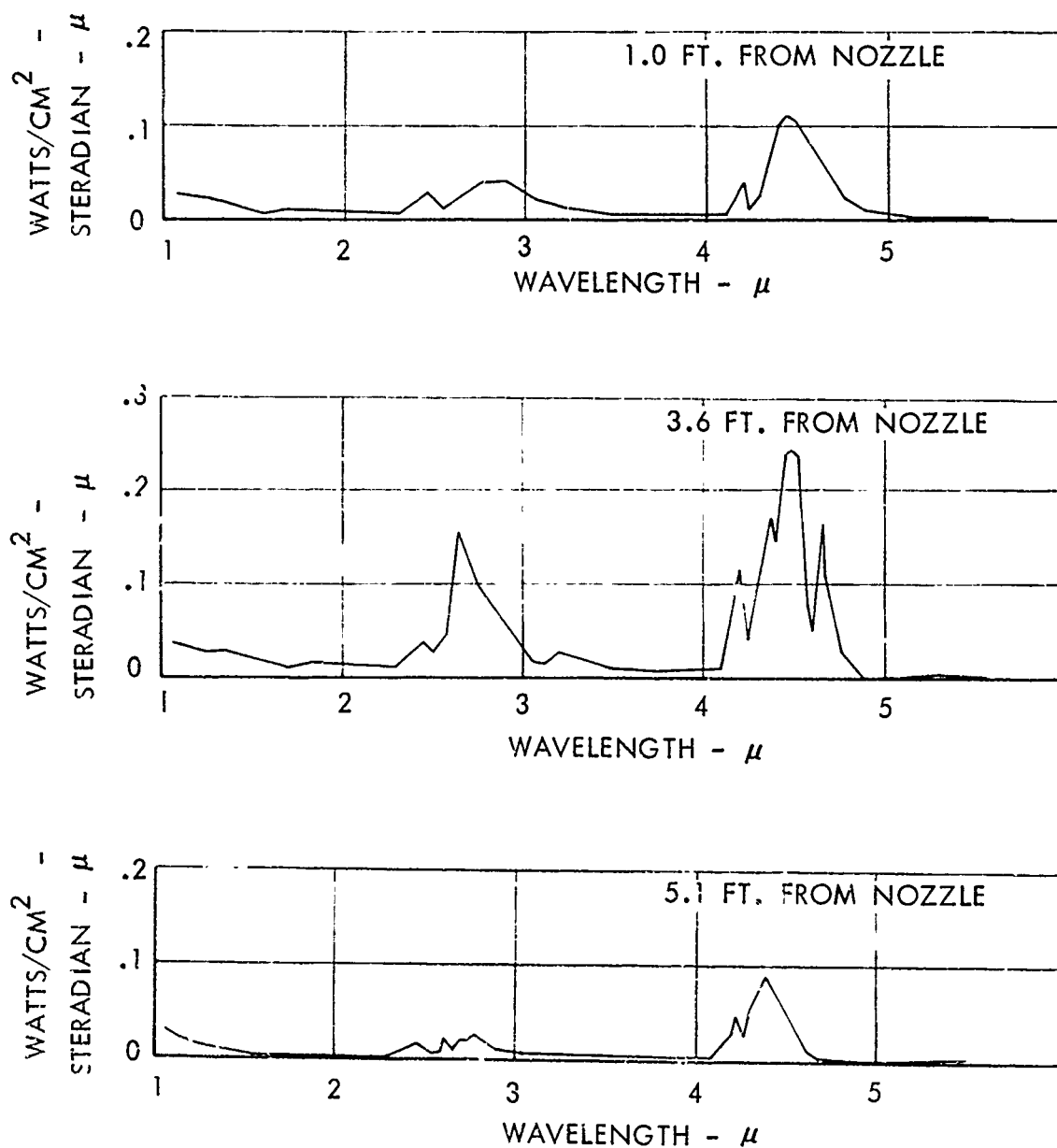
Figure 23b

P'UME SPECTRAL RADIANCE

CONDITIONS

PROPELLANT   SOLID FUEL MOTOR
ALTITUDE   SEA LEVEL
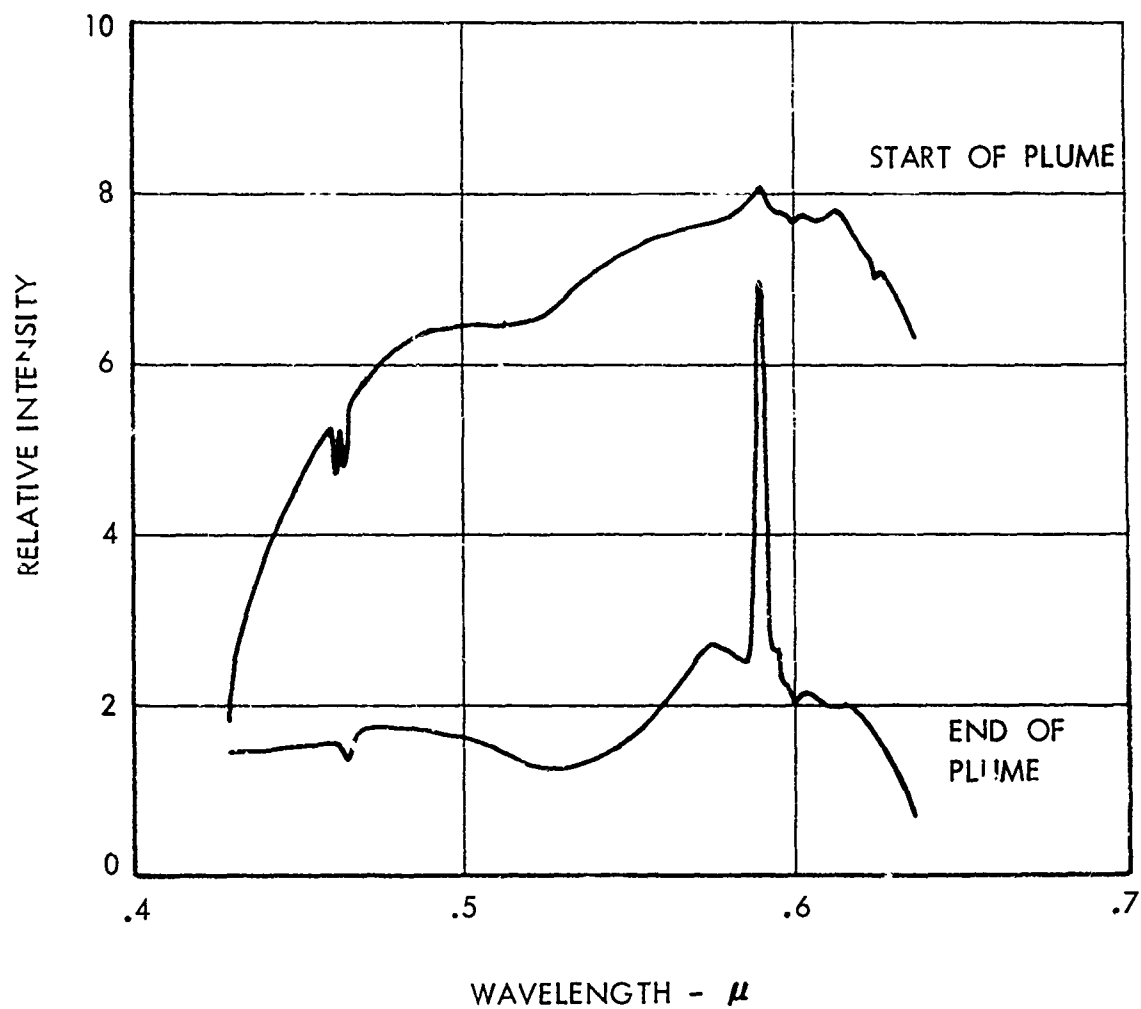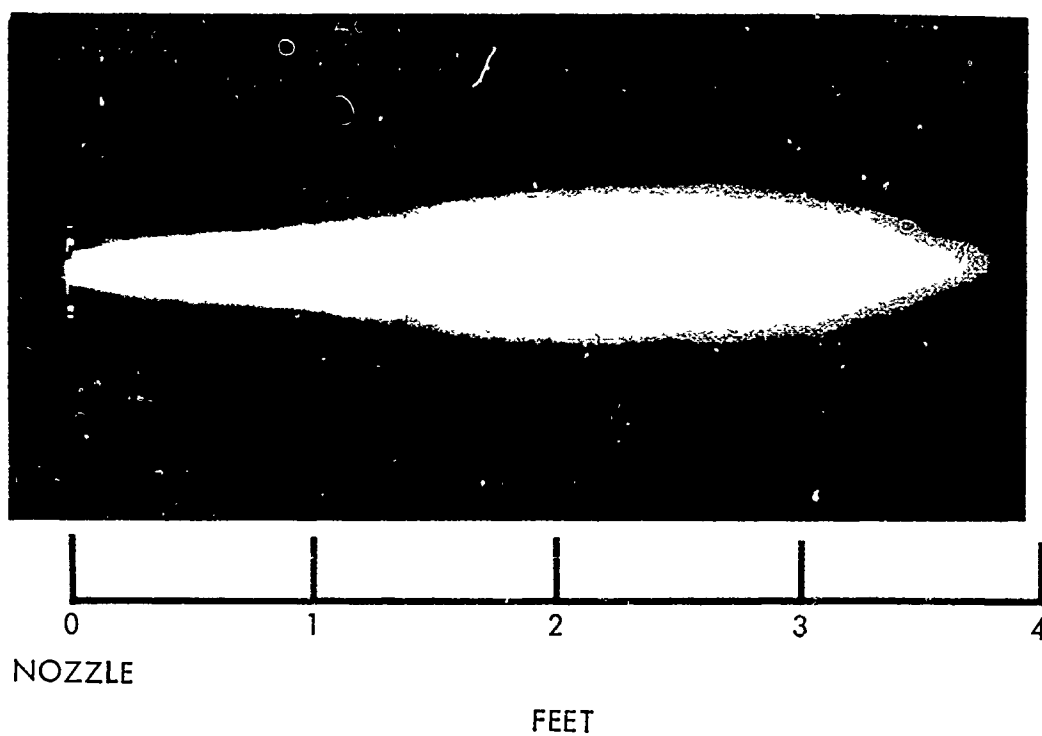
CONDITIONS

PROPELLANT   SOLID FUEL MOTOR
ALTITUDE   SEA LEVEL

Figure 23c

VISIBLE PLUME SPECTRA

75

```
|    |    |    |    |    |
0    1    2    3    4
```

NOZZLE

FEET

CONDITIONS

PROPELLANT	SOLID FUEL
ALTITUDE	SEA LEVEL

Figure 23d

VISIBLE PLUME RADIATION

WATTS/CM² - STERADIAN

DISTANCE FROM NOZZLE - FEET
TOTAL RADIANCE   1.2 μ TO 5.5 μ

MILLIWATTS/CM² - STERADIAN

DISTANCE FROM NOZZLE - FEET
ULTRAVIOLET RADIANCE   .26 μ TO .39 μ

LATERAL PLUME WIDTH - FEET

75%   50%
25%

DISTANCE FROM NOZZLE - FEET
RELATIVE RADIANCE CONTOURS   PbS RESPONSE
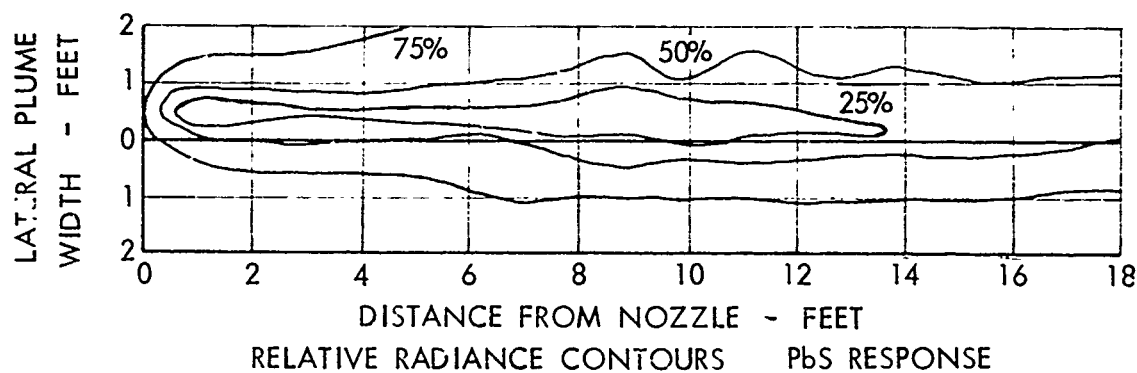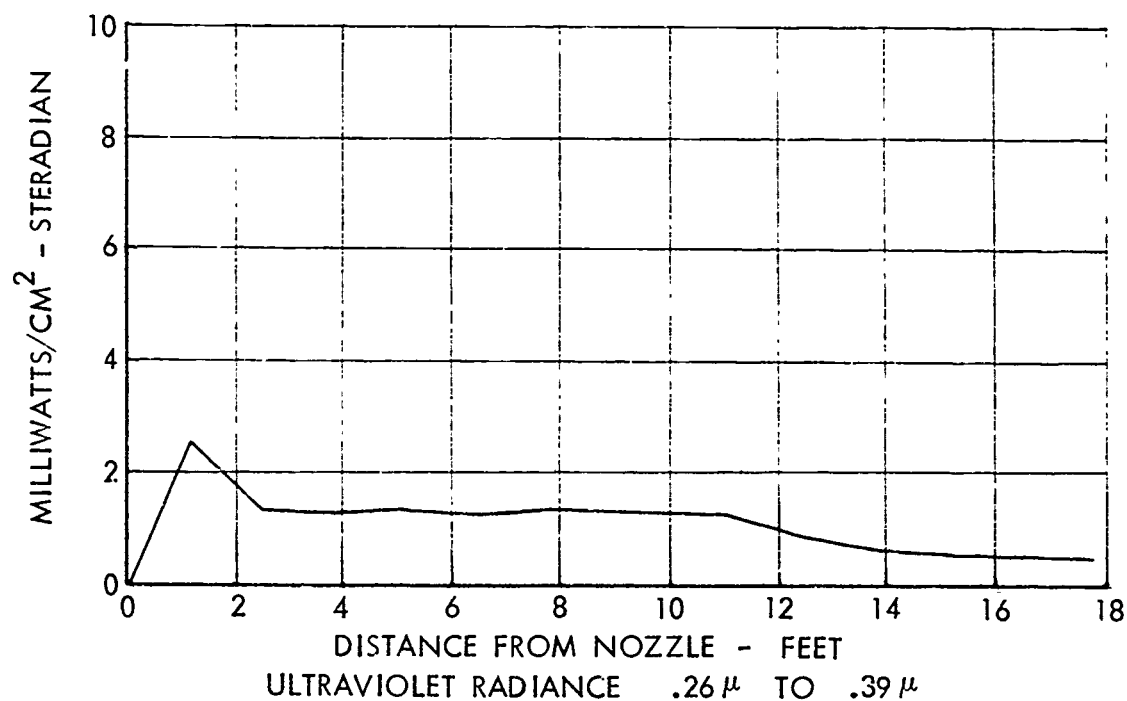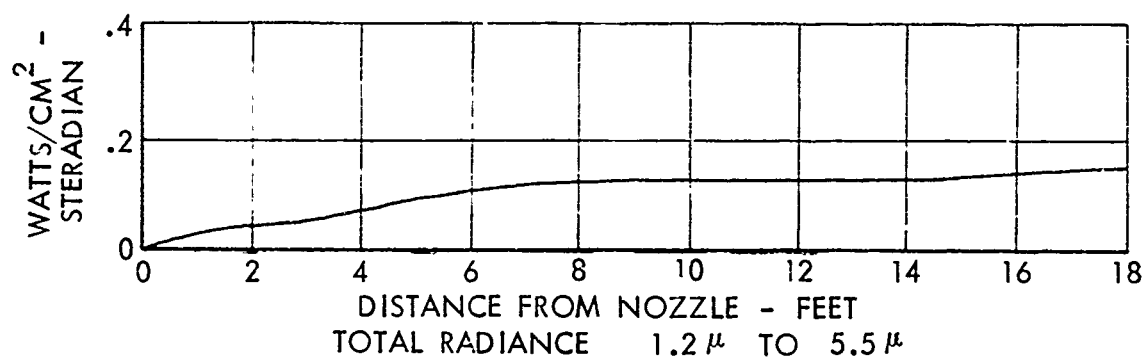
CONDITIONS

PROPELLANT   SOLID FUEL
ALTITUDE   87,000 FT.

Figure 24a

PLUME RADIANCE

77
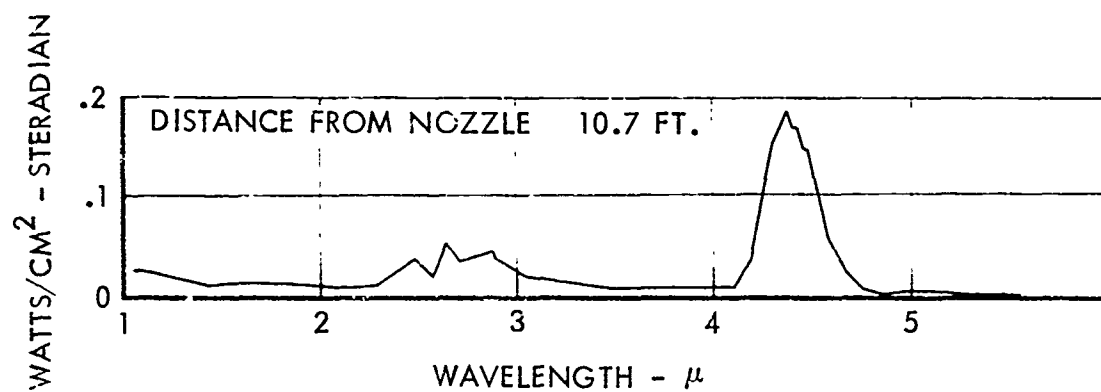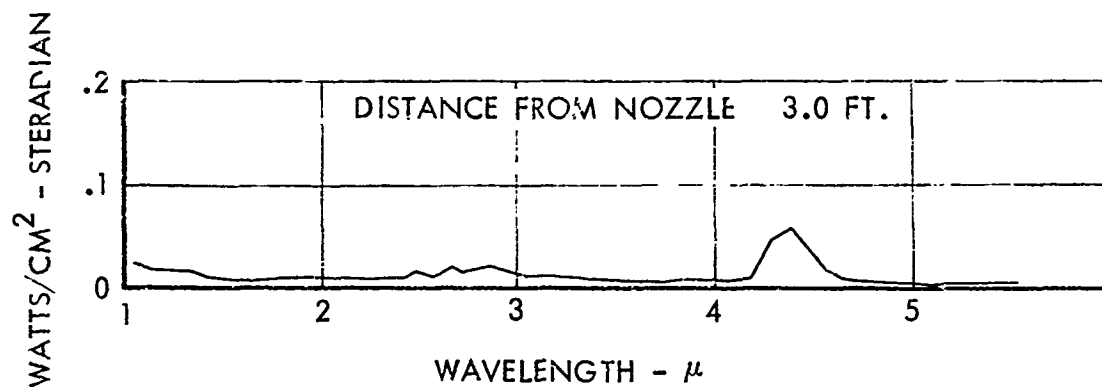
Figure 24b

PLUME SPECTRAL RADIANCE
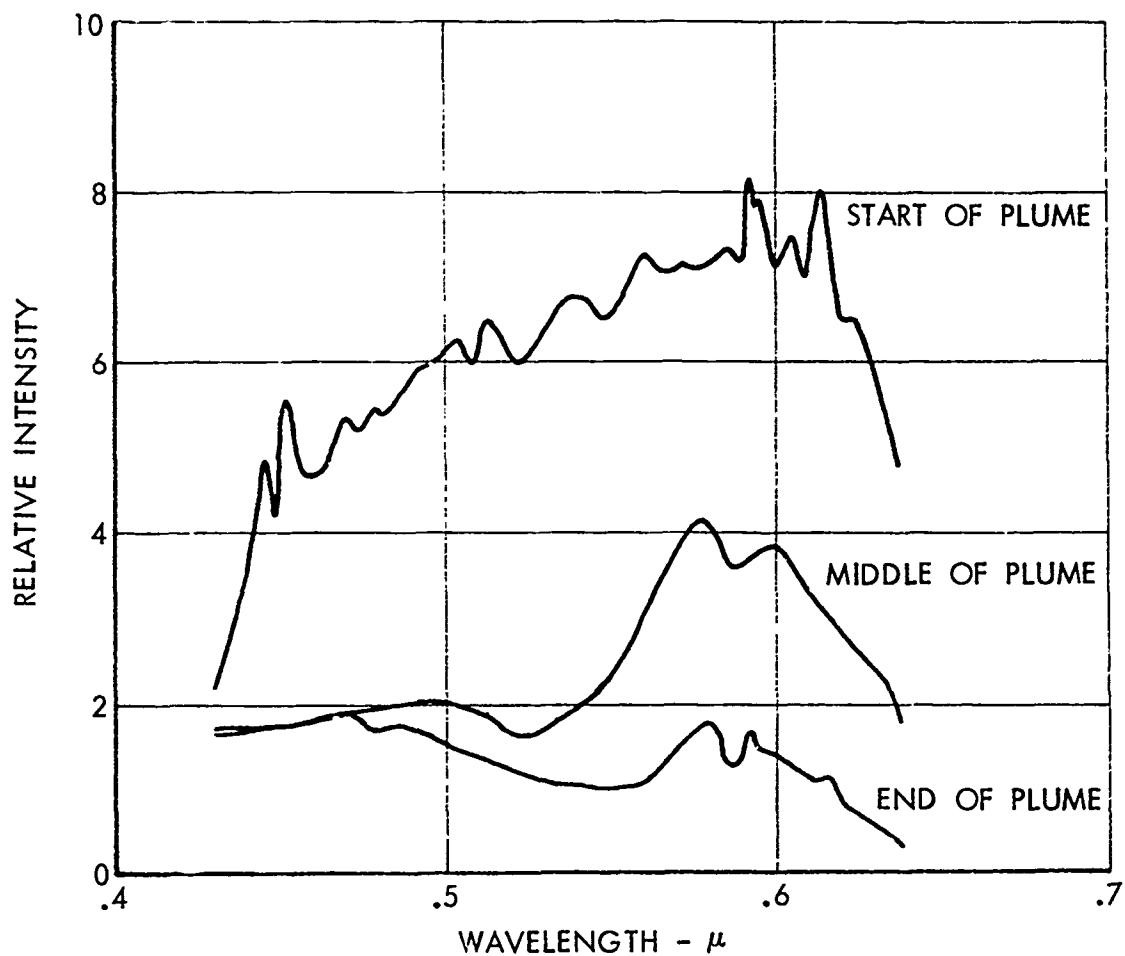
CONDITIONS

PROPELLANT	SOLID FUEL
ALTITUDE	87,000 FT.

Figure 24c

VISIBLE PLUME SPECTRA
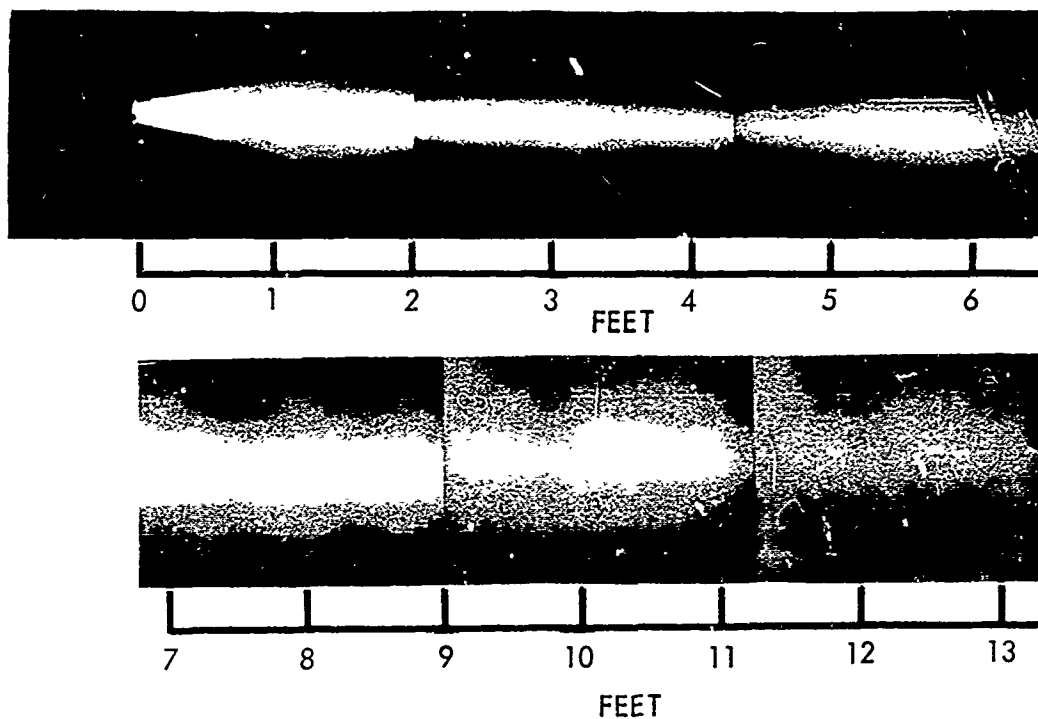
CONDITIONS

PROPELLANT   SOLID FUEL
ALTITUDE   87,000 FEET

Figure 24d

VISIBLE PLUME RADIATION

3.5 AUDIOMODULATION OF PLUME RADIANCE

Preliminary observations of the audiomodulation in the infrared radiance of the plumes were made for the hydrocarbon-oxygen rockets. The significance of the data obtained is limited, due to the rudimentary design of the modulation radiometer and the half-octave bandwidth analyzer utilized in reduction of the data.

For the sea level runs the modulation peaked in the 37 to 75 cycle region, and then decreased regularly to zero at 1000 cycles. In some of the runs a secondary weak maximum was observed between 150 and 212 cycles. Similar observations were made for the altitude runs, except that the secondary peak between 150 and 212 cycles was consistently present and more pronounced than at sea level. The spatial region showing maximum audiomodulation corresponded to the area from which the infrared radiance itself was the greatest.

The vibrations of the altitude chamber were continuously monitored and recorded on a parallel channel. The peak in tank vibrations was centered between 850 and 1200 cycles, with a rapid decrease in power on either side of the peak. These frequencies are well-removed from the data observed for the modulation of the infrared radiance.

Several improvements will be made in the instrumentation before attempting further studies of this type. The D.C. level will be recorded by division of the detector signal, so that the percent modulation can be determined as a function of audio frequency. A narrower bandpass analysis will be performed, utilizing a bandwidth which is constant in frequency increment. In this manner narrow spikes in the noise power spectrum may be located, and their dependence on operating parameters can be determined.

4.0 SUMMARY

The major observations from plume radiance studies of laboratory motors are summarized below:

1. The zone of maximum plume radiance for the hydrocarbon-oxygen propellant combinations rapidly recedes from the nozzle region with increasing altitude. At pressures equivalent to 80,000 to 100,000 feet the maximum value was observed in an elongated source, centered some 80 to 100 nozzle diameters downstream.

2. The maximum radiance in this zone is decreased to some 30 percent of the maximum at sea level. The increased radiating area serves to compensate for the reduced radiance, so that the radiant intensity is at least 50 percent of the sea level value.

3. At altitude the infrared radiance in the region near the nozzle is at least an order of magnitude lower than in the brighter zone.

4. The infrared spectra of hydrocarbon-oxygen exhaust show strong influence of continuum contribution near the nozzle at sea level and in the maximum radiance zone at altitude. For some distance beyond this zone the band radiations in 2.7 and 4.3 micron regions are maintained at uniform or increased intensity.

5. The maximum values of ultraviolet radiance in hydrocarbon-oxygen exhaust are found in the same zones as the maximum in infrared. The ultraviolet radiance decreases rapidly with altitude; the maximum value near 100,000 feet was found to be 1 to 2 percent of the sea level value.

6. The radiation characteristics of kerosene-oxygen systems (JP 4 and RP 1) are not detectably different from those of gasoline-oxygen.

7. At sea level the spectral characteristics for the $UDMH-N_2O_4$ propellant combination are markedly different from those of hydrocarbon-oxygen systems. The continuum contributions do not appear. The 2.7 and 4.3 micron band radiations correspond in intensity to those in the hydrocarbon-oxygen exhaust at sea level.

8. The spectral distribution of infrared radiation from aluminized solid propellant motors is surprisingly similar to that for hydrocarbon-oxygen exhaust. The scattering properties of the alumina particles show a different wavelength dependence from that of the carbon particles in the 1 to 3 micron range.

9. The spatial distribution of radiance in the solid propellant exhaust at altitude is grossly different from the hydrocarbon-oxygen exhaust. A more nearly uniform level of infrared radiance is found for the entire length of the observed plume in the solid exhaust.

REFERENCES

1. "Ballistic Missile Plume Wind Tunnel Research." Convair San Diego Report ZR-AP-061-17. May 1961. SECRET

2. "High Temperature Infrared Emission and Absorption Studies," by Ferriso, Carmine C. General Dynamics - Astronautics Report AF 61-0910. 14 September 1961

3. "Spectral Radiances and emissivities of Rocket Exhaust Plumes," by DeBell, A. G.; Simmons, F. S. and Levin, B. P. Rocketdyne Report R-3216. November 1961. SECRET

4. "Infrared Continuum Radiation from High Temperature Air," by Wentink, T.; Planet, W.; Hammerling, P. and Nivel, B. Journal of Applied Physics, pgs. 29, 4, 742 - 743. April 1958